MAGNETOM Flash

The Magazine of MR

Issue no. 1/2007
ISMRM Edition

SIEMENS
medical

Clinical Orthopedic Imaging

Overview
Biochemical Imaging
Page 6

Molecular Imaging of Articular Cartilage and Cartilage Repair
Page 18

Technology

Metamorphosis of MRI: Seamless Move-During-Scan with *syngo* TimCT
Page 61

Pushing the Boundaries of MR with Siemens MAGNETOM 7T
Page 70

MR Imaging with an 8-Channel RF Transmit Array
Page 75

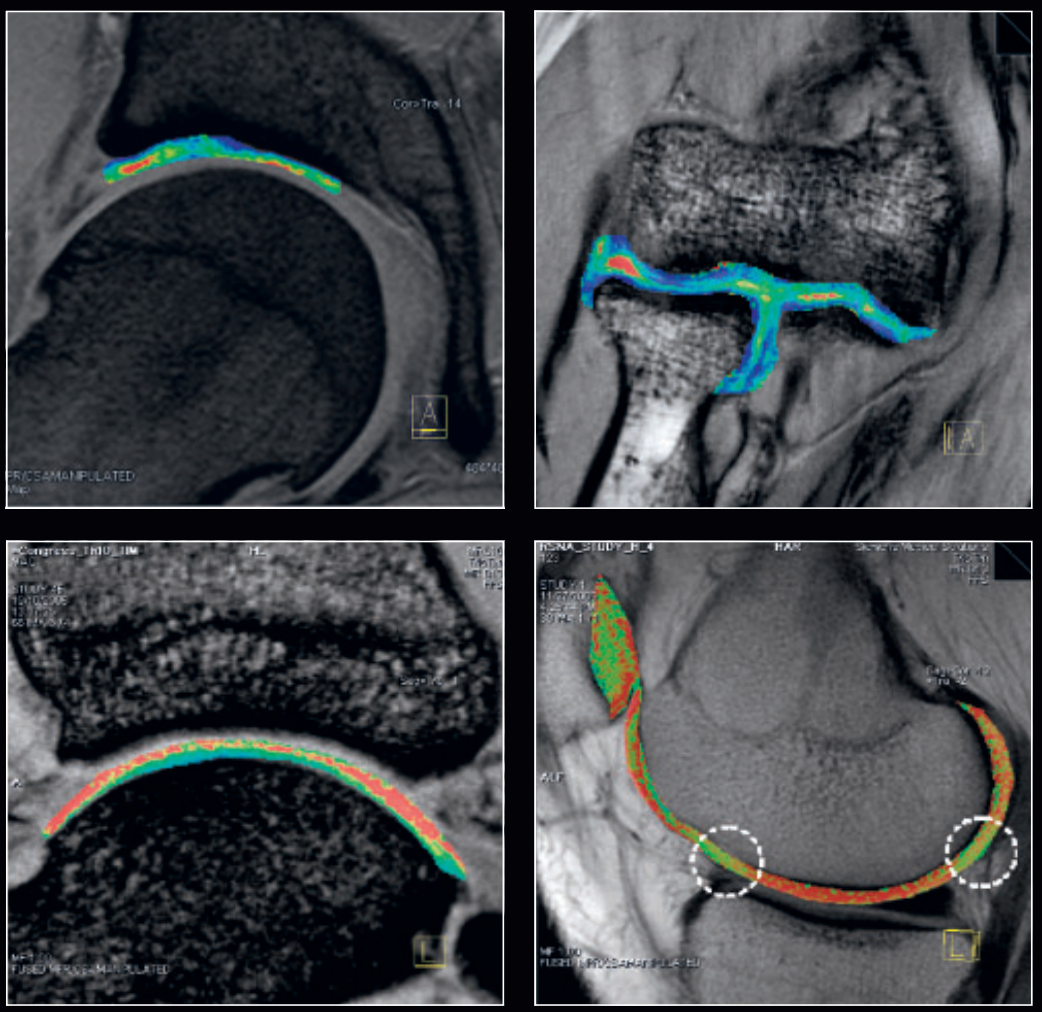

syngo **MapIt**

35

Tallal Charles Mamisch, M.D.
Inselspital, University Bern, Switzerland
Timothy Hughes, Ph.D.
Siemens Medical Solutions, Erlangen, Germany

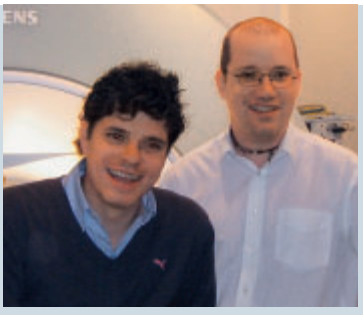

Dear MAGNETOM user,

Musculoskeletal (MSK) diseases are a major problem in our society, affecting millions and resulting in lost working hours and restricted functioning. MRI is increasingly important for the precise diagnosis and monitoring of therapy as it allows non-invasive morphological diagnosis. Furthermore, recent developments are making possible the biochemical assessment of pathologies.
Siemens MAGNETOM MR systems offer a comprehensive solution in Musculoskeletal imaging with special emphasis in four areas:
1. High-resolution fast imaging: using the extra imaging power of Tim (Total imaging matrix) to deliver extremely high in-plane 2D resolution within clinically acceptable examination times. The scan time can also be drastically reduced for users who require increased throughput.
2. 3D Isotropic imaging: a means of delivering enhanced workflow and better diagnosis.
3. Biochemical imaging: for improved diagnostic capability and therapy planning.
4. Orthopedic imaging with dedicated coils: to fully capitalize on the benefits of MAGNETOM systems and indicate new areas of study not previously possible e.g. biochemical imaging of the cartilage in the wrist, ankle or knee.
Our aim in this issue of MAGNETOM Flash is to include articles that give an overview of current approaches in Orthopedic imaging, from routine clinical protocols to new research work. The articles focus on improvements in diagnostic imaging and follow-up of therapy.
Our special thanks are due to Prof. Dr. Siegfried Trattnig (University Vienna, Austria), Dr. Thaddeus Laird (UC Davis Medical Center, Sacramento, USA) and Dr. Stefan Werlen (Sonnenhof Clinics Bern, Switzerland) for all their efforts in bringing the ideas and topics together for this issue. We are aware that the content of this MAGNETOM Flash can only cover a few selected topics from the wide spectrum of applications for MSK imaging.
We encourage MAGNETOM users to give us feedback on these articles and on other approaches they consider of significance. With your help, we can tap into a wide range of experiences, develop new techniques and translate these techniques into the clinical routine of the future.

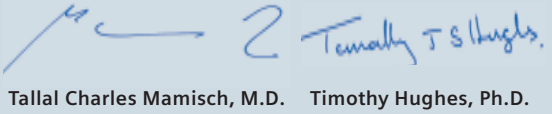

Tallal Charles Mamisch, M.D. **Timothy Hughes, Ph.D.**

Contact
mamisch@bwh.harvard.edu
timothy.hughes@siemens.com

The Editorial Team

We appreciate your comments.
Please contact us at magnetomworld.med@siemens.com

A. Nejat Bengi, M.D.
Editor in Chief

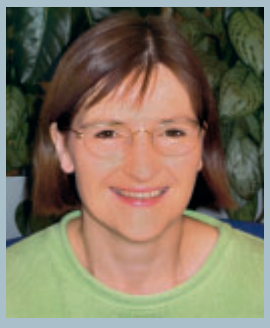

Antje Hellwich
Associate Editor

Dagmar Thomsik-Schröpfer,
Ph.D., MR Marketing-Products,
Erlangen

Cécile Mohr, Ph.D
Head of Market Segment
Management, Erlangen

Heike Weh,
Clinical Data Manager,
Erlangen

Bernhard Baden,
Clinical Data Manager,
Erlangen

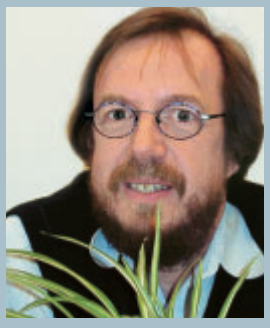

Peter Kreisler, Ph.D.
Collaborations & Applications,
Erlangen

Milind Dhamankar, M.D.
Manager Clinical MR Research
Collaborations, USA

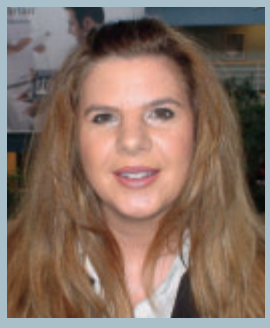

Kathleen Giannini,
US Installed Base Manager,
Malvern, PA, USA

Gary R. McNeal, MS (BME)
Advanced Application Specialist,
Cardiovascular MR Imaging
Siemens Medical Solutions USA

Dr. Sunil Kumar S.L. Manager
Applications MRI, Siemens
Medical Solutions, India

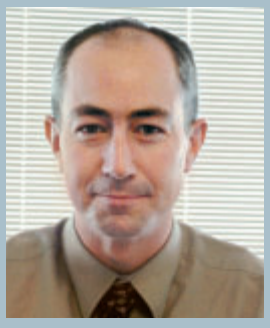

Tony Enright, Ph.D.
Asia Pacific Collaborations,
Australia

Content

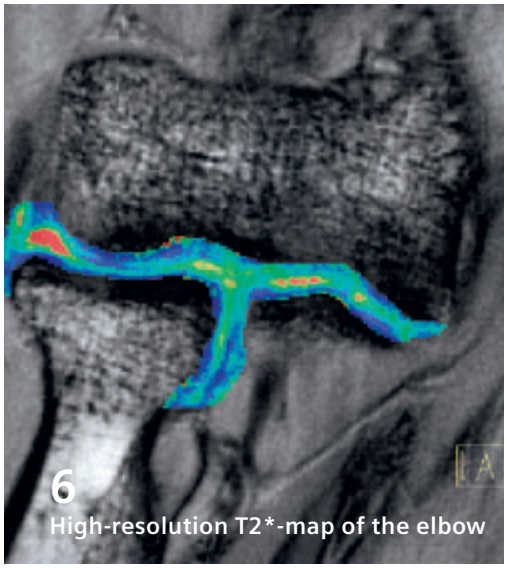

Orthopedic Imaging

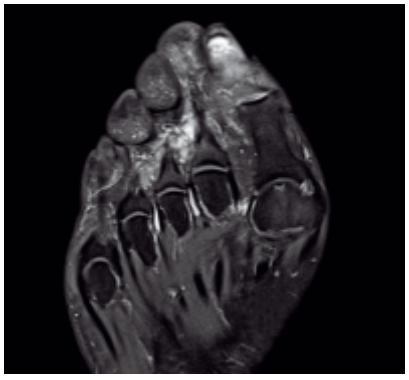

48 In this issue of MAGNETOM Flash we launch a "How I do it" section with application tips.

Clinical Orthopedic Imaging

6 Overview: Biochemical Imaging

8 Overview: High-Resolution (Fast-) Imaging

10 Overview: Isotropic 3D Imaging

14 Overview: Orthopedic Coils

18 Molecular Imaging of Articular Cartilage and Cartilage Repair

22 Delayed Gadolinium Enhanced MRI of Cartilage (dGEMRIC) in Hip Dysplasia

24 T2 Mapping of Articular Cartilage in Hip Joint

26 3D-$T_{1\rho}$-Mapping of Cartilage at 3T with integrated Parallel Imaging Technique (*syngo* GRAPPA)

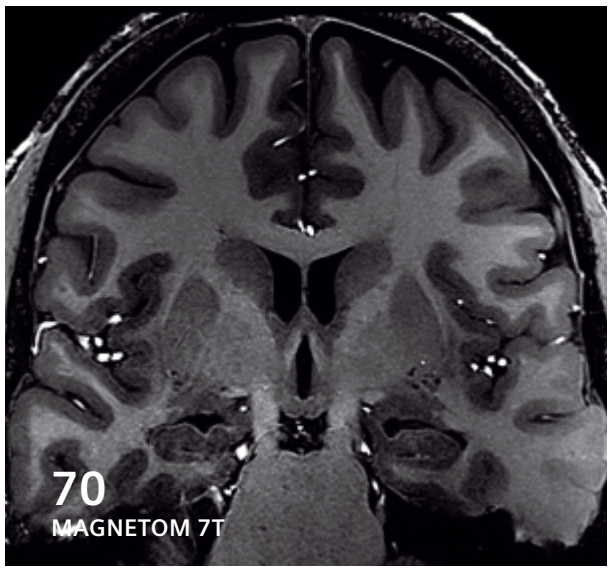

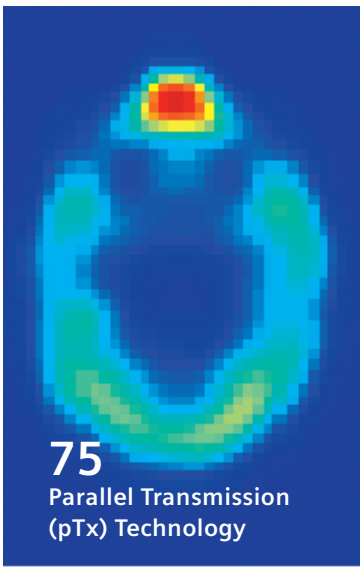

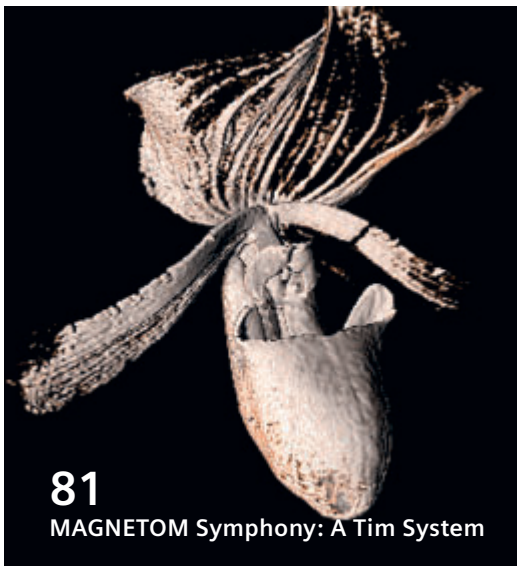

Clinical Gastro-intestinal Imaging

28 Image Gallery Orthopedic Imaging

36 Isotropic MR Arthrography of the Shoulder. Case Reports

38 MR-Arthrography of the Hip

40 Direct MR-Arthrography

42 Wrist Imaging with MAGNETOM Espree: Changing a Practice

44 Water Excitation in Musculoskeletal Low-Field MR Imaging

Orthopedic Imaging → How I do it

48 Application Hints for MR Orthopedic Imaging: The Knee Examination

50 MR Imaging of the Carpometacarpal Joint of the Thumb

52 MRI of the Forefoot

55 *syngo* REVEAL Images

56 MRI with MR Fistulogram for Perianal Fistula: A Successful Combination

Technology

61 Metamorphosis of MRI: Seamless Move-During-Scan with *syngo* TimCT

70 Pushing the Boundaries of MR with Siemens MAGNETOM 7T

75 Parallel Transmission (pTX) Technology

Product News

81 Image Gallery MAGNETOM Symphony, A Tim System

82 MAGNETOM Symphony With New Applications. Power-class with *syngo* MR A30

Life

86 Your verdict: "Great job – keep doing what you're doing!"

87 Innovations '07: Siemens Education Symposium for Medical Technologists and IT Customers

Biochemical Imaging

Besides improvements in morphological imaging, the ability to assess and quantify biomarkers is increasingly important in MSK imaging. The use of biochemical imaging instead of morphological imaging is gaining importance as a means of both improving accuracy of diagnosis and of planning and monitoring the effectiveness of therapy.
Based on the different biomarkers, there are several approaches to biochemical imaging described and used for clinical imaging. The different biomarkers can be obtained by contrast and non-contrast examination techniques resulting in T1-, T2- and T2*-maps. Thanks to *syngo* MapIt today it is possible to obtain parametric mapping results automatically. *syngo* MapIt can be used fro all joints in the body (Figs. 1–5). All of the images were prepared within the *syngo* environment from maps which were created automatically, using Inline Technology. These maps can then be retrieved and post-processed using any of the standard *syngo* tools, such as Region of Interest (ROI), pixel lens, etc. Furthermore, it is possible to use *syngo* Fusion to overlay these maps with their corresponding anatomical image and to conduct manual carti-

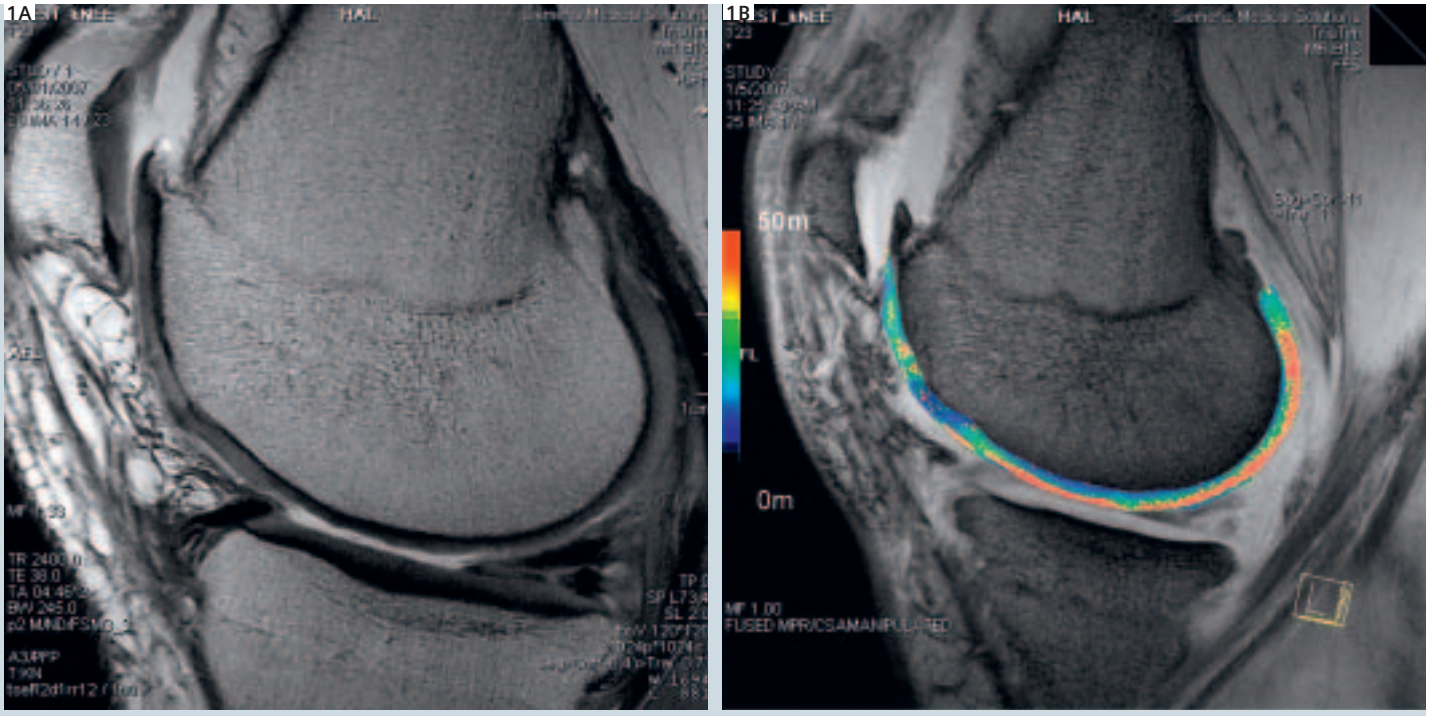

1 Example of a high in-plane resolution (0.3 x 0.3 x 2 mm) protondensity-weighted (PD) TSE image and the corresponding biochemical (T2*) high-resolution image in a patient with cartilage lesion.

lage segmentation. There is now no need to transfer any data offline, as everything can be accomplished on the measurement console.
It is also necessary to expand the biochemical imaging capabilities. To this end new sequence techniques are being examined to evaluate the cartilage. One of the most promising candidates for this is Steady State Free Procession (SSFP) diffusion imaging using a PSIF sequence, with of course Inline mapping. An alternative approach is to use Echo Planar Imaging (EPI) diffusion which has also delivered good results making advanced techniques such as tensor imaging possible. First examples of the use of SSFP diffusion are shown in Fig. 5 in a patient with cartilage degeneration in comparison to a T2-mapping.

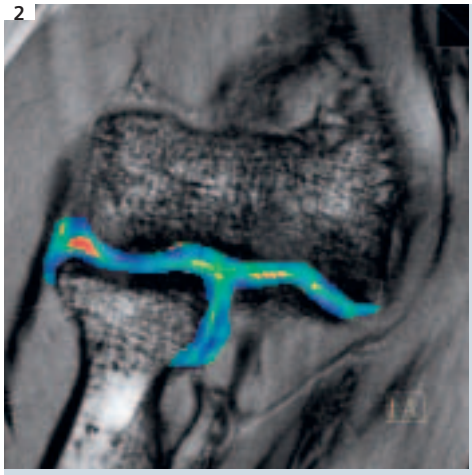

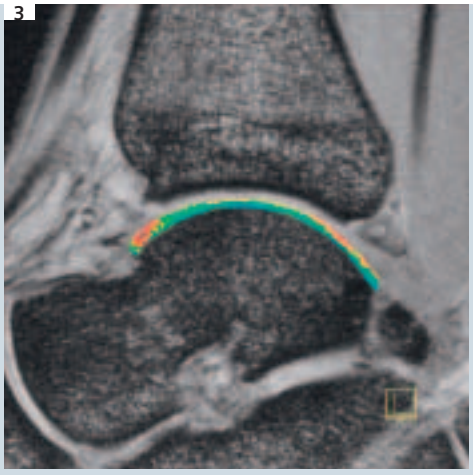

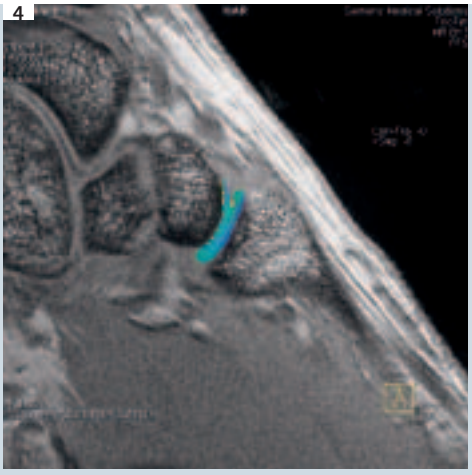

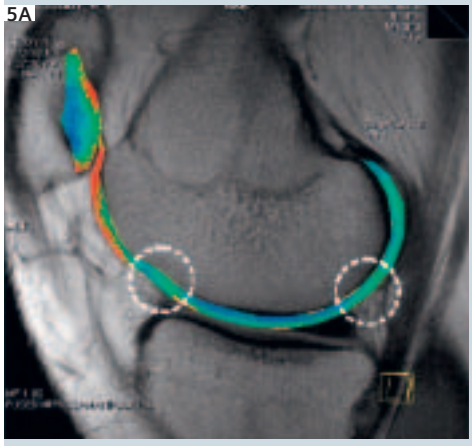

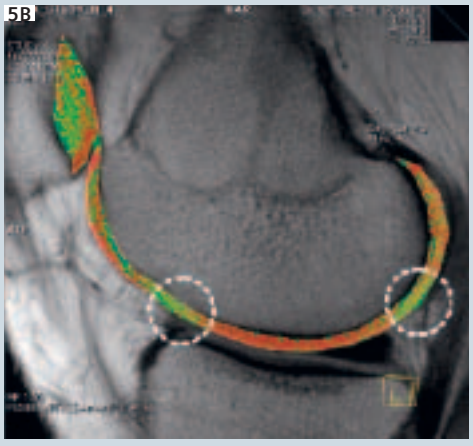

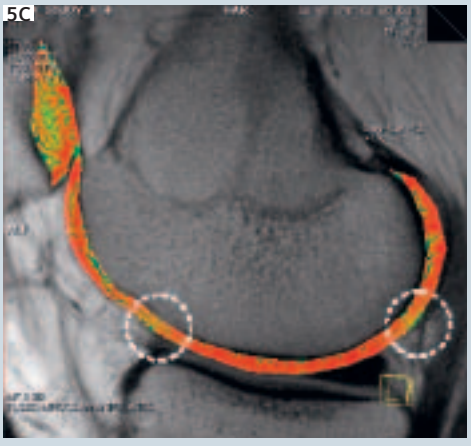

2 **Elbow imaging with the small flex coil. High-resolution T2*-map.**

3 **The 8-channel foot-ankle coil is used to produce high-resolution T2* cartilage mapping at 3T (0.3 x 0.2 x 2 mm) under load restriction over time.**

Courtesy of Prof. Siegfried Trattnig, Medical University Vienna, Austria

4 **T1-mapping in the carpometacarpal (CMC) joint for diagnosis of rheumatoid arthritis.**

5 **A–C: Comparison of a T2-mapping (4A) with the diffusion map in read (4C) and phase (4B) direction (qualitative mapping based on SSFP diffusion sequence).**

High-Resolution (Fast-) Imaging

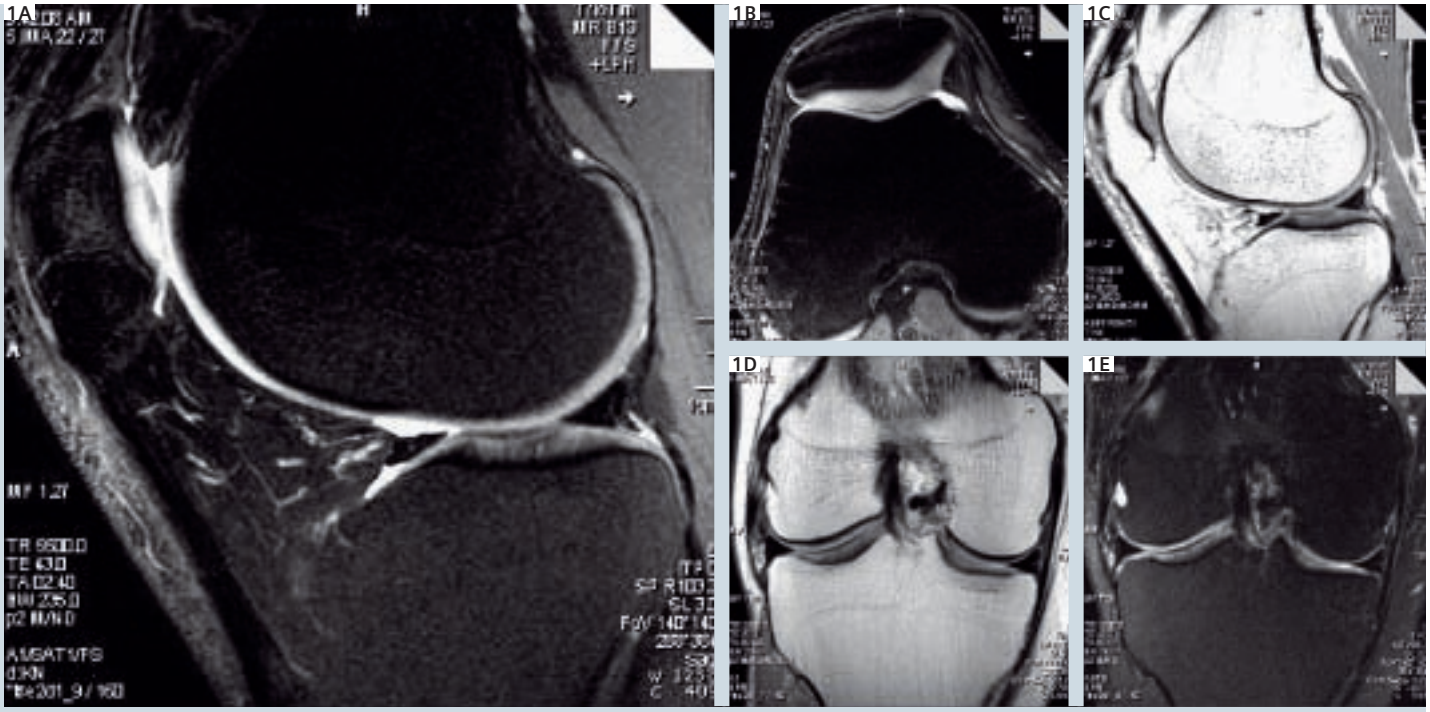

1 **A series of five high-resolution examinations of the knee completed in under 15 minutes. Sequences used:**
A: Sagittal protondensity-weighted Turbo Spin Echo (TSE) image with fat saturation (fatsat), 512 matrix.
B: Axial T2-weighted image with fatsat, 512 matrix.
C: Sagittal T1-weighted image, 512 matrix.
D: Coronal T1-weighted image, 512 matrix.
E: Coronal protondensity-weighted TSE image with fatsat, 512 matrix.

The first goal to achieve in musculoskeletal (MSK) imaging is a high resolution with the necessary contrast for precise detection of the small and complex structures of the MSK system. This requirement leads to the use of Turbo Spin Echo (TSE) sequences optimized for maximum matrix size and small FoV.
Beside more accurate diagnosis there is also a competing requirement for increased throughput. Due to lower reimbursements, a study must be optimized to allow for a total MSK joint study within 15 to 30 minutes. Fig. 1 shows an example of a standard knee study consisting of 5 series using an 8-channel knee coil (Invivo, Latham, NY, USA) and integrated Parallel Imaging Technique (iPAT), with a PAT factor of 2. Total scan time is just under 15 minutes for these high-resolution images.
This optimization has taken the form of more efficient utilization of the imaging gradients coupled with a flexible reordering scheme and parallel imaging techniques.
The new reordering techniques for TSE sequences allow a more flexible choice of TE to allow better optimization of protocols so as to maintain image contrast whilst using longer echo train lengths.
The advantages of this new sequence are shown in Fig. 2. In (A–D) the length of the echo train is increased thus decreasing the scan time from 4 min to 80 s and with the new enhanced sequence the TE can be kept constant resulting in similar contrast properties between the 4 images. Furthermore even numbered Echo Train Lengths (ETLs) are now possible. In (E–H) the TE has been varied to allow for different contrasts. As can be seen, the TSE sequence is now completely flexible and can be configured in any manner.
By using these new sequences coupled with clinical 3T machines and dedicated MSK coils, it is possible to achieve a new level in accurate clinical diagnosis as demonstrated in Fig. 3 where a cartilage delamination in a patient with femoro-acetabular impingement is diagnosed with the help of a non-contrast protondensity (PD)-weighted TSE high-resolution scan (0.3 x 0.3 x 3 mm) with fat suppression.

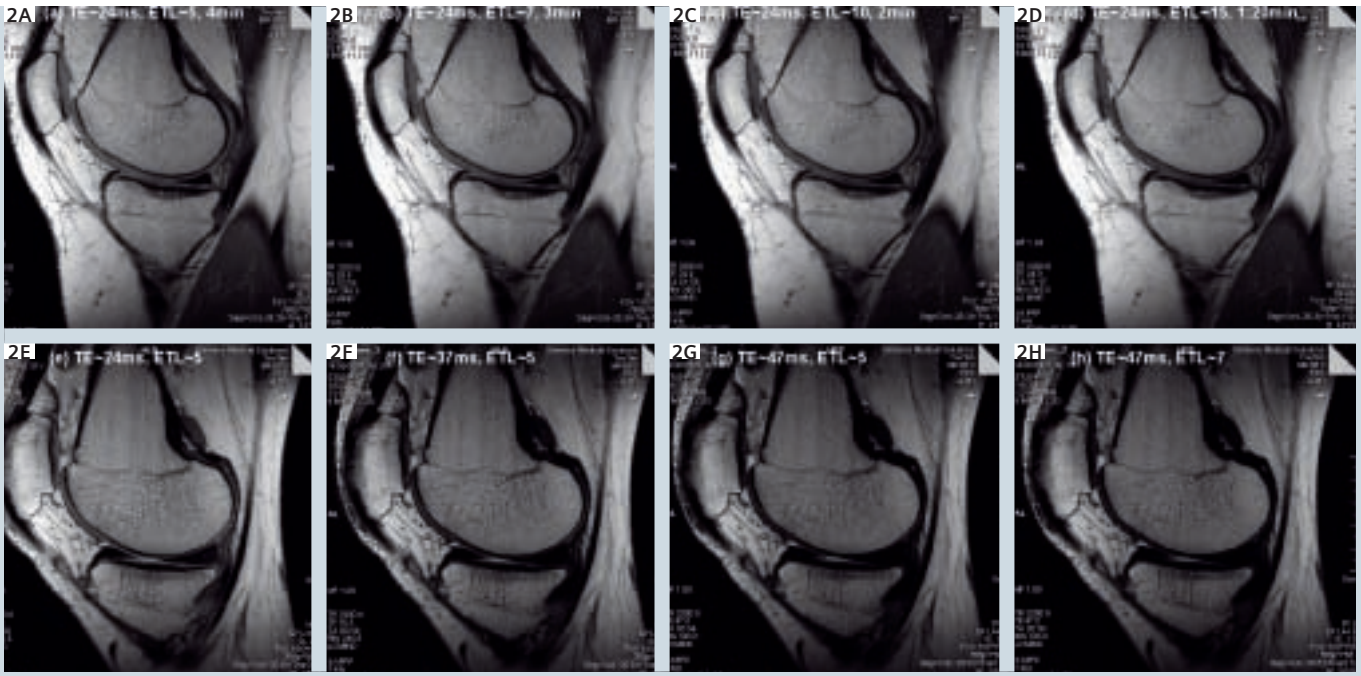

2 The enhanced flexibility of the TSE sequence is demonstrated within this series where in (A–D) scan time has been reduced from 4 min to 80 s. In the second row (E–H) the ability to select intermediate echo times is shown.

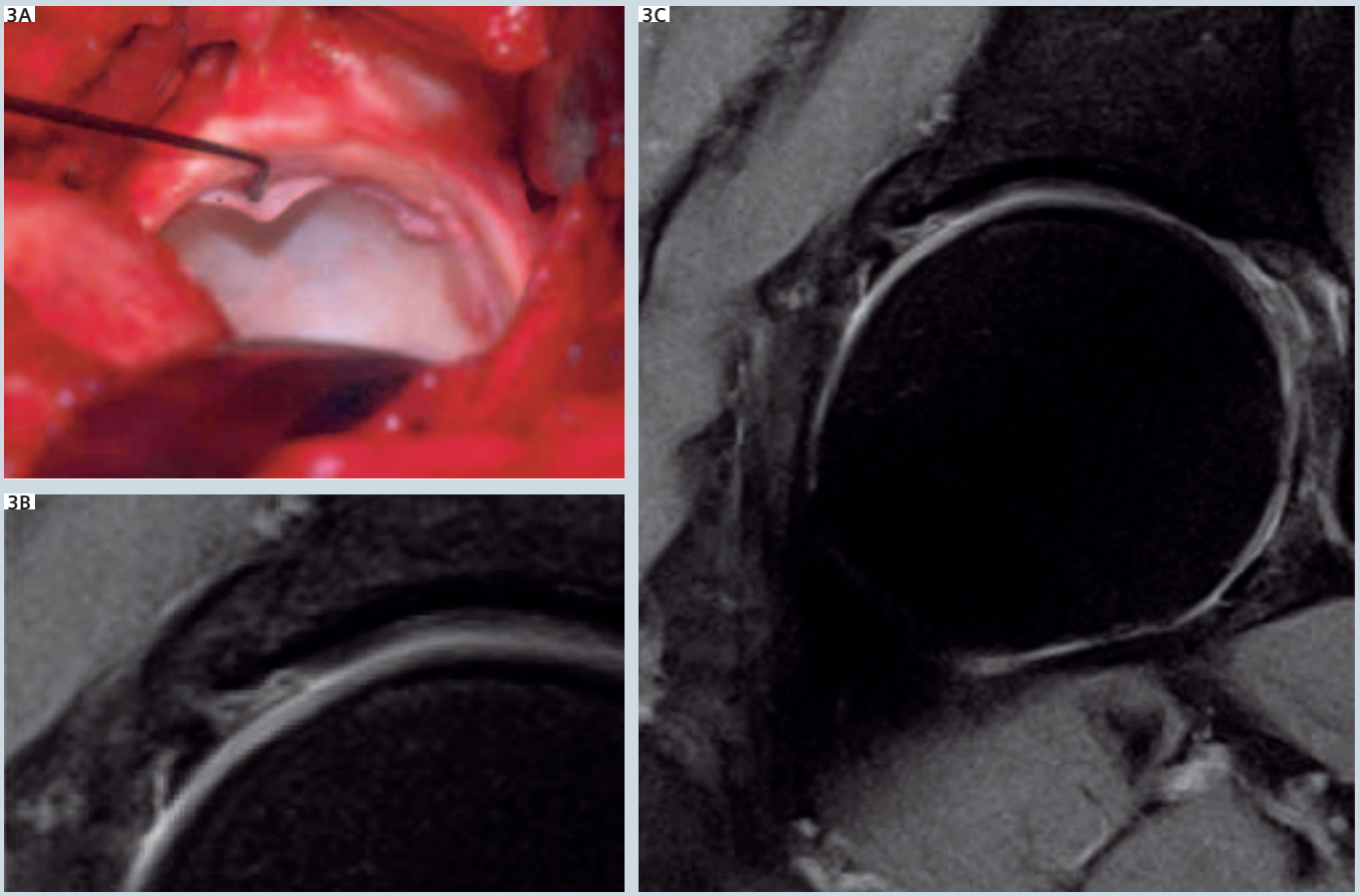

3 A–C High in-plane resolution (0.3 x 0.3 x 3 mm) image (fat suppressed PD-weighted TSE) of a cartilage flap in the hip joint. Patient with femoro-acetabular impingement.

Courtesy of T. C. Mamisch, University Bern, Switzerland.

Isotropic 3D Imaging

High-resolution, sub-millimeter, fast 3D isotropic imaging is becoming increasingly important as a means of enhancing workflow and providing more accurate diagnosis.

The philosophy behind this innovation is that 3D imaging allows total flexibility of examination i.e. by reformatting the joint can be examined in any plane.

The advantages associated with this new philosophy can be summarized as follows:

- Spatial localized diagnosis of the meniscus. Current research emphasizes the role of a more precise diagnosis of the localization of the meniscal injury for the possibility of applying different therapy concepts. In addition, in terms of monitoring of the meniscus after injury and therapy a reproducible localization is necessary.
- Accurate diagnosis of the cruciate ligaments requires angulations of the diagnostic plane to the position of the ligament within the joint. This can be done in a reproducible manner using the isotropic sequence as shown in Fig. 2.
- Diagnosis of cartilage damage or monitoring of cartilage therapy requires accurate determination of the spatial extent of the cartilage lesion or repair tissue. Using International Clinical Scoring Systems for accurate diagnosis requires reproducible and spatially accurate imaging data. This can be achieved with isotropic sequences which allow flexible and accurate reformatting along well defined diagnostic planes.

These examples summarize how isotropic sequences enable the accurate diagnosis of internal structures such as cartilage, meniscus and ligaments based on free angulations reconstruction. Through the use of an isotropic 3D sequence these areas can be reformatted in a reproducible way with a high resolution. This provides further workflow improvements by acquiring one 3D sequence that can be reformatted in the different planes needed for precise diagnosis.

Another example is an anatomical complex situation such as in the hip joint, where different angulations based on anatomical landmarks are necessary for precise diagnosis. By using an isotropic sequence as shown in Figure 5, these reconstructions can be done within one scan.

Recent developments in 3D sequences allow different contrasts to be achieved i.e. using DESS (Dual Echo Steady State), MEDIC (Multi-Echo Data Image Combination), VIBE (Volume Interpolated Breath-hold Examination) and TrueFISP. Most interesting is the capability now to achieve 3D TSE contrast with high signal-to-noise ratio using SPACE (Sampling Perfection with Application optimized Contrasts using different flip angle Evolutions) with long echo trains within a reasonable imaging time.

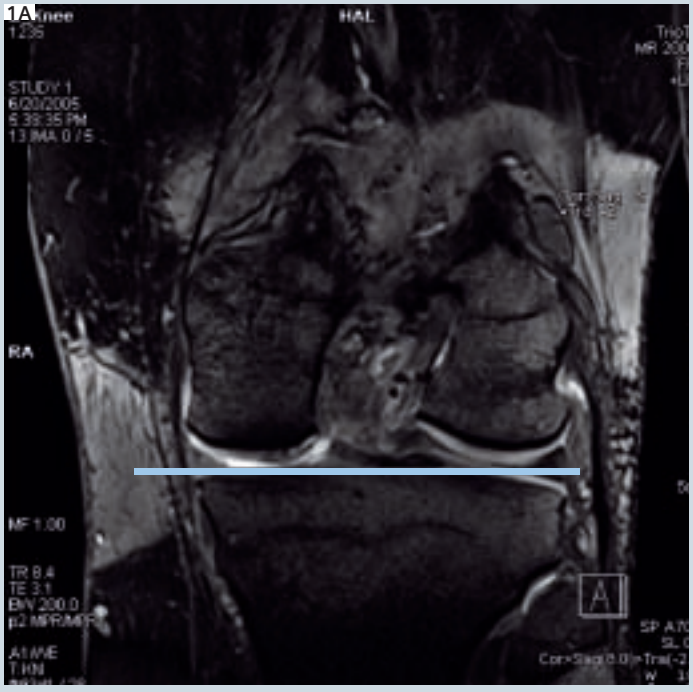

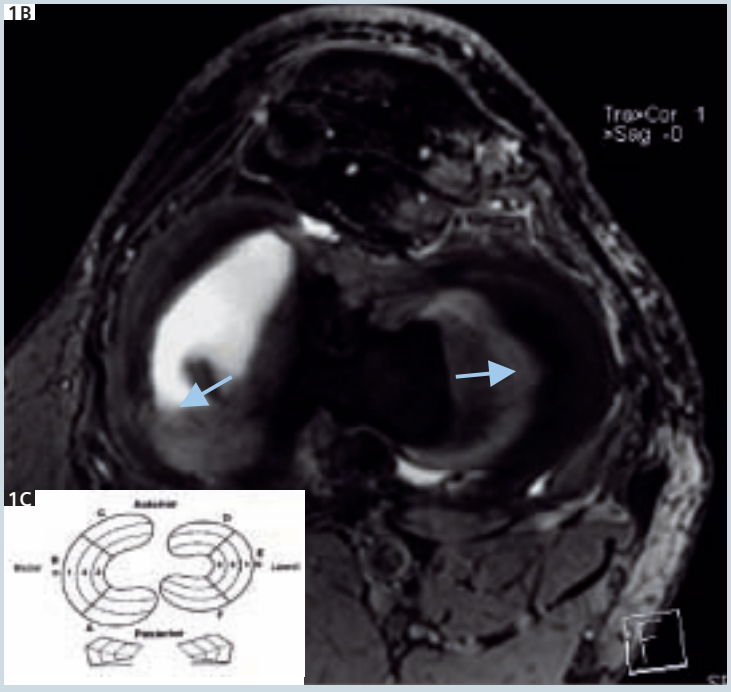

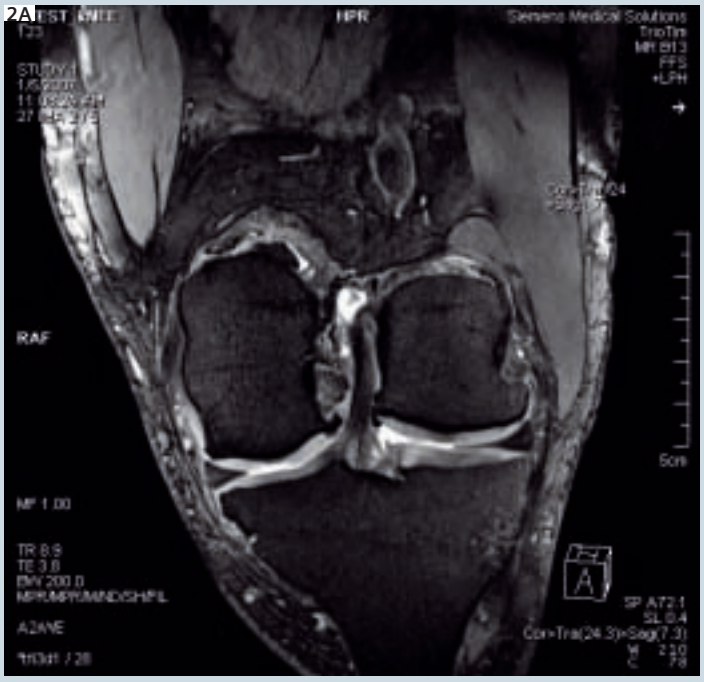

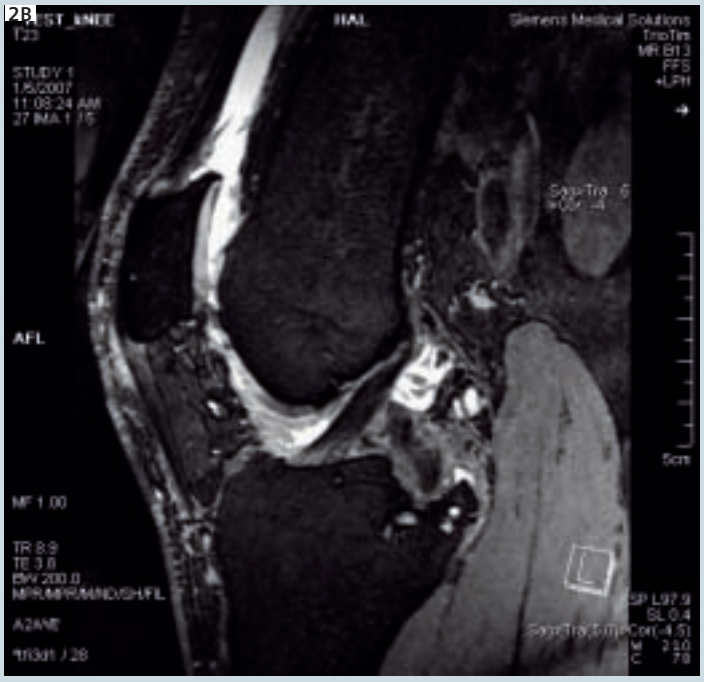

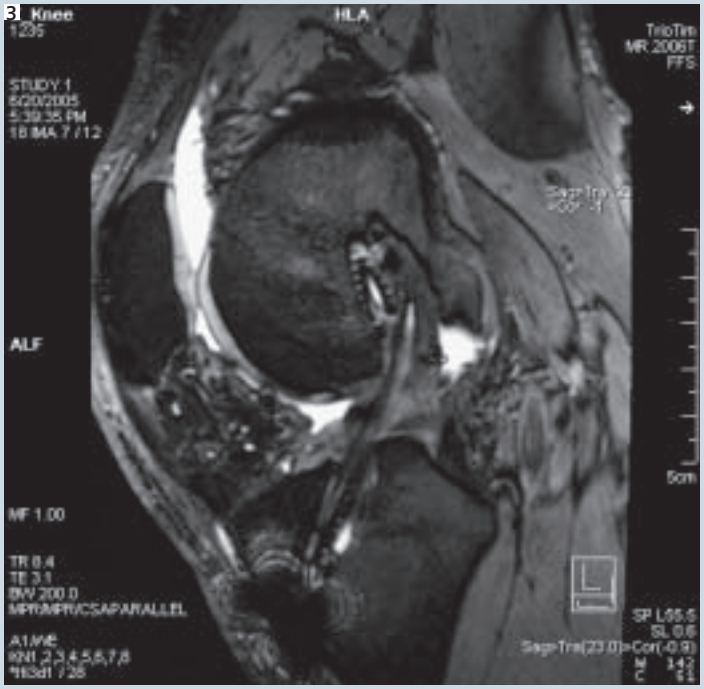

1 **A–C: Example of patient after partial lateral meniscal resection after trauma. Oblique axial plane reconstruction of the meniscus for precise localization for follow up and diagnosis.**

2 **A, B: Visualization of the anterior cruciate ligament oblique coronal and sagittal based on a 3D TrueFISP (isotropic resolution 0.4 x 0.4 x 0.4 mm).**

3 **Visualization after replacement of anterior cruciate ligament for monitoring of therapy.**

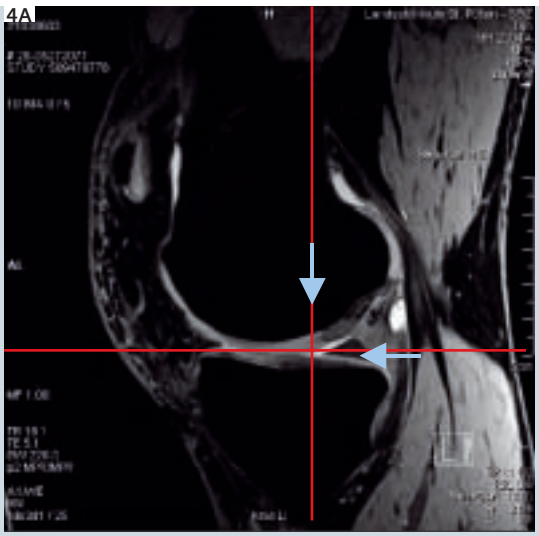

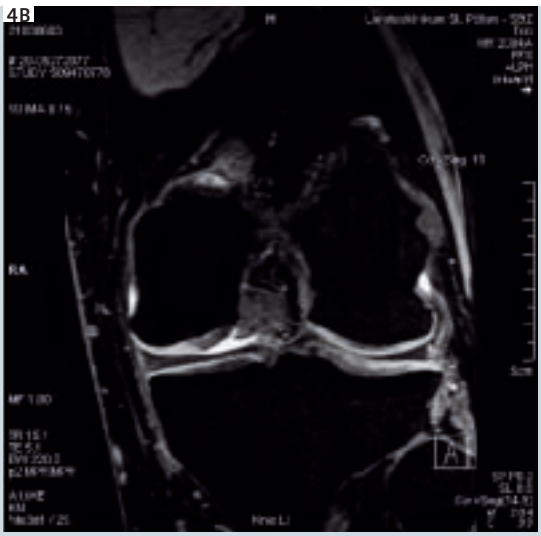

4 A–D: 3D TrueFISP of patient with cartilage repair procedure (matrix-associated autologous chondrocyte transplantation – MACT technique). Reconstruction of ana tomical image planes for localization of the damaged tissue based on classification cartilage repair society scheme (Fig. 4D).

Courtesy: Siegfried Trattnig M.D., Medical University of Vienna, Austria

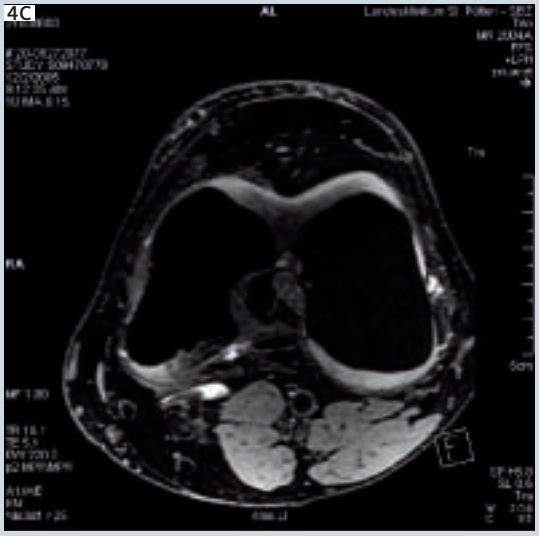

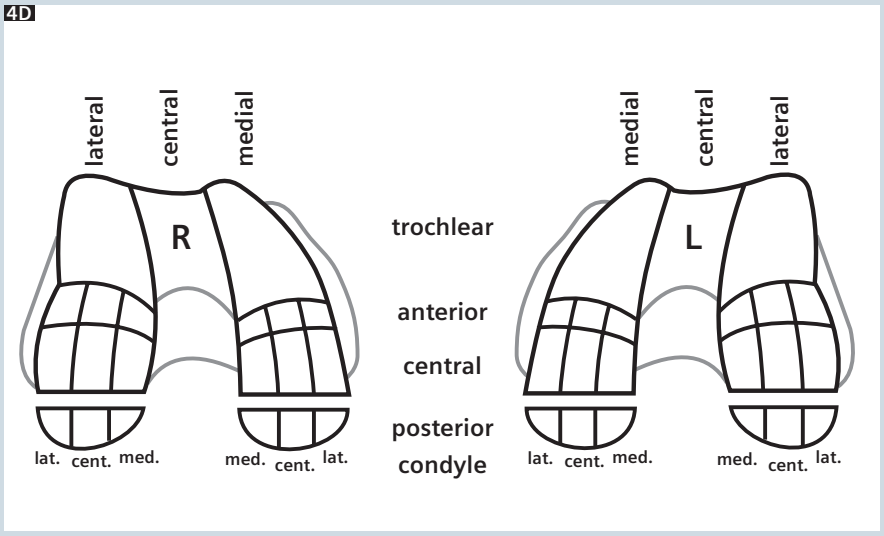

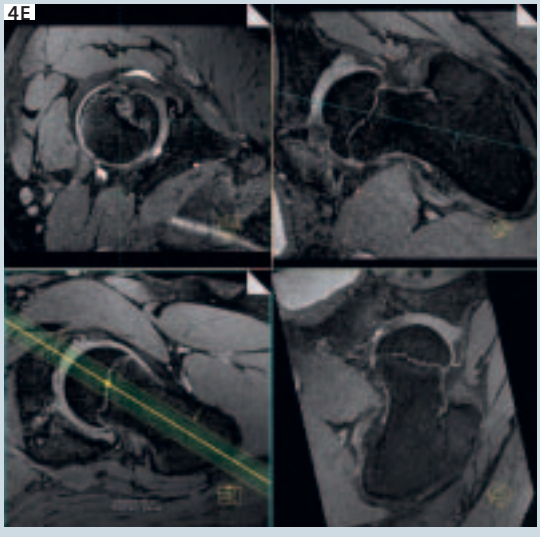

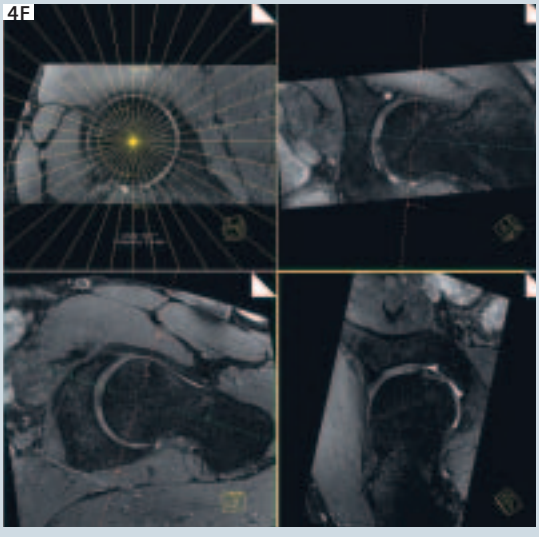

4 E–F: Hip joint evaluated from different angles with the help of isotropic imaging.
E: Oblique coronal.
F: Radial reconstruction for the assessment of labrum and cartilage morphology.

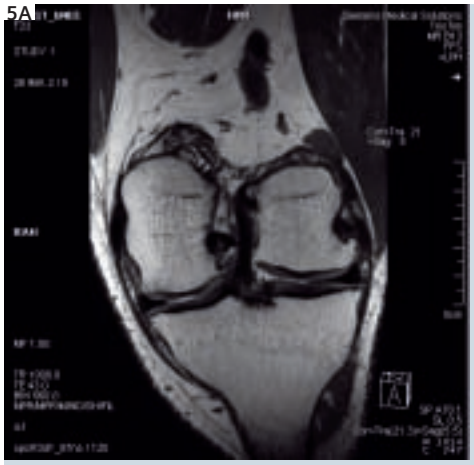

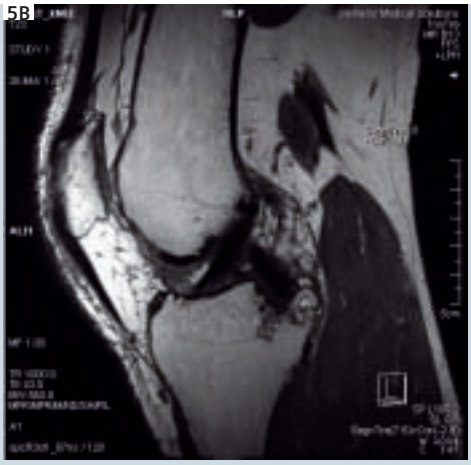

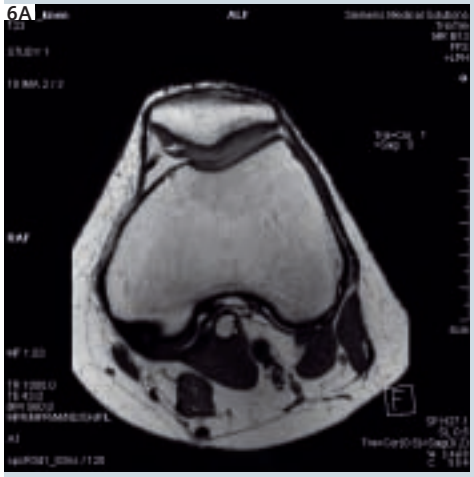

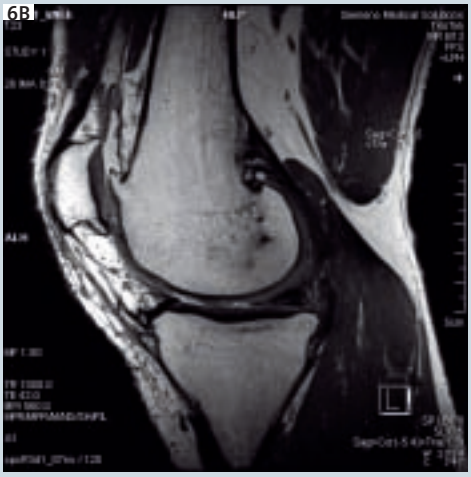

5 6 **Figures 5 and 6 show the cruciate ligament and a cartilage diagnostic view angulated based on a 3D PD-weighted SPACE sequence (0.6 x 0.6 x 0.6 mm isotropic resolution).**

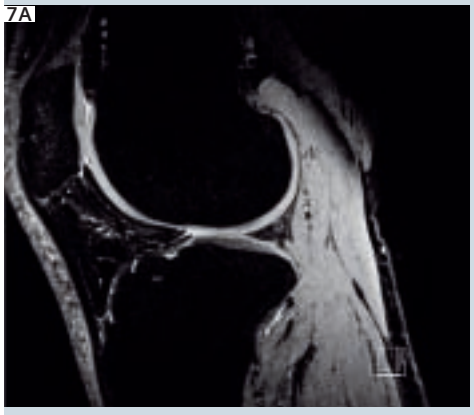

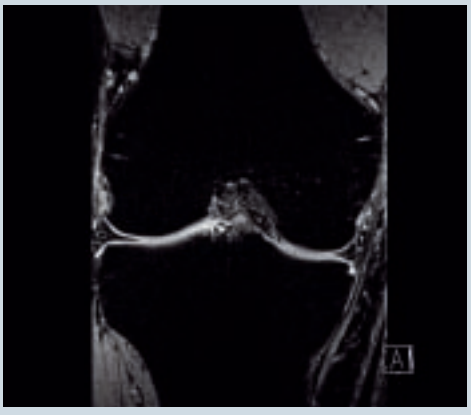

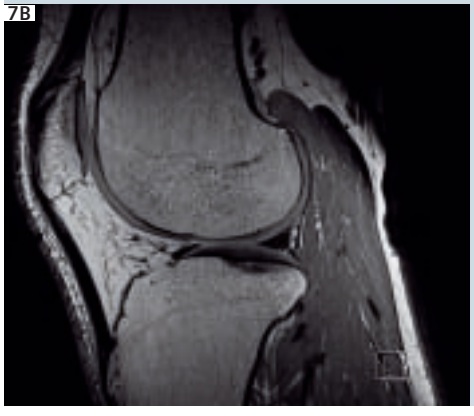

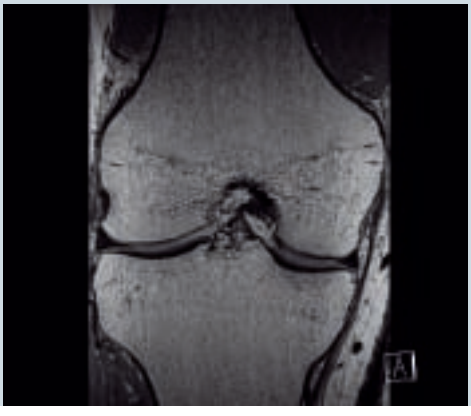

7 **A–B: Protondensity-weighted SPACE sequence with (A) and without (B) SPAIR fat suppression.**

Orthopedic Coils

The advances in resolution, image quality, workflow, scan speed and availability of new imaging techniques (biochemical) are made possible with Tim technology (Total imaging matrix) and are also due to orthopedic imaging dedicated phased array coils supported by Siemens MAGNETOM MR systems. These coils provide high signal-to-noise ratio (SNR), are compatible with parallel imaging techniques and allow comfortable imaging of all musculoskeletal relevant anatomical areas.

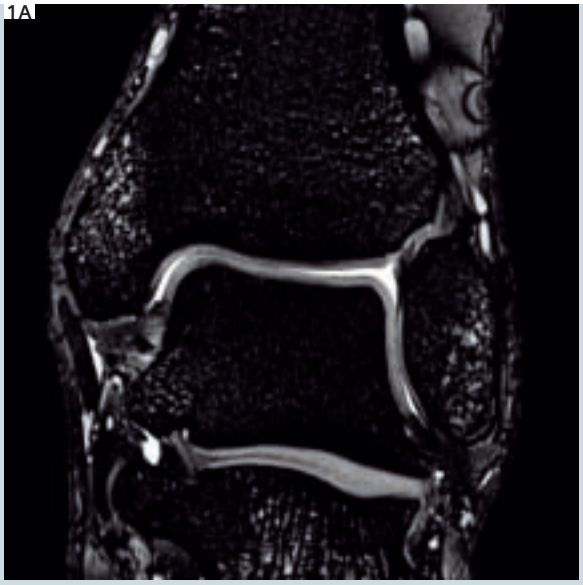

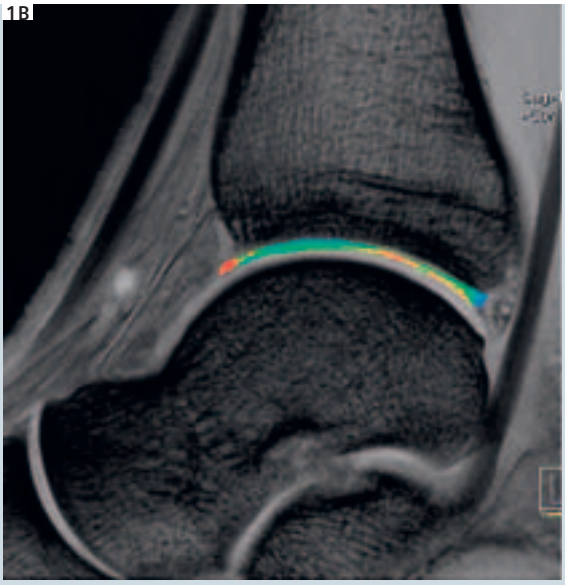

1 Figure 1 shows images of an ankle, using an 8-channel coil (Invivo 8-channel foot/ankle).

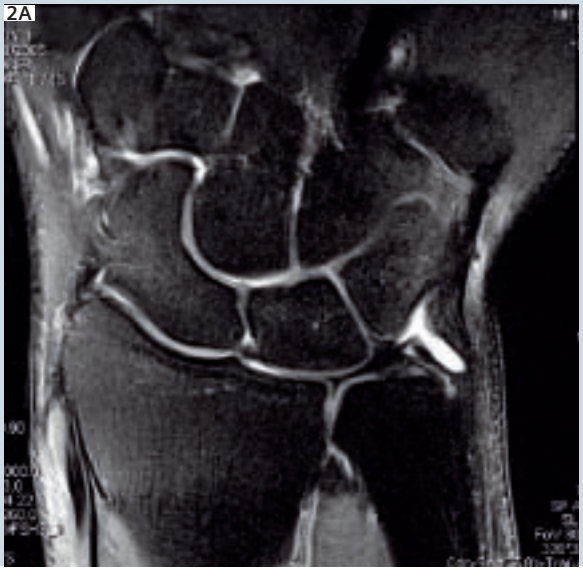

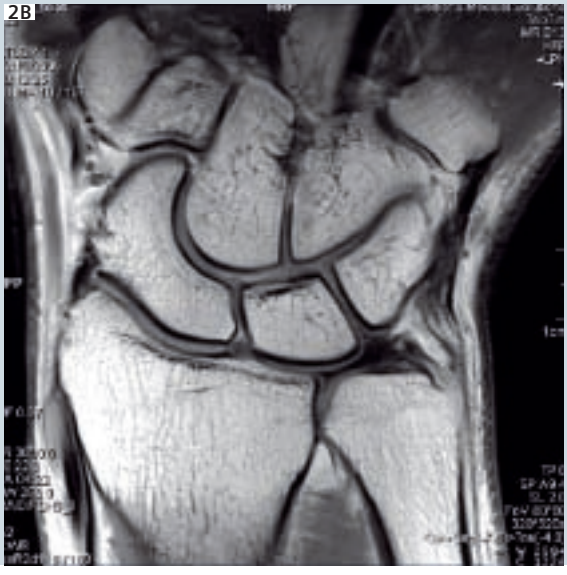

2 Figure 2 shows images of a wrist, using an 8-channel wrist coil (Invivo 8-channel wrist). Protondensity-weighted image with (A) and without (B) fat suppression (FS). FoV 8 cm, matrix 320, 0.26 x 0.26 x 2 mm. Also available are an 8-channel knee coil and a 4-channel shoulder coil (Invivo).

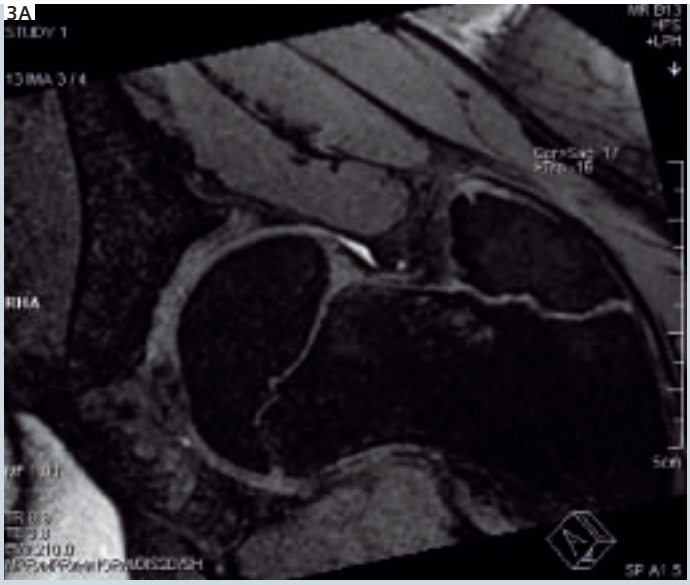

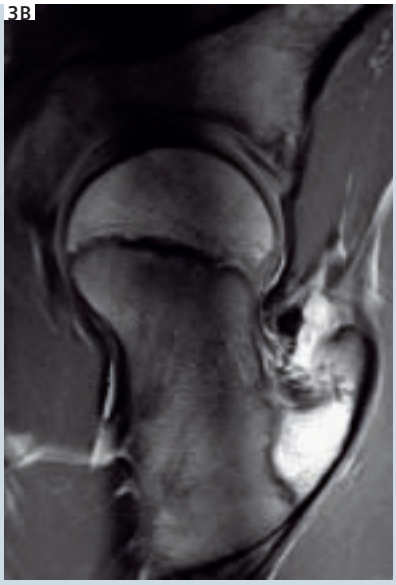

3 Figure 3 shows CP flex coil used for pediatric imaging of the hip joint. Flex coils large and small can also be used to image the elbow (Fig.4).

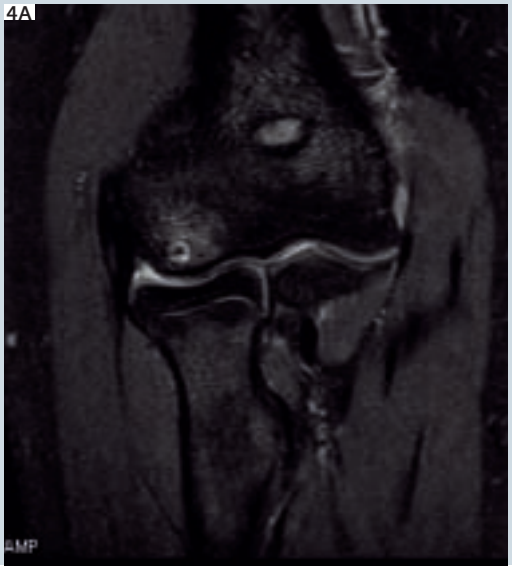

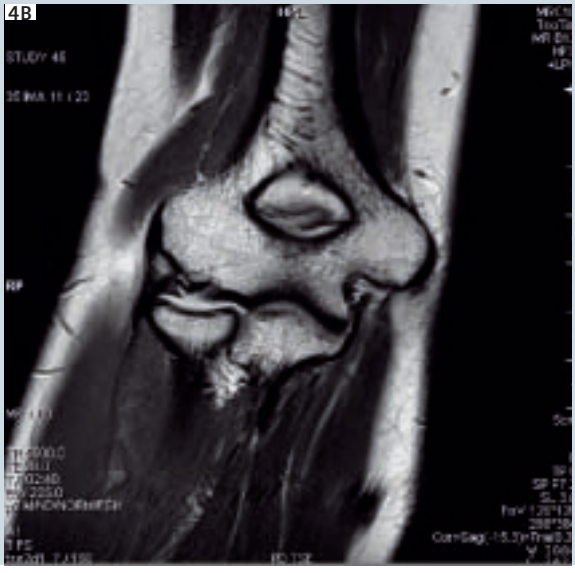

4 Elbow imaging with the small flex coil.Protondensity-weighted TSE image with (A) and without (B) fat sat.

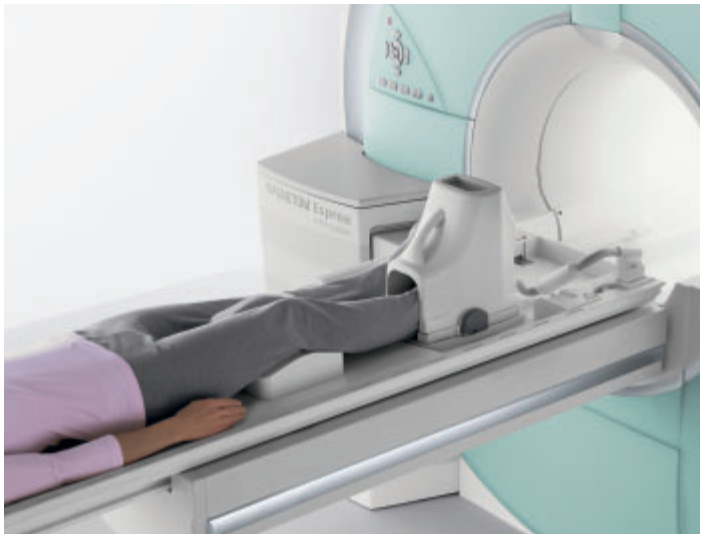

8-channel foot/ankle coil.

8-channel wrist coil.

CP extremity coil (send and receive).

1.5T 4-channel flex coil small.

4-channel flex coil large.

8-channel knee coil.

Proven Outcomes in Magnetic Resonance.

Get ready for T-class, the next generation of MRI. With *syngo*® TimCT™ – Continuous Table move – the new MAGNETOM® T-class shifts the paradigm to CT-like scanning. No stops. Just continuous scanning. And not a single second wasted. Powered by Tim®, T-class combines increased diagnostic confidence with dramatically increased throughput. Find out more at our website. And see for yourself why at Siemens, the innovation never stops.

SIEMENS
medical

MR-Z998-2-7600

Molecular Imaging of Articular Cartilage and Cartilage Repair

Siegfried Trattnig, M.D.[1]; Götz Welsch, M.D.[2]; Stefan Marlovits, M.D.[3]; Tallal Charles Mamisch, M.D.[4]

[1]*Department of Radiology, Medical University of Vienna, Austria*
[2]*Department of Radiology, AKH Vienna, Austria*
[3]*Department of Trauma Surgery, AKH Vienna, Austria*
[4]*Inselspital, University Bern, Switzerland*

MR imaging of the morphology of cartilage and cartilage repair tissue has significantly improved in recent years due to the development of clinical high-field MR systems operating at 3 Tesla. The improved performance has also been achieved as a result of the higher gradient strengths and the application of dedicated coils with modern configuration, such as phased array coils. The combination of these technological advances now allows high-resolution imaging of cartilage within reasonable scan times. In addition to the evaluation of gross cartilage morphology by MRI, there is growing interest in the visualization of ultra small structural components of cartilage by MR in two fields:

1. Osteoarthritis is manifested by significant changes in biochemical composition of articular cartilage. Loss of glycosaminoglycans (GAG) and increased water content represent the earliest stage of cartilage degeneration, while the collagenous component of the extracellular matrix remains mainly intact during this early phase of cartilage degeneration [1].

2. During recent years many new cartilage surgical techniques have been developed based on tissue engineering techniques such as autologous chondrocyte implantation (ACI) and matrix-associated autologous chondrocyte transplantation (MACT).

In addition to morphological MR imaging of cartilage repair tissue, an advanced method for non-invasively and quantitatively monitoring parameters reflecting the biochemical status of cartilage repair tissue is a necessity for studies which seek to elucidate the natural maturation of MACT grafts and the efficacy of the technique. Therefore, several MR techniques have been developed which allow detection of biochemical changes that precede the morphological degeneration in cartilage:

Delayed gadolinium-enhanced MRI of cartilage (dGEMRIC) [2]

Based on the fact that GAG molecules contain negatively charged side chains which lead an inverse proportionality in the distribution of the negatively charged contrast agent molecules. Consequently, T1 which is determined by the Gd-DTPA2-concentration becomes a specific measure of tissue GAG concentration. The dGEMRIC technique has provided valuable results in studies on hip dysplasia, in comparative studies with arthroscopically determined cartilage softening in early osteoarthritis, and demonstrated the positive effects of moderate exercise on glycosaminoglycan content in knee cartilage [3]. However there are two main problems, firstly the standard dGEMRIC technique is either limited to single slices in 2D acquisition or is time consuming in 3D sequences such as 3D inversion recovery prepared fast spoiled gradient recalled acquisition in the steady state. This therefore limits the attractiveness of dGEMRIC for clinical use. The second problem with dGEMRIC is more specific to cartilage repair tissue. Previous clinical studies of early cartilage degeneration showed that the differences in the pre-contrast T1 values between degenerative cartilage and normal cartilage were so small that they could be ignored [4]; however, this is not true for cartilage repair tissue. For a correct evaluation of glycosaminoglycan concentration in cartilage repair tissue, the pre-contrast T1 values also have to be calculated [4]. If a quantitative T1 analysis is also performed prior to contrast administration, it is possible to calculate the concentration of Gd-DTPA in the cartilage. The concentration is represented by Δ R1, the difference in relaxation rate (R1 = 1/T1) between T1 pre-contrast and T1 post-contrast. This places time limitation problems on the patient evaluation since both pre-contrast MR imaging and delayed post-contrast MR imaging must be performed in cartilage repair patients. To overcome these problems we used fast T1 determination by using different excitation flip angle values in gradient echo based sequences. For the follow-up of cartilage implants, quantitative T1-mapping based on a 3D GRE sequence, Volume Interpolated Breath-hold Examination (VIBE), with a TR 50 ms, TE 3.67 ms, flip angle 35/10°, a field of view (FoV) of 183 x 200 mm and a matrix size of 317 x 384 was performed, resulting in a resolution in plane of 0.6 x 0.5 mm with an effective slice thickness of 1 mm. The scan time was 6 min 53 s. The repetition time of 50 ms was chosen as a compromise between signal-to-noise ratio (SNR) and the reduction of any slice profile effects. The flip angle combination of 35°–10° proved to be the best compromise for obtaining reliable T1 values in the long range of T1 values present in the pre-contrast repair tissue (800–1200 ms) as well as in the short range of T1 values seen in post-contrast repair tissue (300–500 ms) as demonstrated by a good correlation with inversion recovery sequence in both T1 value ranges in the phantom study. In the in vivo part of this study we have shown that it is feasible to apply this 3D variable flip angle dGEMRIC technique in patients following MACT surgery in clinically acceptable scan times as a way to obtain information related to the long-term development and maturation of

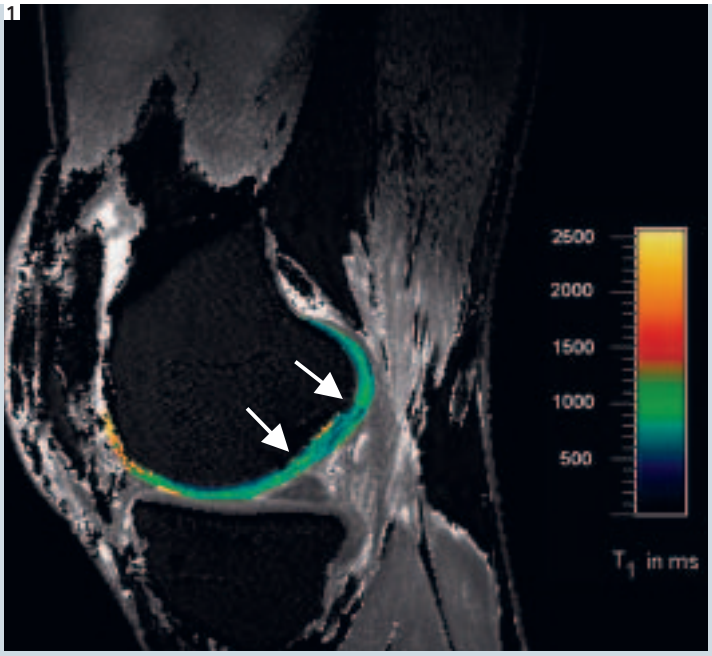

1 **Pre-contrast.** **Image of T2-map shows the pseudo-colour T2 values distribution within MACT. Corresponding T2 values are shown in the color-bar. Transplant cartilage shows higher T2 values, compared to the hyaline cartilage reference. The MR measurement was conducted 5 months after the surgery. White arrows mark the borders of the cartilage transplant.**

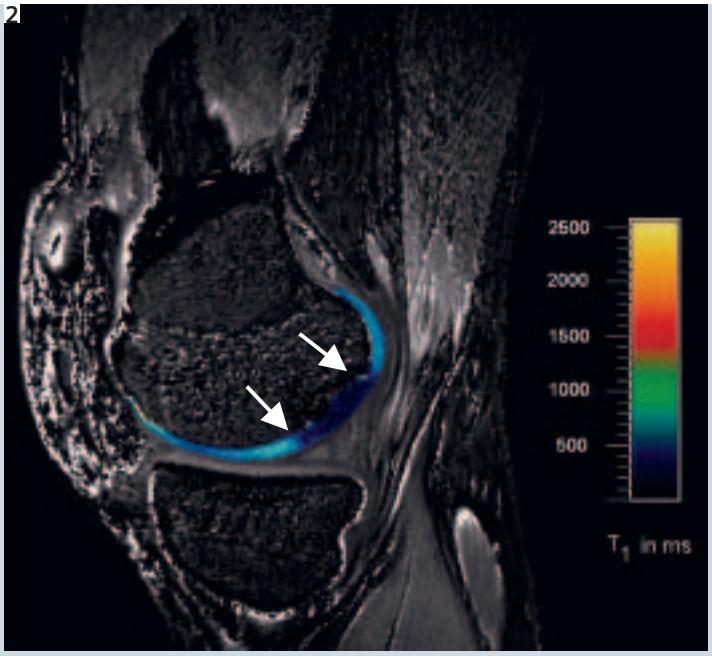

2 **Post-contrast.** **Figure shows color coded cartilage transplant post-contrast T1-map. This figure shows contrast enhancement of cartilage transplant after i.v. administration of contrast agent. White arrows mark the borders of the transplant.**

grafts. Thus, we found that the GAG content is significantly lower in repair tissue than in normal hyaline cartilage and does not change even after 3 to 4 years.
While GAG content reflects stiffness properties of repair tissue, the organisation of the collagen matrix in repair tissue over time is important too, as failure within the collageneous fibre network is considered to entail further cartilage breakdown.

Quantitative T2-mapping

Reported to be sensitive to collagen content and organization. In our examinations the T2 relaxation times were obtained from T2-maps reconstructed using a multi-echo spin echo (SE) measurement with a repetition time (TR) of 1.650 s and six echo times (TE) of 12.9 ms, 25.8 ms, 38.7 ms, 51.6 ms, 65.5 ms and 77.4 ms. Field of View (FoV) was 200 x 200 mm, pixel matrix 320 x 320 and voxel size of 0.63 x 0.63 x 1 mm. Using quantitative T2-mapping of patients at different post operative intervals after MACT surgery, we found significantly higher T2 values in cartilage repair tissue in the early stage (3–6 months) compared to native hyaline cartilage. Furthermore, we found a decrease in repair tissue T2 values over time with the T2 values becoming similar to native healthy cartilage by approximately one year. One encouraging alternative to these sequence modalities for the evaluation of cartilage microstructure is the use of DWI.

DWI: Diffusion-weighted sequences [8]

Diffusion-Weighted Imaging (DWI) is based on molecular motion that is influenced by intra- and extra-cellular barriers. Consequently, it is possible, by measuring the molecular movement, to reflect biochemical structure and architecture of the tissue. Conventional DWI based on spin-echo (SE) sequences is relatively insensitive to susceptibility effects, but diffusion-weighted SE sequences require a long acquisition time which, for practical reasons, in a clinical examination is inapplicable. Echo planar imaging (EPI)-based diffusion sequences, the gold standard of DWI in neuro applications, suffer from image distortions due to susceptibility changes as well as from limitations in contrast due to the rather long echo times needed. Both render them impracticable for low T2 tissues like cartilage and muscles. Alternatively, diffusion imaging can be based on steady state free precession sequences (SSFP) which realize a diffusion weighting in relatively short echo times. This is achieved by the application of a mono-polar diffusion sensitizing gradient which, under steady state conditions, leads to a diffusion weighting of consecutive echoes (spin

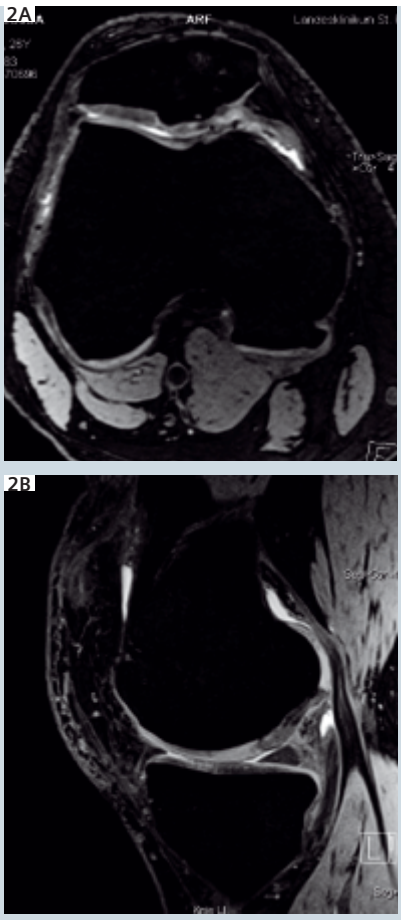

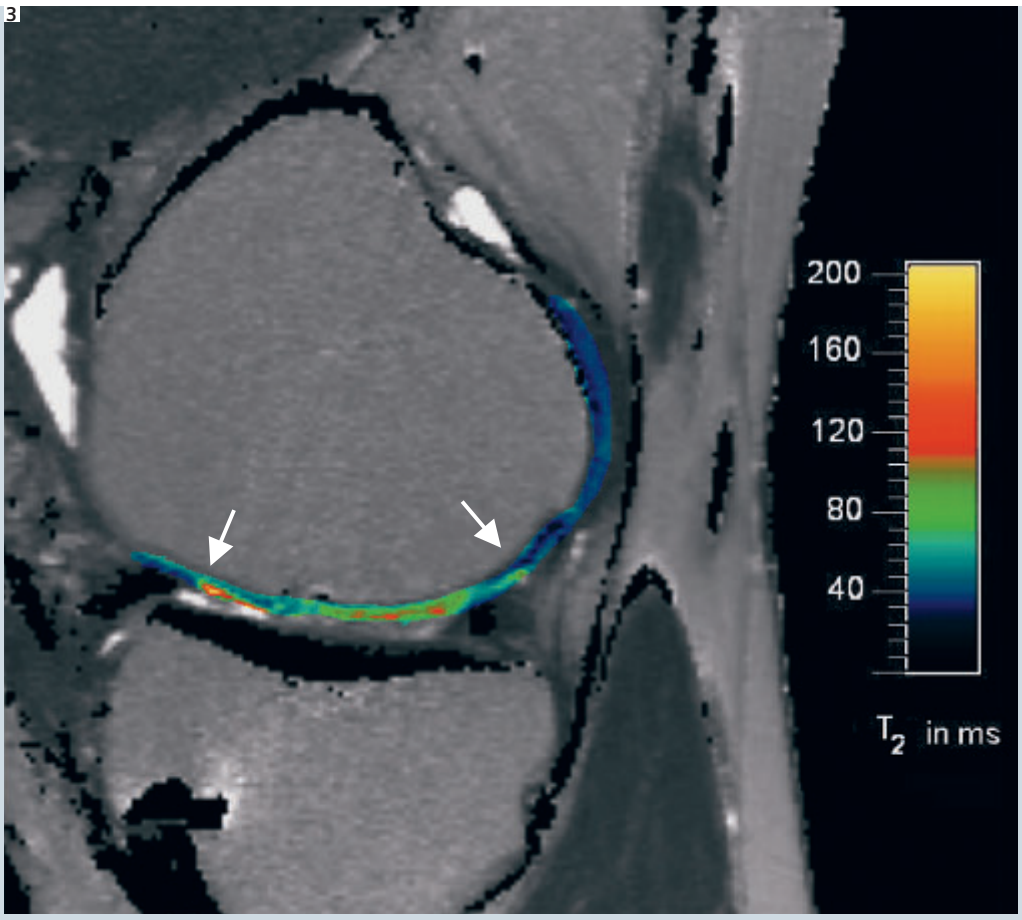

2 **A, B: 3D Morphological imaging: 3D DESS sequence for assessment of cartilage repair axial (top) and sagittal (bottom).**

3 **T2: Post-contrast. Pseudo-color image of T2-map of the measurement after the surgery shows lower T2 values presented in cartilage transplant, compared to the normal hyaline cartilage reference. White arrows mark the borders of the cartilage transplant. Corresponding T2 values are shown in the color-bar.**

echoes and stimulated echoes). For the assessment of diffusion-weighted images, a three-dimensional steady state diffusion technique, called PSIF (which is a time reversed FISP (Fast Imaging by Steady State Precession) sequence), has been used [9]. Imaging parameters of the DW-PSIF acquisition for cartilage were as follows: TR 16.3 ms, TE 6.1 ms, flip angle 30°, 48 sagittal slices, 170 x 170 mm FoV, 256 x 256 matrix size, slice thickness 1.5 mm, voxel size 0.6 x 0.6 x 1.5 mm^3. Scan time for each diffusion-weighted sequence was 4:40 min. In order to allow a semi-quantitative assessment of the diffusional behaviour in the cartilage, the diffusion sequence protocol consisted of 2 separate but immediately consecutive measurements using none (0), and 75 mT*ms*m-1 monopolar diffusion gradient moments for Diffusion-Weighted Imaging (DWI) and otherwise identical imaging parameters. For evaluation, the quotient image (non-diffusion-weighted /diffusion-weighted image) was calculated on a pixel-by-pixel basis. In a series of 15 patients after MACT we could demonstrate the feasibility of diffusion-weighted PSIF imaging with high resolution in vivo. The results show that in the follow up at different time points after MACT the diffusion behaviour of the transplants is changing. In the earlier period after MACT the diffusion was higher restricted which declined in the later follow up, but even after a period of up to 42 months there was still a difference in diffusion values between repair tissue and normal hyaline cartilage. With imaging techniques such as DW PSIF and a semi-quantitative evaluation forming the quotient, functional analysis of cartilage and cartilage repair with high SNR and high resolution can be achieved within comparably short acquisition times. In this context, diffusion-weighted imaging can practicably complement the information obtained from approaches which rely on relaxation properties such as dGEMRIC or T2-mapping. In comparison to dGEMRIC imaging of cartilage and cartilage repair procedures, no contrast medium is needed, coverage and resolution is improved and scan times reduced. It may be another tool of biochemical evaluation of cartilage transplants in the near future and could be added in a clinical setting to dGEMRIC and T2-mapping for evaluation of cartilage repair outcomes.

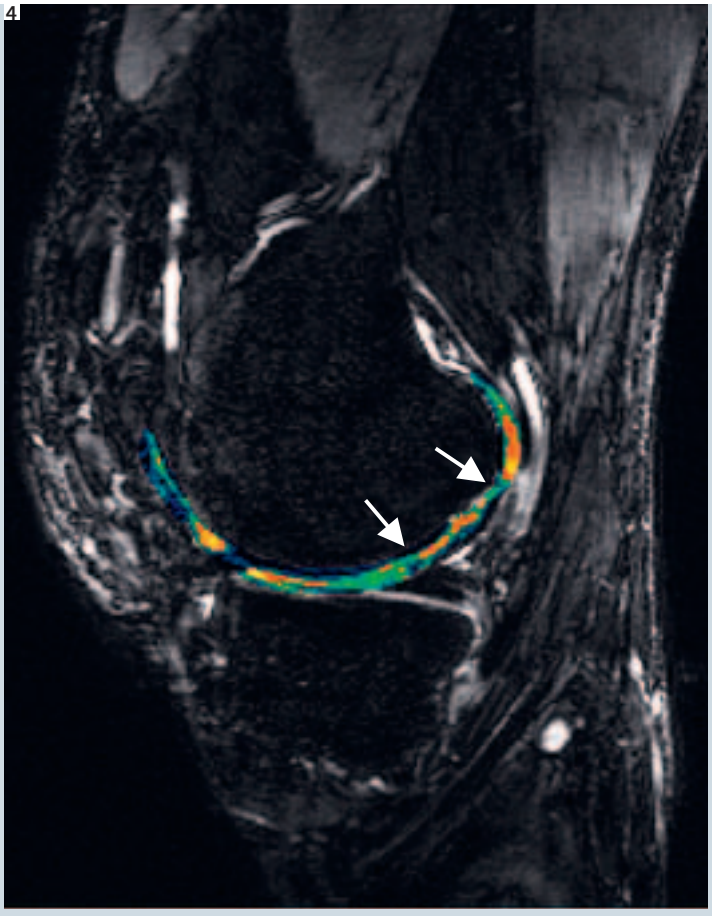

4 **DIFF: None.** **This is not a diffusion-weighted image. The intensity of the greyscaled part of the image was modified for better representation. The intensity of the pseudo-colored cartilage part was not modified and can be evaluated using the colorbar.**

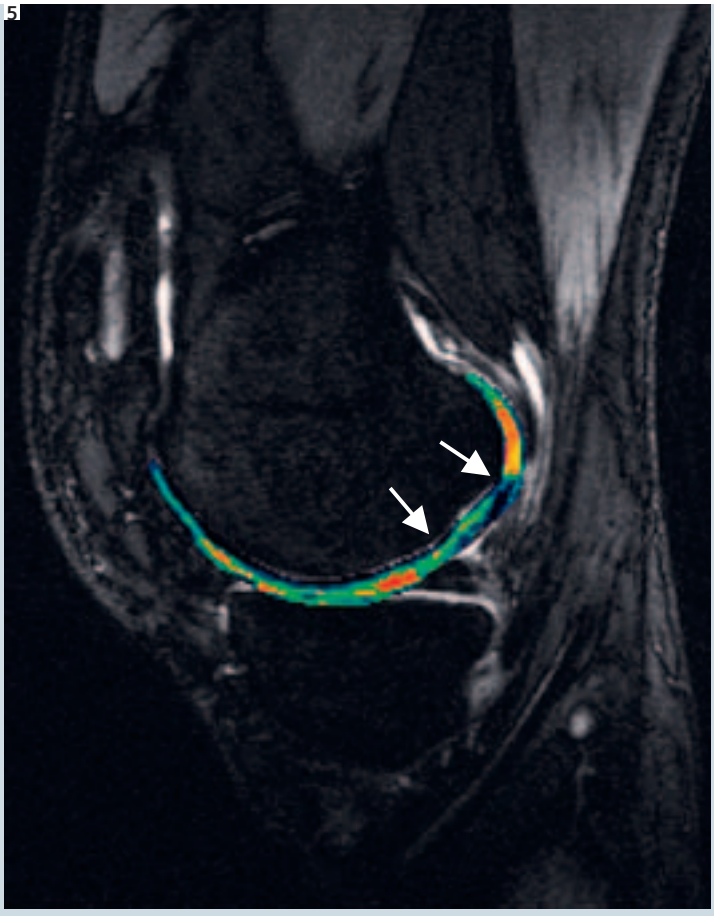

5 **DIFF: 75.** **The colored diffusion image in a medial condyle from central weight bearing zone aspects. The cartilage transplant is visible (arrows). Whereas in the central aspects the diffusivity is a little higher, it reduces to the more peripheral areas.**

References

1 Grushko G, Schneiderman R, Maroudas A. Some biochemical and biophysical parameters for the study of the pathogenesis of osteoarthritis: a comparison between the processes of aging and degeneration in human hip cartilage Connect Tissue Res 1989; 19: 149–76.

2 Brittberg M, Lindahl A, Nilsson A, Ohlsson C, Isaksson O, Peterson L. Treatment of Deep Cartilage Defects in the Knee with Autologous Chondrocyte Transplantation. New Engl J Med 1994; 331(14): 889–895.

3 Bashir A, Gray ML, Burstein D. Gd-DTPA2- as a measure of cartilage degradation. Magn Reson Med 1996; 36: 665–73.

4 Burstein D, Velyvis J, Scott KT et al. Protocol issues for delayed Gd(DTPA) (2-) enhanced MRI (dGEMRIC) for clinical evaluation of articular cartilage. Magn Reson Med 2001; 45: 36–41.

5 Watanabe A, Wada Y, Obata T, et al. Delayed gadolinium-enhanced MR to determine glycosaminoglycan concentration in reparative cartilage after autologous chondrocyte implantation: Preliminary results. Radiology 2006; 239(1): 201–208.

6 Miller KL, Hargreaves BA, Gold GE, et al. Steady-state diffusion-weighted imaging of in vivo knee cartilage. *Magn Reson Med.* Feb 2004; 51(2): 394–398.

Delayed Gadolinium Enhanced MRI of Cartilage (dGEMRIC) in Hip Dysplasia

Marcel Dudda, M.D.[1, 2]; Young Jo Kim, M.D., Ph.D.[1]

[1] *Dept. of Orthopaedic Surgery, Children's Hospital Boston, Harvard Medical School, Boston, USA*
[2] *Dept. of Surgery, University Hospital Bergmannsheil, Ruhr-University-Bochum, Germany*

Developmental dysplasia of the hip results in a shallow and unstable hip joint that leads to early osteoarthritis (OA) because of an increased mechanical stress of the cartilage [1–3]. It is estimated in some clinical series that up to 20 % of hips undergoing total hip replacement is due to this developmental disorder [4].
The delayed Gadolinium Enhanced MRI of Cartilage (dGEMRIC) is a non-invasive imaging technique that is able to monitor the loss of charge density in articular cartilage seen in early OA. dGEMRIC is a better marker of OA in hip dysplasia than traditional X-Ray measurements, such as minimal joint space width. Only dGEMRIC correlates with the patient's symptoms and with the severity of dysplasia [5].
dGEMRIC examines the cartilage's fixed-negative-charge density comprised of negatively charged glycosaminoglycans (GAG) [6, 7]. GAG provide the cartilage with its compressive stiffness and are lost early in the course of osteoarthritis [8].
In dGEMRIC, the anionic contrast agent gadopentetate ($Gd\text{-}DTPA^{2-}$), is given intravenously and distributes in cartilage in an inversely proportional manner to the concentration of negatively charged GAG. The concentration of $Gd\text{-}DTPA^{2-}$ will be relatively low in normal cartilage with abundant GAG and will be relatively high in degraded cartilage from which GAG have been lost. The concentration of $Gd\text{-}DTPA^{2-}$ in tissues can be determined from magnetic resonance measurements of T1, with T1 being proportional to the cartilage GAG content. Several in vitro and in vivo validation studies have been performed in the past [6, 9–13].
The dGEMRIC scans are performed with a 1.5T Siemens MAGNETOM Avanto scanner after administration of a double dose (0.4 mL/kg) of intravenous Magnevist ($Gd\text{-}DTPA^{2-}$; Berlex Laboratories, Wayne, NJ, USA) thirty minutes prior to the study [12]. Patients are required to walk for 10 to 15 minutes.
The dGEMRIC value is calculated as the average of the T1 values of the acetabular and femoral head articular cartilages in the weight-bearing zone (as designated from the edge of the acetabular rim to the indentation at the site of fovea's attachment to the femoral head) across all 3 coronal slices. Figs. 1 and 2 illustrate examples of dGEMRIC scans. The three

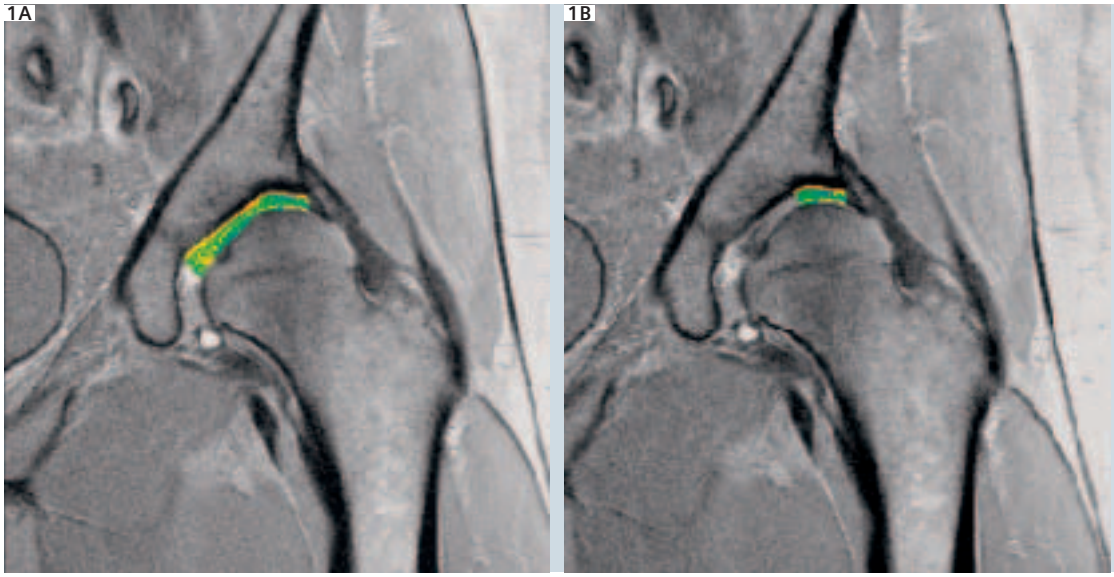

1 **A, B: T1 dGEMRIC of the hip.**
Color-coded T1-map of a left hip. 35-year-old patient with hip dysplasia.
Green color indicating a high dGEMRIC index (good cartilage status and good predictive value for reorientating surgery).

coronal slices cover most of the weight bearing surface of the hip joint. The femoral and acetabular cartilages from the labral edge to the acetabular fossa were included in the analysis.
The scans are performed under the following protocol:

Sequences	Time
Fast T1 localizer TA	*0.13 min*
T2 truefi 3d we sag TA	*1.42 min*
T2 star map 2d cor TA	*5.59 min*
DESS cor TA	*6.42 min*
Psif 2d sag we r75 384 TA	*9.02 min*
Psif 2d sag we n384 TA	*9.02 min*
T2 truefi 3d we sag 0.6 iso TA	*7.45 min*
Pd tse cor TA	*4.58 min*
Pd tse sag TA	*4.58 min*
Fl 3d vibe T1 Map 4 mm cor TA	*5.46 min*
Fl 3d vibe T1 Map 4 mm sag TA	*5.46 min*

Conclusion

Kim et al. demonstrated that the dGEMRIC index correlates with pain and severity of hip dysplasia as a sign of the biochemical integrity in cartilage [5]. In addition it has been shown that this technique is a better predictor of surgical outcome after periacetabular osteotomy (PAO) than plain radiographic and clinical measurements [14]. The T1 value does correlate with severity of dysplasia which is consistent with the increased incidence of early osteoarthritis in severe dysplasia. It is very important for the surgical treatment and outcome in periacetabular osteotomies to know the status of degenerated cartilage and integrity of cartilage in hips with developmental dysplasia to identify poor candidates for this procedure.

References

1 Murphy, S.B., R. Ganz, and M.E. Muller, The prognosis in untreated dysplasia of the hip. A study of radiographic factors that predict the outcome. J Bone Joint Surg Am, 1995. 77(7): p. 985–9.
2 Harris, W.H., Etiology of osteoarthritis of the hip. Clin Orthop Relat Res, 1986(213): p. 20–33.
3 Murray, R.O., The aetiology of primary osteoarthritis of the hip. Br J Radiol, 1965. 38(455): p. 810–24.
4 Solomon, L., Patterns of osteoarthritis of the hip. J Bone Joint Surg Br, 1976. 58(2): p. 176–83.
5 Kim, Y.J., et al., Assessment of early osteoarthritis in hip dysplasia with delayed gadolinium-enhanced magnetic resonance imaging of cartilage. J Bone Joint Surg Am, 2003. 85–A(10): p.1987–92.
6 Bashir, A., M.L. Gray, and D. Burstein, Gd-DTPA2- as a measure of cartilage degradation. Magn Reson Med, 1996. 36(5): p. 665–73.
7 Bashir, A., et al. MRI of Glycosaminoglycan distribution in Cartilage Using Gd(DTPA)2- in vivo. in Fifth Annual Meeting of the International Society for Magnetic Resonance in Medicine. 1997. Berkeley, CA.
8 Venn, M. and A. Maroudas, Chemical composition and swelling of normal and osteoarthrotic femoral head cartilage. I. Chemical composition. Ann Rheum Dis, 1977. 36(2): p. 121–9.
9 Tiderius, C.J., et al., Gd-DTPA2)-enhanced MRI of femoral knee cartilage: a dose-response study in healthy volunteers. Magn Reson Med, 2001. 46(6): p. 1067–71.
10 Bashir, A., et al., Glycosaminoglycan in articular cartilage: in vivo assessment with delayed Gd(DTPA)(2-)-enhanced MR imaging. Radiology, 1997. 205(2): p. 551–8.
11 Bashir, A., et al., Nondestructive imaging of human cartilage glycosaminoglycan concentration by MRI. Magn Reson Med, 1999. 41(5): p. 857–65.
12 Burstein, D., et al., Protocol issues for delayed Gd(DTPA)(2-)-enhanced MRI (dGEMRIC) for clinical evaluation of articular cartilage. Magn Reson Med, 2001. 45(1): p. 36–41.
13 Mlynarik, V., et al., The role of relaxation times in monitoring proteoglycan depletion in articular cartilage. J Magn Reson Imaging, 1999. 10(4): p. 497–502.
14 Cunningham, T., et al., Delayed Gadolinium Enhanced MRI of Cartilage (dGEMRIC) as a Predictor of Early Failure after Bernese Periacetabular Osteotomy for Hip Dysplasia. J Bone Joint Surg, 2006.

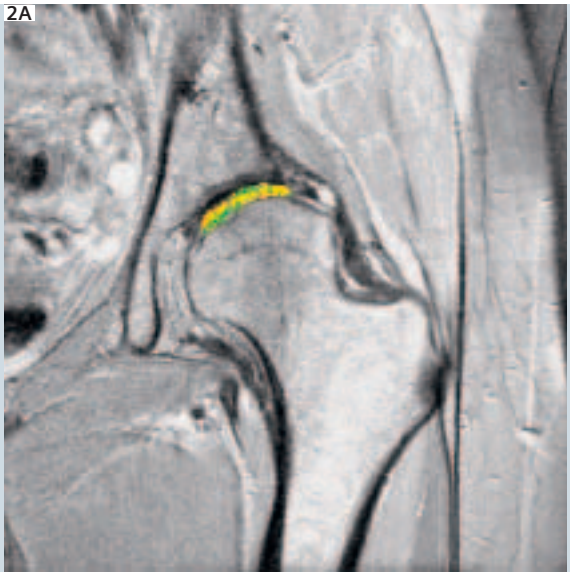

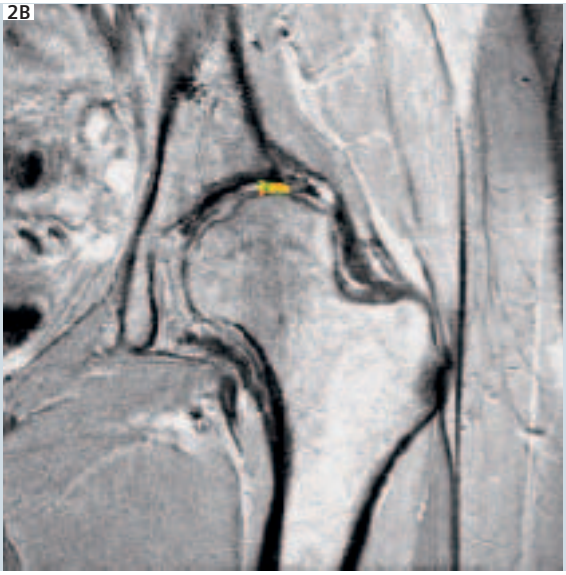

2 A, B: T1 dGEMRIC of the hip. Color-coded T1-map of a left hip. 26-year-old patient with hip dysplasia. Yellow color indicating a lower dGEMRIC index and therefore a cartilage degeneration. This corresponds in this case with osteoarthritic changes in the X-ray images (Tönnis Grade 1–2).

T2 Mapping of Articular Cartilage in Hip Joint

Atsuya Watanabe, M.D.[1, 2]; Chris Boesch, M.D.[1]; Tallal C. Mamisch, M.D.[3]; Suzanne E. Anderson, M.D.[1, 2]

[1]Department of Clinical Research, Unit for MR Spectroscopy and Methodology, University of Bern, Switzerland
[2]Department of Diagnostic, Interventional and Pediatric Radiology, Inselspital, University of Bern, Switzerland
[3]University Hospital Bochum, Bergmannsheil Clinics, Department of Trauma Surgery, Bochum, Germany

Introduction

T2 (transverse relaxation time) mapping is an MR imaging technique which is able to evaluate the cartilage matrix status, such as collagen fiber integrity and hydration in cartilage [1]. As early degeneration of cartilage is characterized by deterioration of the extracellular matrix components, T2 mapping has the potential to identify cartilage degeneration in an early stage.
It has been known that there is a variation of cartilage matrix composition in the joint, and that T2 of cartilage is sensitive to the relationship between the collagen network and orientation of the static magnetic field (B_0) due to the orientation dependent dipolar interaction [2, 3]. To inspect the cartilage degeneration, it is important to understand the regional differences of T2 in a specific joint. There have been several clinical studies of T2 mapping in knee joints; however, few studies of T2 mapping have involved the hip joint.
The aim of this study is to demonstrate the ability of T2 mapping in detecting early degeneration of cartilage in the hip joint.

Examination and Analysis

Healthy volunteers and patients with femoro-acetabular impingement (FAI) syndrome diagnosed by previous examinations were evaluated.
MR imaging was performed with a 3.0 Tesla system (MAGNETOM Trio, A Tim System; Siemens, Erlangen, Germany). A dedicated Body Matrix coil (Tim system) was used to image both hip joints.
T2 measurement was performed at an oblique coronal plane, which was parallel to the femoral neck and passed through the center of the femoral head. A multi-spin-echo sequence was used for T2 measurements. The scanning parameters were 1500 msec repetition time, 10 echo times of 10.3–103 msec, 150×150 mm field of view, 4.0 mm slice thickness, 512×512 matrix, and 1 excitation. Color-coded T2-calculated maps were generated using MATLAB software (Mathworks, Natick, MA, USA) with a mono-exponential curve fit. The appearance of cartilage T2 maps in healthy hip joints were compared with that in hips with FAI syndrome.

Findings

T2 maps of acetabular and femoral cartilage in healthy hips for a representative case are shown in figures 1A and 1B respectively. The T2 in cartilage was slightly longer in the superficial layer than in the deep layer. In addition, slightly high T2 was observed in the lateral areas of femoral cartilage located symmetrically with each other.
The main cause of the high T2 observed at these areas might be the orientation dependent dipolar interaction, as magic angle effect is supposed to be observed when the collagen network structure is oriented 54.7° relative to B_0.
T2 map and T1- and T2-weighted MR images of acetabular cartilage in the same slice position of the hip for a representative patient with early stage of FAI syndrome are shown in figures 2A, 2B, and 2C respectively.
In the conventional T2-weighted MR

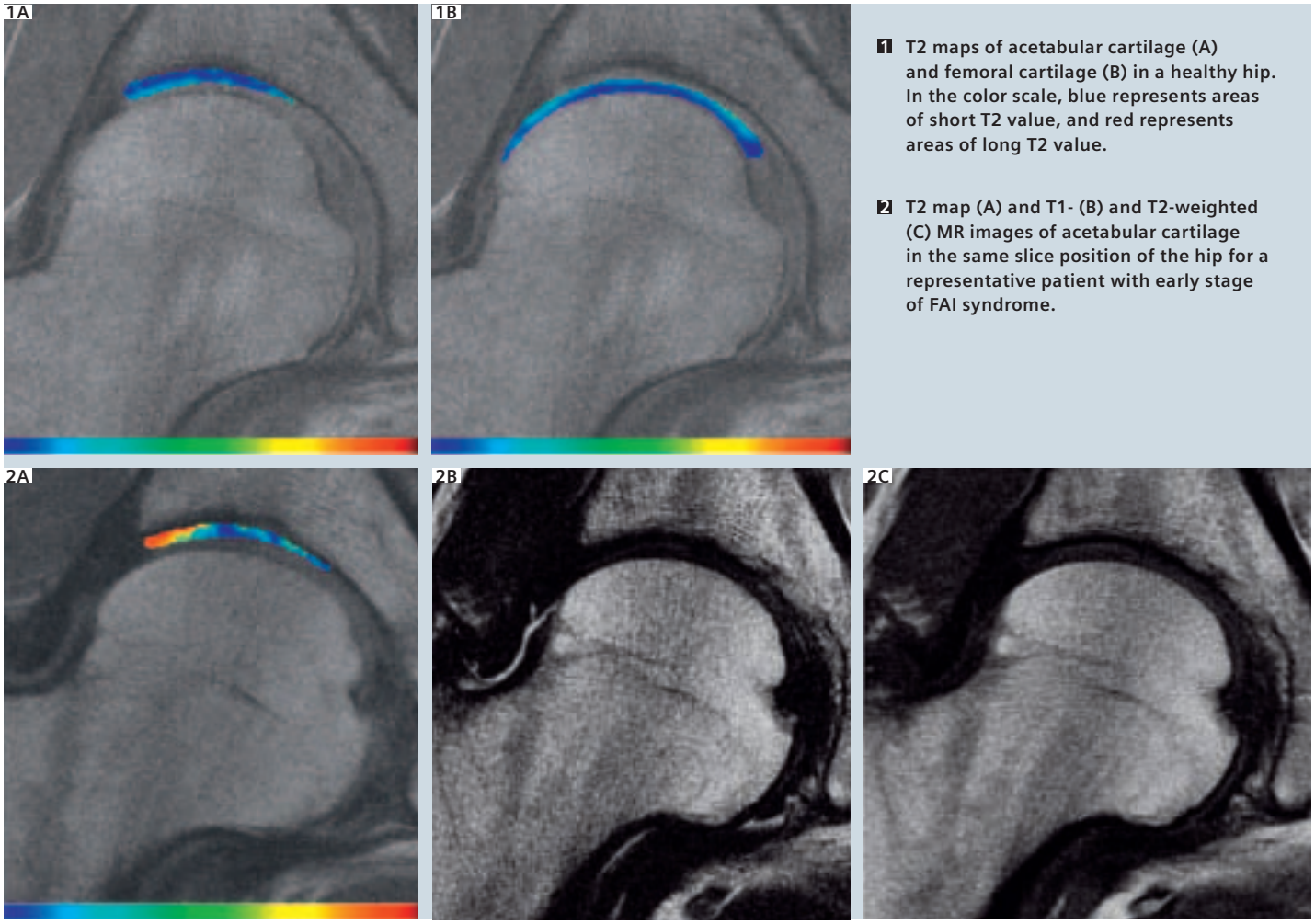

1 T2 maps of acetabular cartilage (A) and femoral cartilage (B) in a healthy hip. In the color scale, blue represents areas of short T2 value, and red represents areas of long T2 value.

2 T2 map (A) and T1- (B) and T2-weighted (C) MR images of acetabular cartilage in the same slice position of the hip for a representative patient with early stage of FAI syndrome.

image, degeneration of acetabular cartilage was not clearly evident. However, high T2 in the lateral acetabular cartilage was observed with the T2 map, indicating the presence of degeneration within this area.

Discussion

T2 mapping may be able to detect early degeneration better than the conventional MR imaging techniques. The ability to detect early degeneration of hip articular cartilage may contribute to better understanding of the progression of degeneration seen with degenerative hip disease. It has been shown that the outcome of joint-preserving operations in hip joints correlates with the initial joint condition [4], the ability to evaluate cartilage status prior to operation could improve the predictability of post-operative outcomes. In this study, relatively large topographic variation of hip cartilage T2 in young healthy volunteers was observed. As this variation of T2 can lead to possible misinterpretation regarding cartilage degeneration, special attention should be paid when T2 mapping is applied to patients with degenerative cartilage of the hip joint.

References

1 Nieminen MT, Rieppo J, Toyras J, et al. T2 relaxation reveals spatial collagen architecture in articular cartilage: a comparative quantitative MRI and polarized light microscopic study. Magn Reson Med 2001; 46: 487–493.

2 Goodwin DW, Zhu H, Dunn JF. In vitro MR imaging of hyaline cartilage: correlation with scanning electron microscopy. Am J Roentgenol 2000; 174: 405–409.

3 Mosher TJ, Smith H, Dardzinski BJ, Schmithorst VJ, Smith MB. MR imaging and T2 mapping of femoral cartilage: in vivo determination of the magic angle effect. AJR Am J Roentgenol. 2001; 177: 665–669.

4 Trousdale RT, Ekkenkamp A, Ganz R, Wallrichs SL. Periacetabular and intertrochanteric osteotomy for the treatment of osteoarthrosis in dysplastic hips. J Bone Joint Surg 1995; 77A: 73–85.

3D-$T_{1\rho}$-Mapping of Cartilage at 3T with integrated Parallel Imaging Technique (*syngo* GRAPPA)

Ravinder R. Regatte, Ph.D.; Mark E. Schweitzer, M.D.

Center for Biomedical Imaging, Department of Radiology, New York University School of Medicine, New York, USA

Introduction

Osteoarthritis (OA) affects over 50 million Americans and has a substantial impact on the economy and the health care system. Currently, there is no cure for this debilitating chronic disease and the effective treatment is, at best, focused on symptomatic relief. The conventional imaging techniques have shown promise for the identification of more subtle morphologic alterations as determined by cartilage thickness, volume, or surface fibrillation. However, even the more innovative of these conventional techniques have not been consistent in detecting the earliest stages (biochemical/functional integrity) of cartilage degeneration.

The loss of proteoglycan content (PG) is an initiating event in the early stages of OA. Currently, the loss of PG can be measured via contrast enhanced MRI of cartilage (dGEMRIC) or $T_{1\rho}$-MRI (spin-lattice relaxation time in the rotating frame) or ^{23}Na-MRI. For clinical applications, dGEMRIC requires an exogenous contrast agent ($Gd\text{-}DTPA^{2-}$) with long temporal delay after intravenous injection (~90 minutes). However, sodium MRI is highly specific to PG but it requires RF hardware modification and high static magnetic fields (B_o) and has inherently low sensitivity, all of which limit this techniques clinical utility. Alternatively, $T_{1\rho}$ relaxation mapping has been shown to be sensitive to early biochemical changes in cartilage especially PG. It is well suited for probing low-frequency interactions between macro molecular protons (e.g. –NH and –OH sites) and bulk water protons. In cartilage, $T_{1\rho}$ is strongly correlated with PG content and is being studied for its potential as a biochemical marker of early OA. However, the clinical applications of 3D-$T_{1\rho}$ -relaxation mapping at high field systems (e.g. 3T and above) are currently limited due to the long imaging times as well as significant radio-frequency (RF) energy deposition. The combination of 3D-$T_{1\rho}$-weighted MRI with multi-coil RF technology and parallel imaging (GRAPPA) should be able to address both of these problems (total imaging time and RF energy deposition). The main purpose of the article is to demonstrate the feasibility of rapid $T_{1\rho}$- relaxation mapping of cartilage in early OA subjects at 3T clinical scanner with parallel imaging.

Examination and Data Analysis

Osteoarthritis subjects were recruited based on clinical symptoms and Kellgren-Lawrence grades. 3D-$T_{1\rho}$-relaxation mapping with parallel imaging was performed employing 3.0 Tesla clinical MRI system (MAGNETOM Trio, A Tim System; Siemens Medical Solutions, Erlangen, Germany). All the MRI experiments were performed employing a phased-array (PA) RF coil (18 cm diameter, 8-channel transmit-receive). We utilized a 3D-FLASH sequence in combination with parallel imaging (GRAPPA with 24 reference k-space lines) to acquire 3D-$T_{1\rho}$-weighted images. In order to achieve $T_{1\rho}$ magnetization preparation, we used a "self-compensating" spin-lock pulse cluster (duration of each 90° pulse = 200 µs). Four 3D- $T_{1\rho}$-weighted images with varying spin-lock pulse lengths (TSL = 2, 10, 20 and 30 ms) were acquired in order to construct $T_{1\rho}$ maps. Color coded $T_{1\rho}$-maps were generated using MATLAB software (Mathworks, Natick, MA, USA).

Results and Discussion

Representative $T_{1\rho}$ maps from a data set of 16 slices obtained with parallel imaging (PAT factor = 2) from two osteoarthritis subjects are shown in Fig. 1 (early OA, 35-year-old female volunteer) and Fig. 2 (moderate OA, 45-year-old male volunteer). In the group of early OA subjects studied, there is an approximately 15–20% elevation in $T_{1\rho}$ relaxation times (shown by white arrows) when compared to age-matched asymptomatic subjects. However in the case of moderate OA (Fig. 2), there is ~20–45% increase in $T_{1\rho}$ numbers as well as more compartments are involved in the progression of OA (shown by white arrows). The 3D-$T_{1\rho}$ in combination with parallel imaging (PAT factor = 2) show excellent *in-vivo* reproducibility for cartilage imaging (data not shown). Therefore, these preliminary studies clearly demonstrate the potential of rapid $T_{1\rho}$ with parallel imaging as a non-invasive biochemical marker of proteoglycan loss as well as early degeneration at high field systems (3T) without exceeding the RF energy deposition.

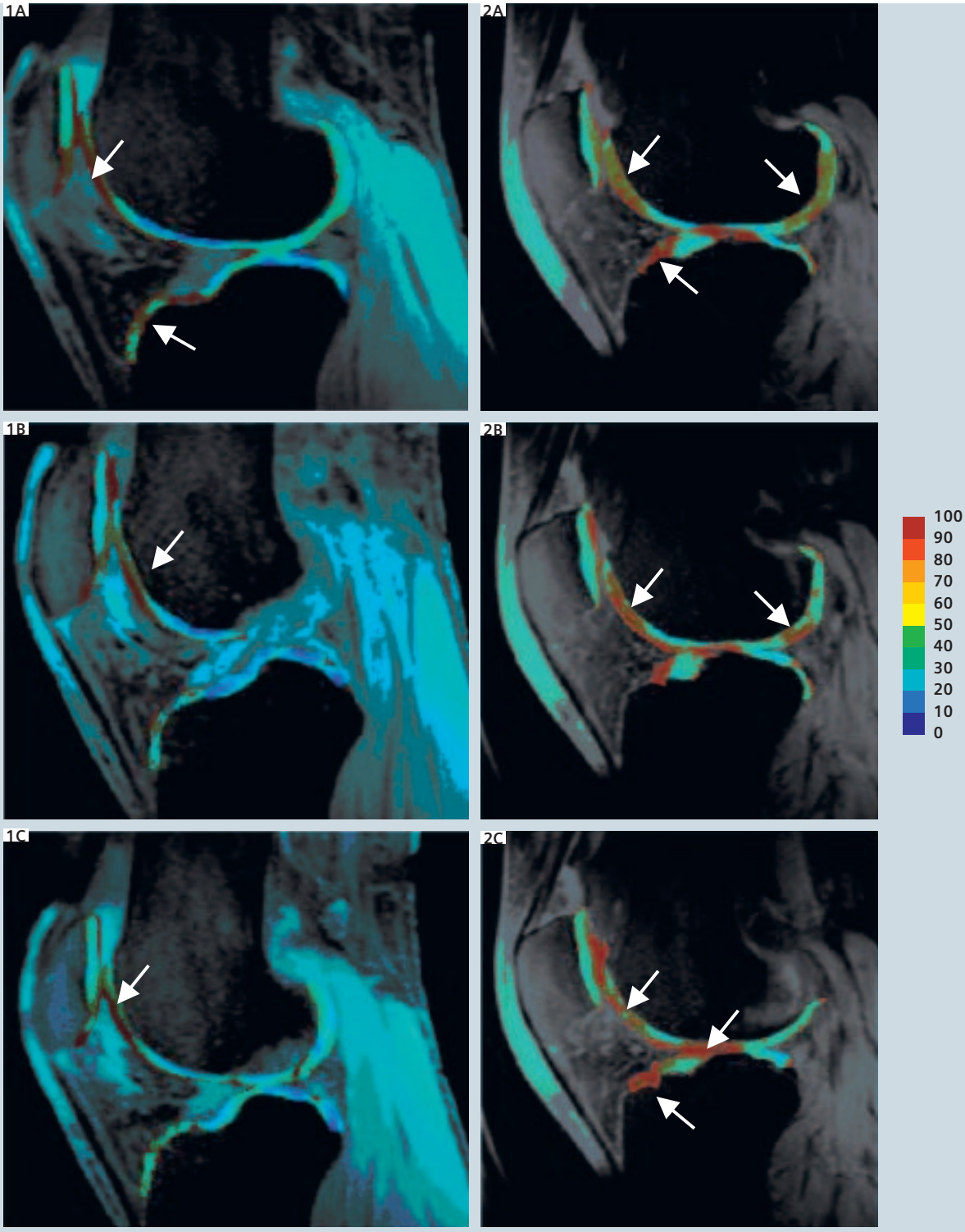

1 2 Representative $T_{1\rho}$-maps computed from two OA subjects are shown in Fig. 1 (early OA) and 2 (moderate OA) respectively. The 3D- $T_{1\rho}$-weighted imaging (GRAPPA with PAT factor = 2) was performed using $T_{1\rho}$ preparation pulse cluster and 3D-FLASH as a readout. The imaging parameters are TR 175ms; TE 3 ms; flip angle 25; slices 16; matrix 256 x 256; bandwidth 130 Hz/pixel, spin-lock amplitude 250 Hz. The color bar scale at the right indicates the $T_{1\rho}$-relaxation times in the cartilage (0–100 ms).
The elevated pixels in both OA subjects are shown by white arrows.

Orthopedic Imaging

Thaddeus Laird, M.D.

UC Davis Medical Center, Dept. of Radiology, MSK Division, Sacramento, USA

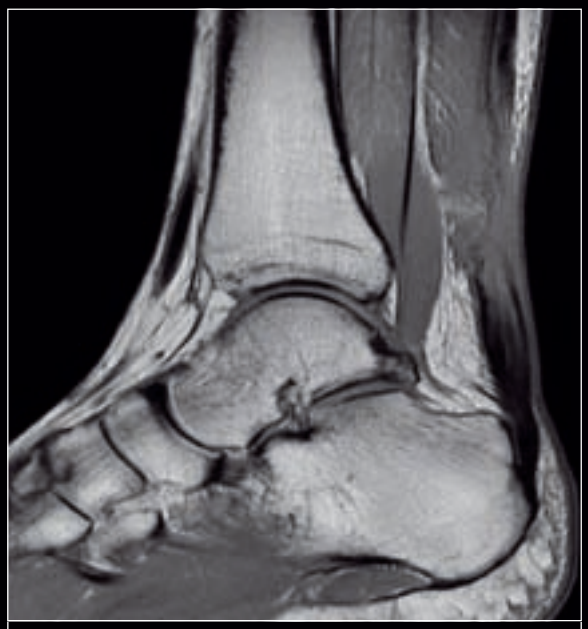

1 T1-weighted image, achilles tendon tear.

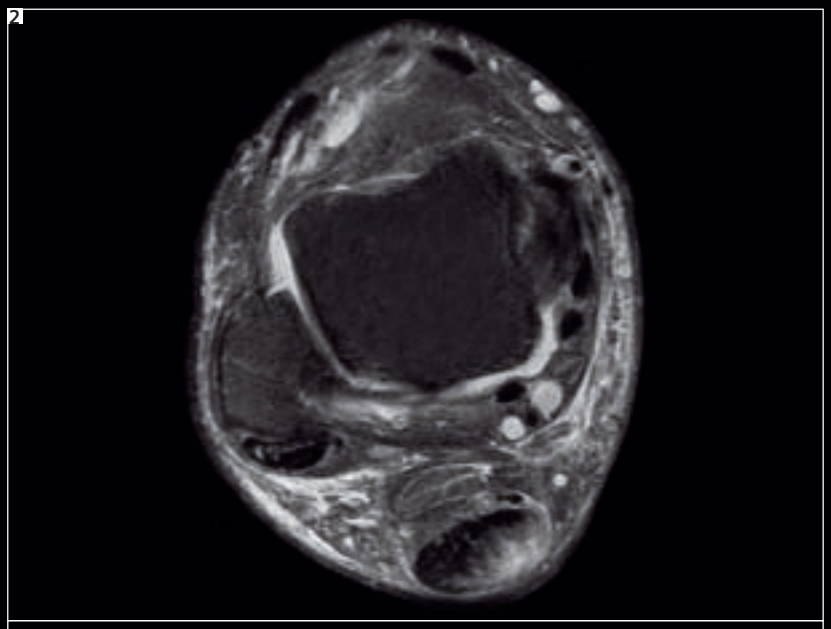

2 Protondensity-weighted (pd) image with fat suppression (fs), achilles tendon tear.

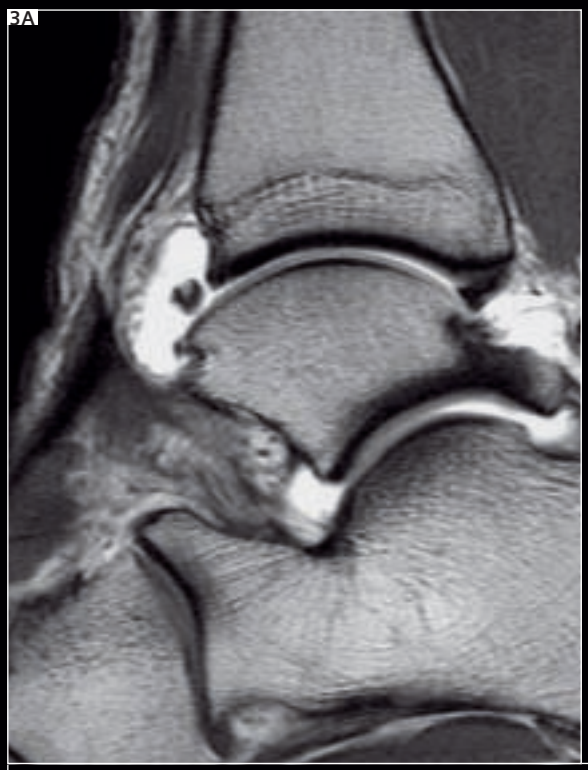

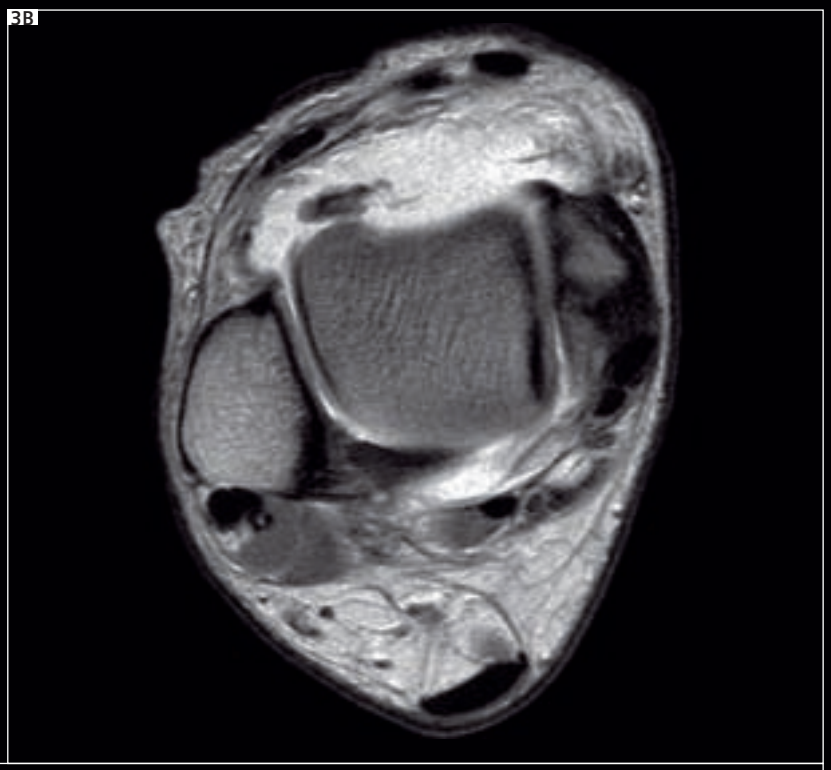

3 Sagittal T1-weighted and axial protondensity-weighted sequence: loose body in the anterior capsular recess of tibiotalar joint.

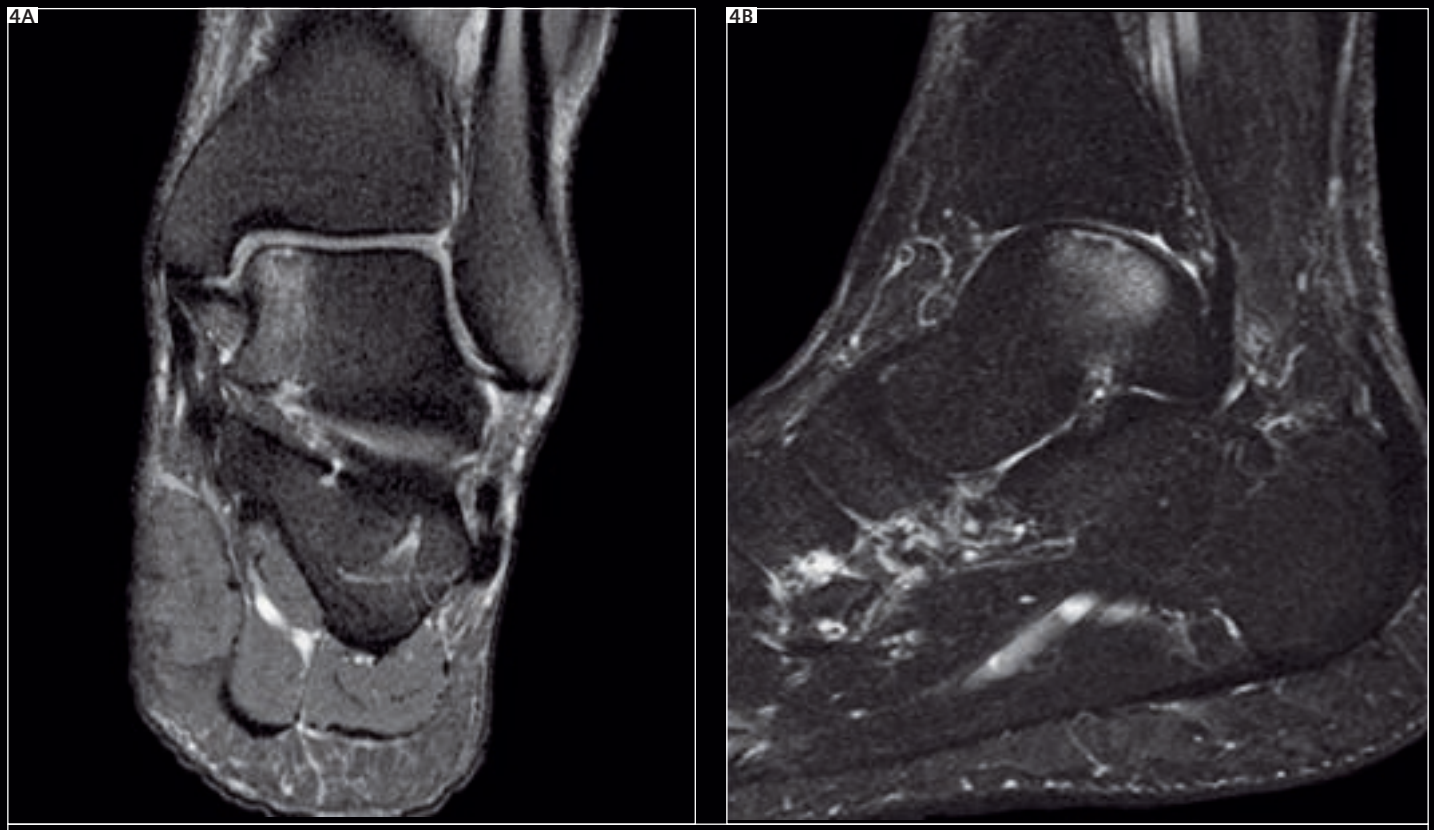

4 Ankle, osteochondritis dissecans. 4A: Protondensity-weighted image with fat suppression. 4B: STIR sequence.

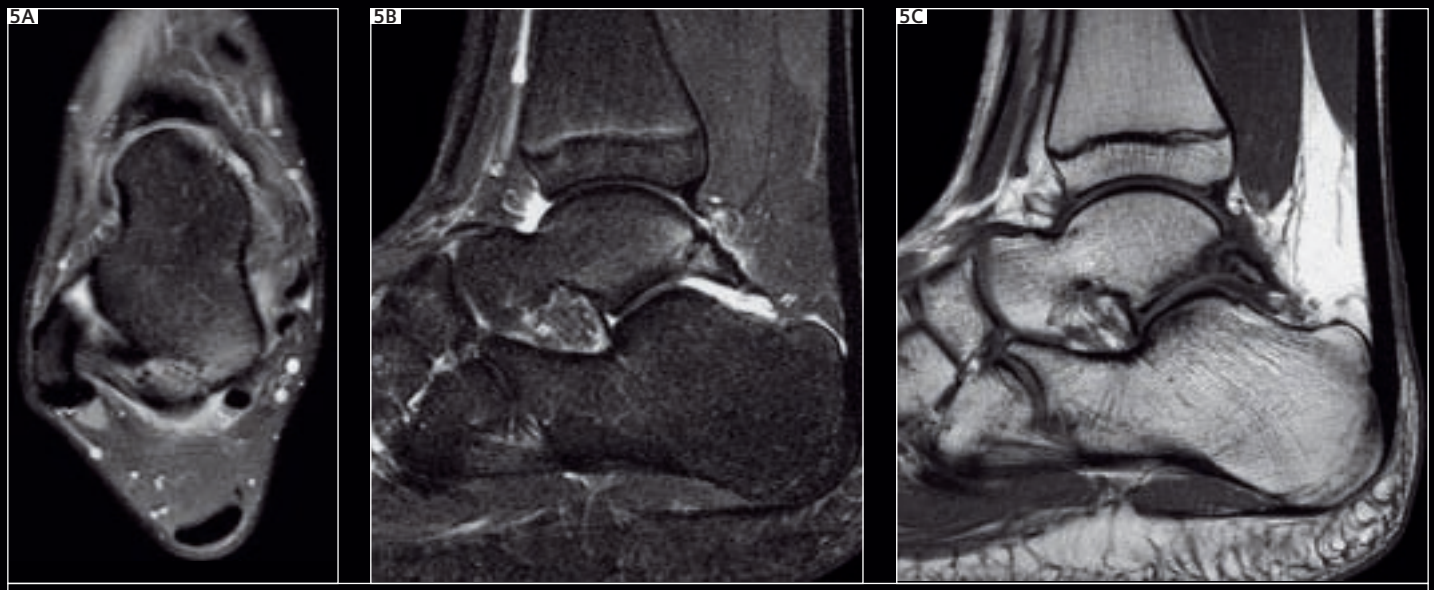

5 Posterior impingement syndrome. 5A: Protondensity-weighted image with fat suppression. 5B: STIR sequence. 5C: T1-weighted image.

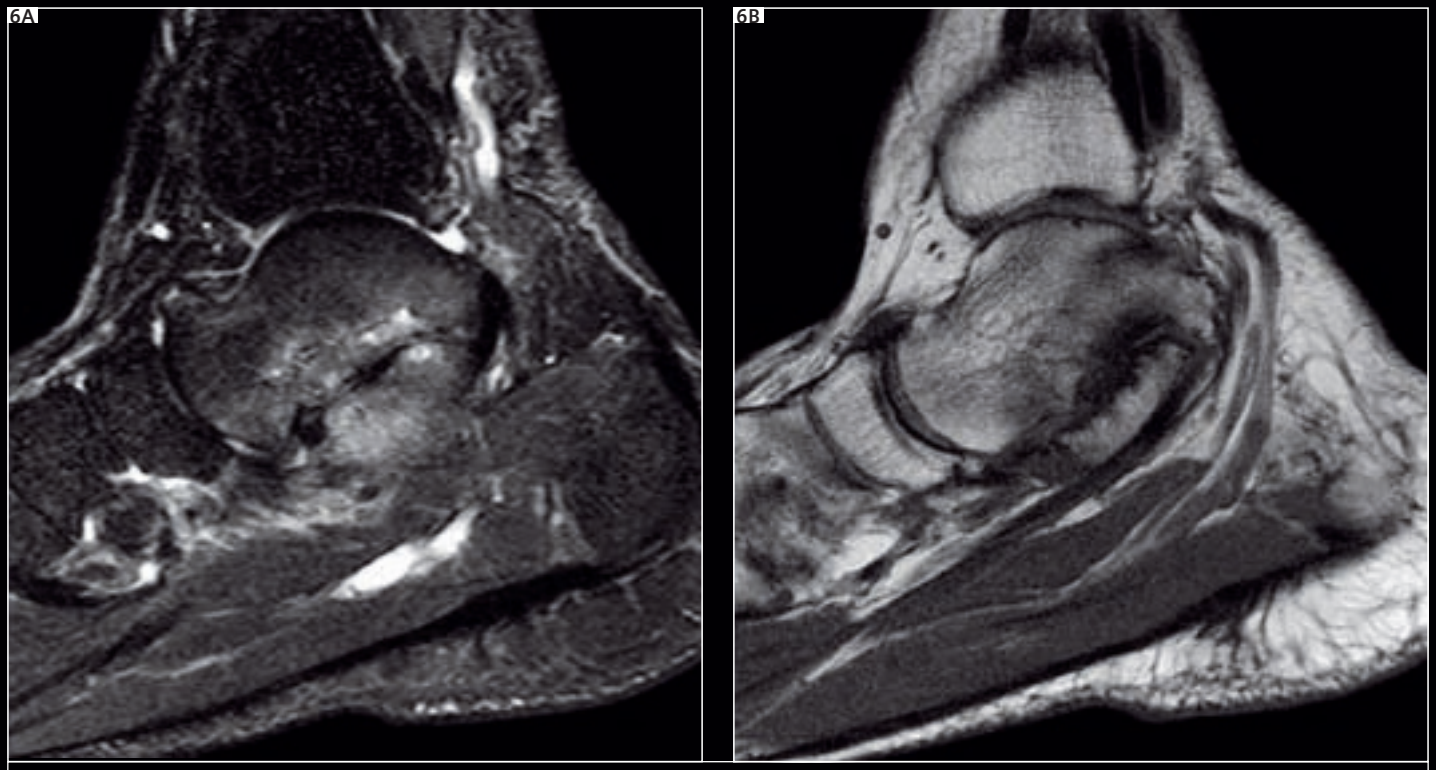

6 Tarsal coalition. 6A: STIR sequence. 6B: T1-weighted image.

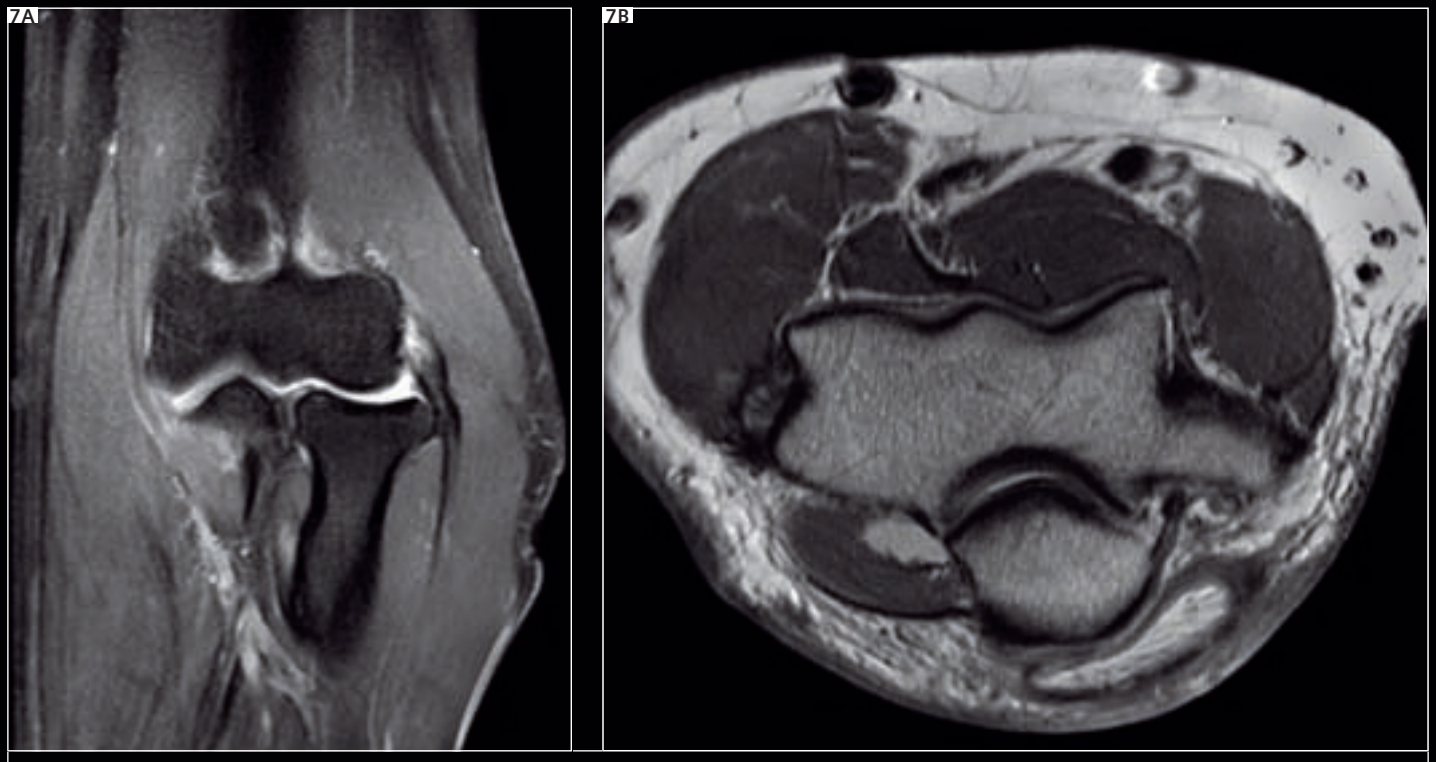

7 Tendon tear. 7A: Protondensity-weighted image with fat suppression, common extensor. 7B: Olecranon bursitis, T2-weighted image.

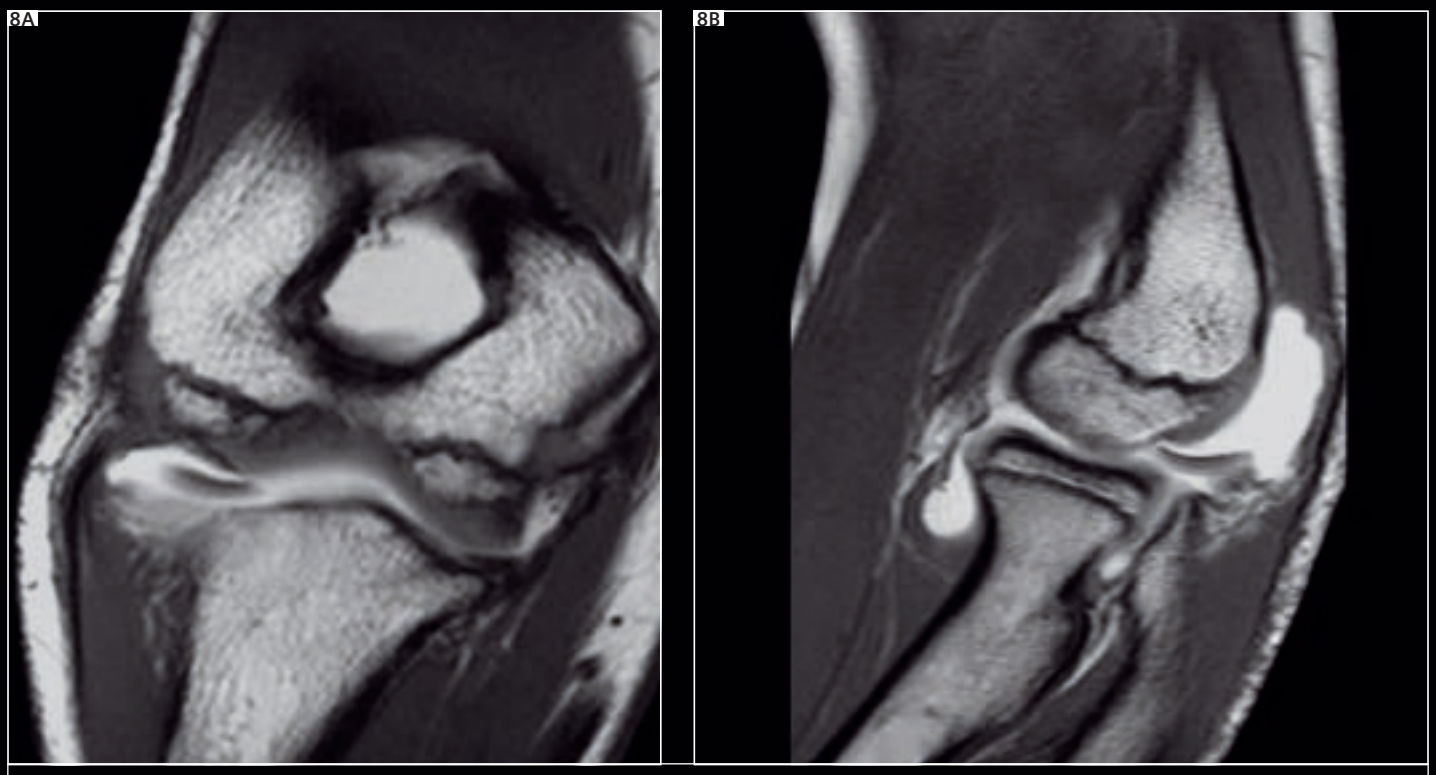

8 Coronal and sagittal T1-weighted sequences: cartilage flake from a lesion of the capitellum humeri dislocated into the dorsal capsular recess.

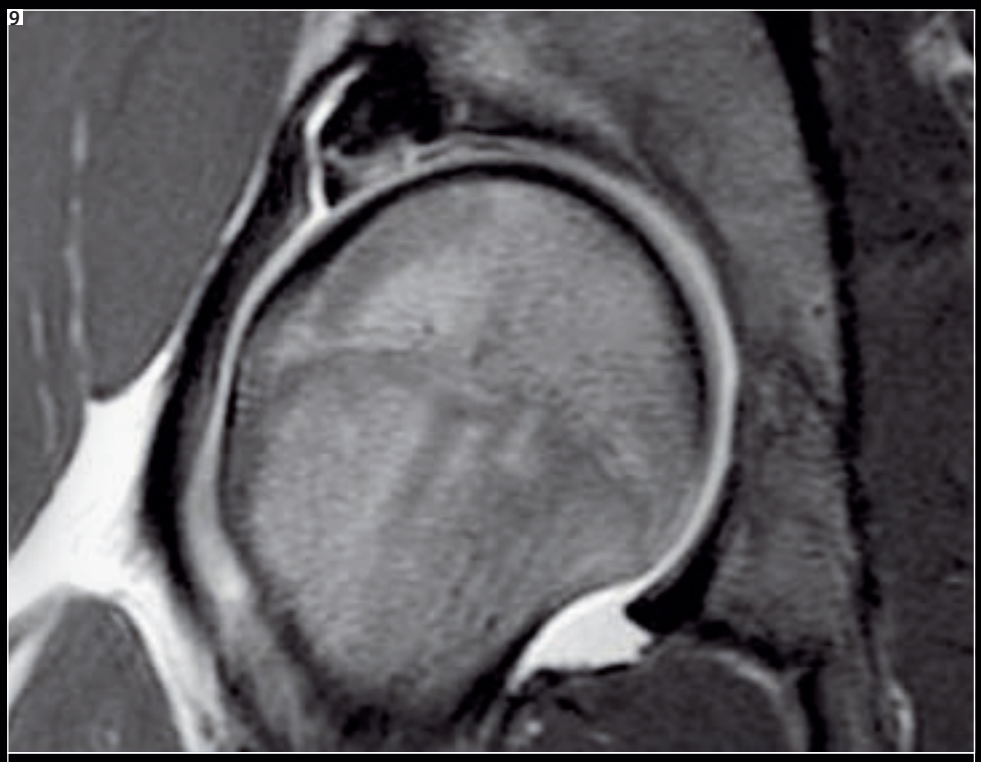

9 Hip, coronal protondensity-weighted image, cartilage delamination.

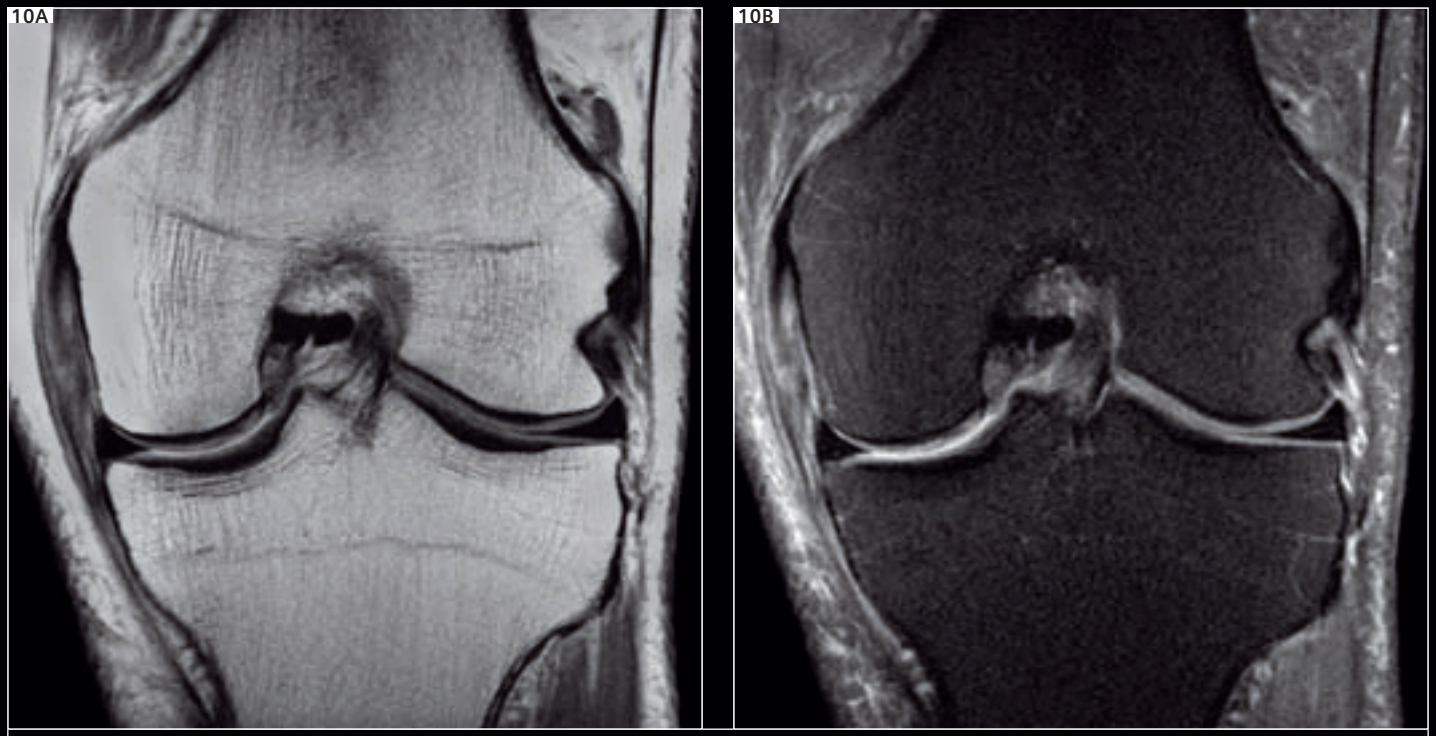

10 Knee, protondensity-weighted image. 10B: With fat suppression. Tear of the medial collateral ligaments (MCL).

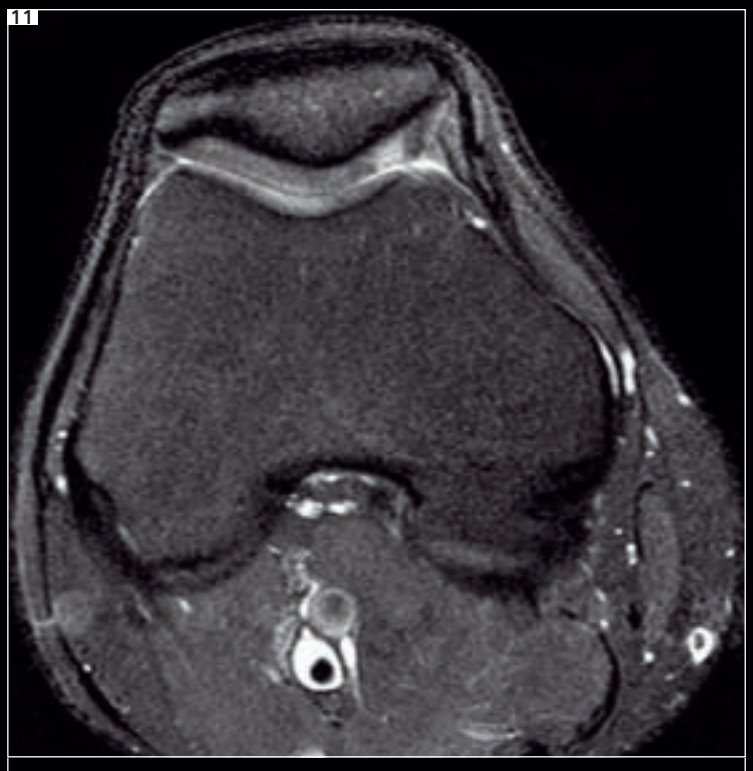

11 Protondensity-weighted image with fat suppression of an axial patellar chondral injury.

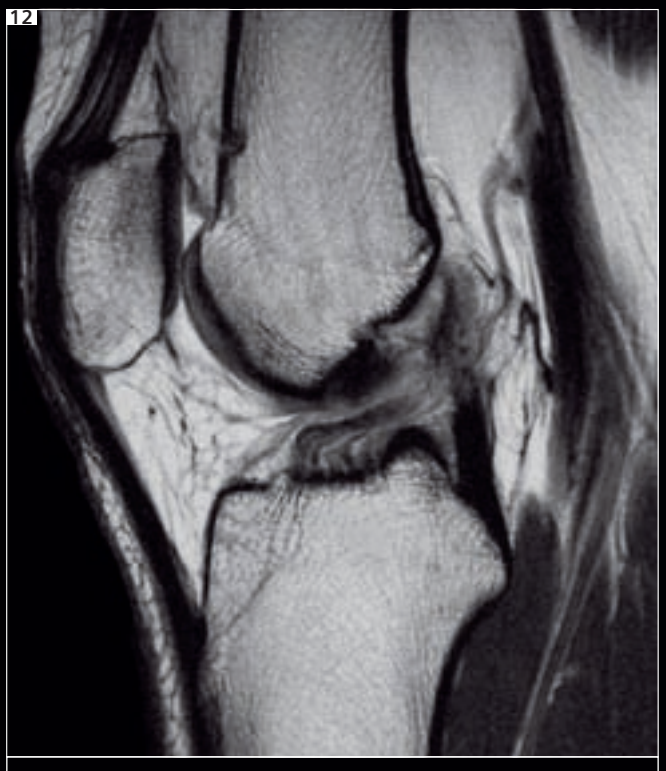

12 Protondensity-weighted image of an anterior cruciate ligament (ACL) tear.

13

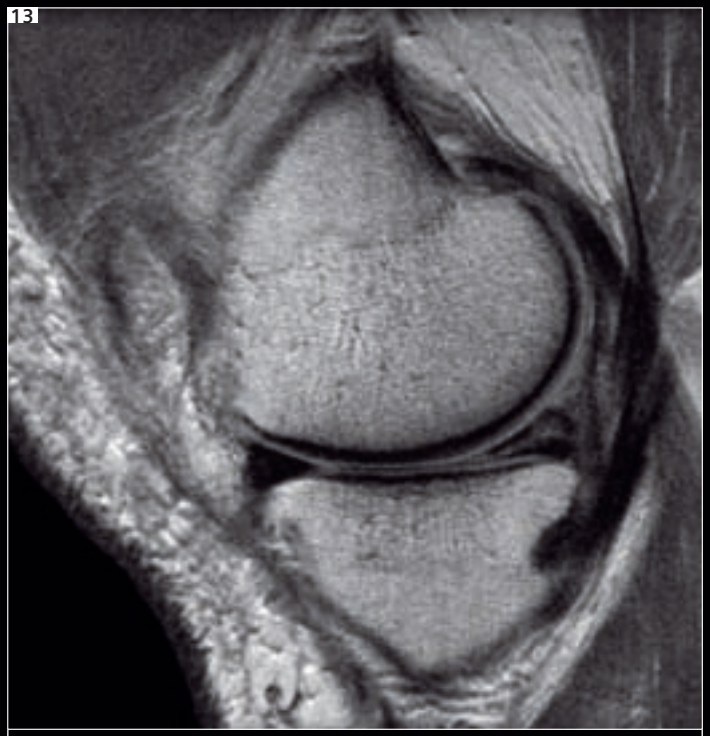

13 Knee, medial meniscus tear, sagittal.

14A

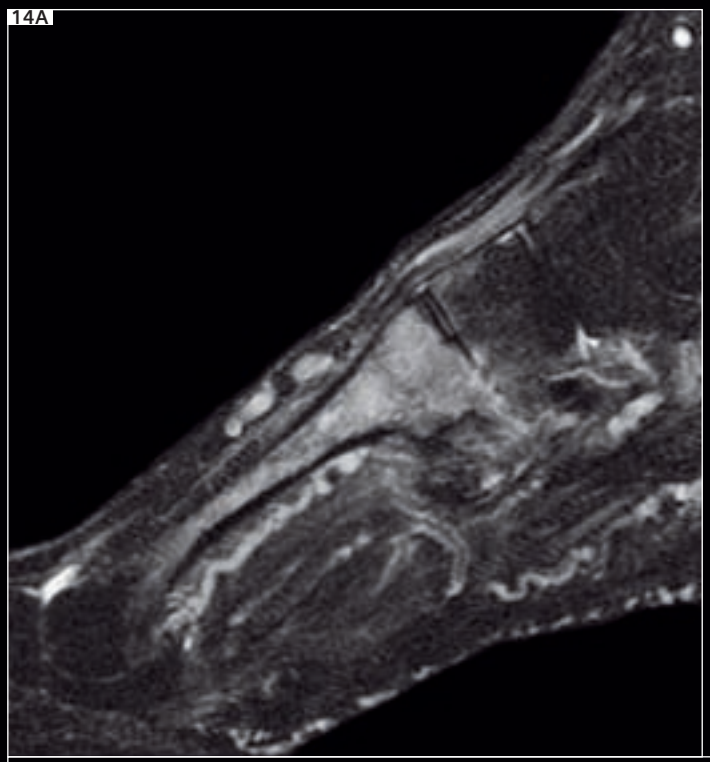

14B

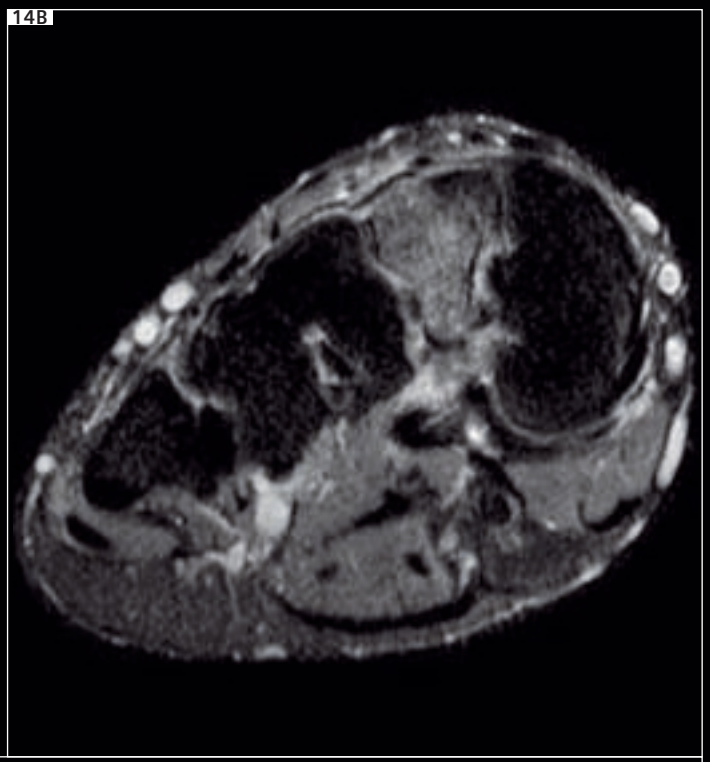

14 2nd metatarsal stress fracture. 14A: STIR sequence. 14B: Protondensity-weighted image with fat suppression.

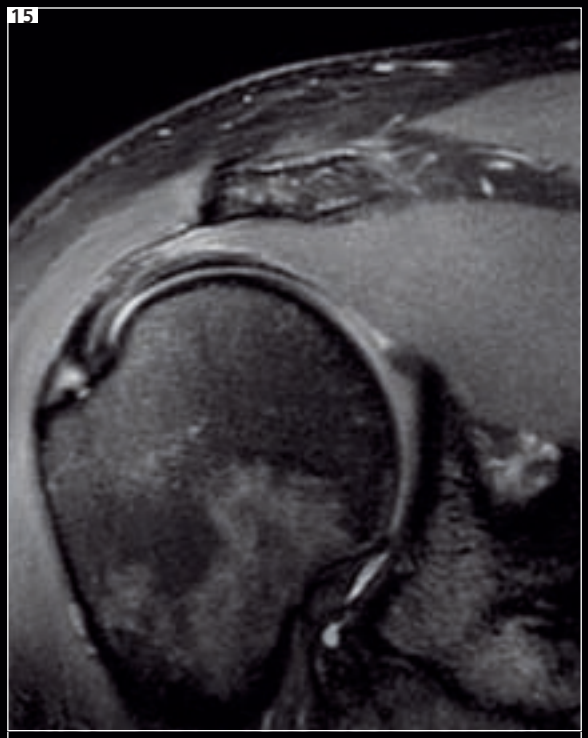

15 Partial tear of the rotator cuff. Protondensity-weighted image with fat suppression.

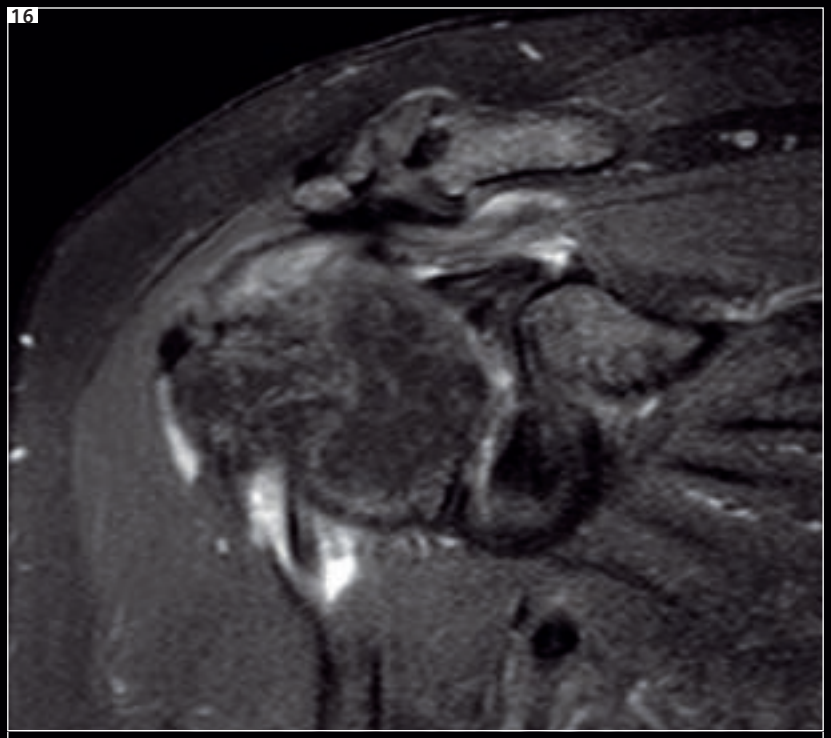

16 Impingement. Protondensity-weighted image with fat suppression. Tear of the medial collateral ligaments (MCL).

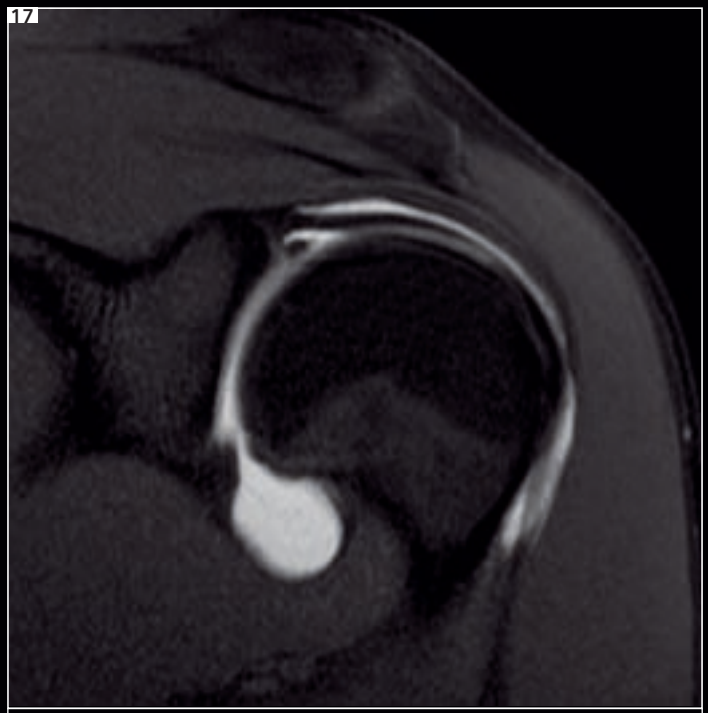

17 Superior labrum anterior-posterior (SLAP) tear.

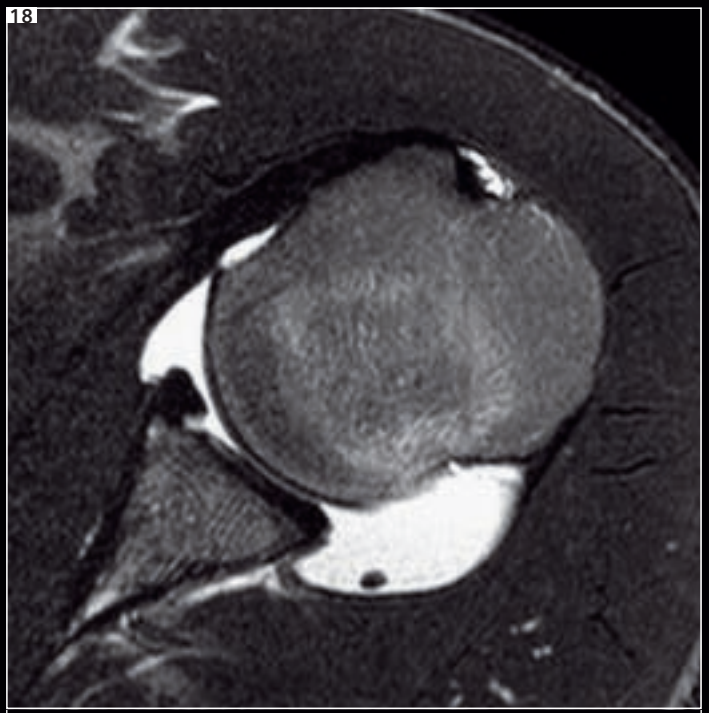

18 Loose body.

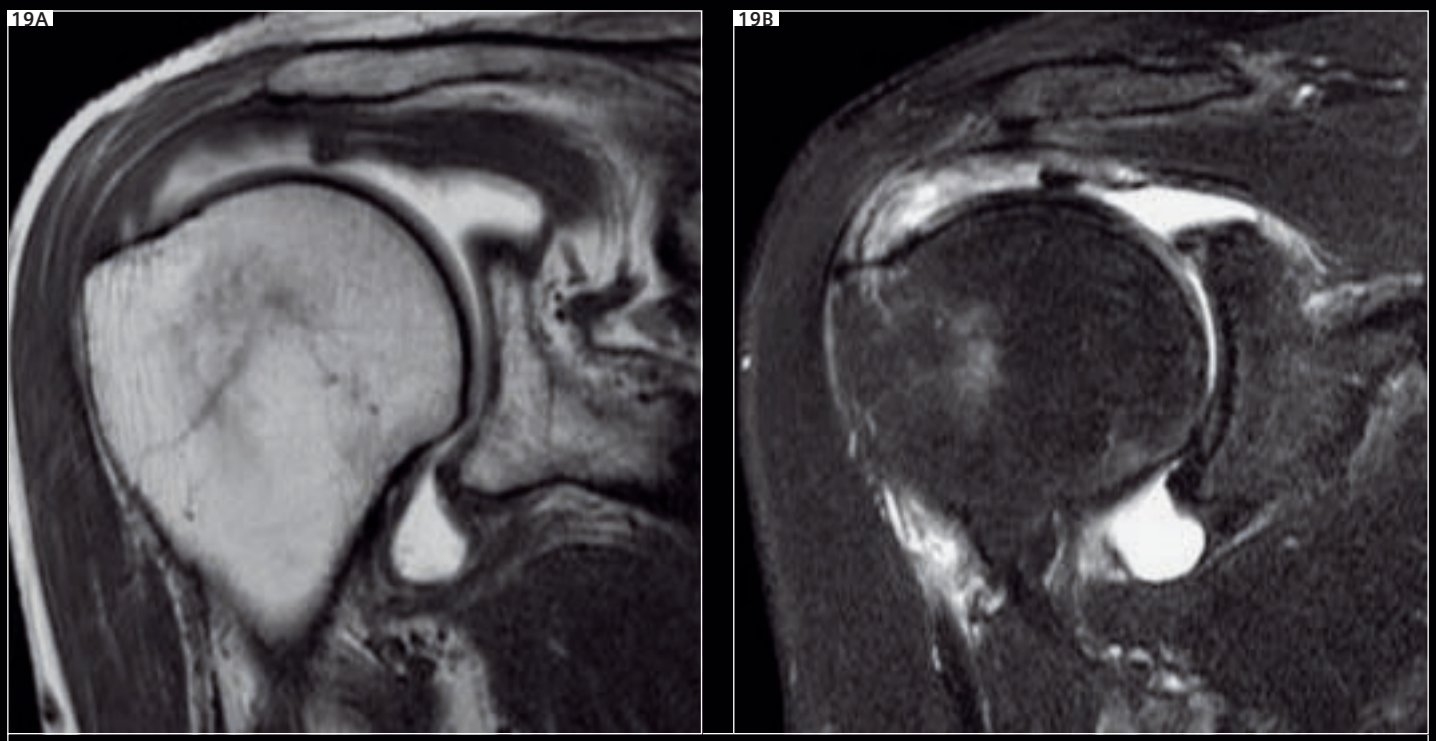

19 Coronal T1- and T2 FS-weighted sequences: delamination type undersurface partial tear of the supraspinatustendon.

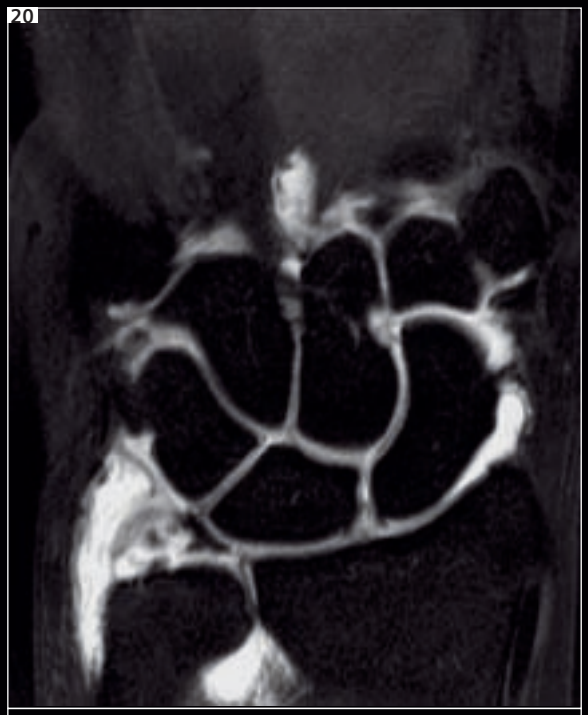

20 T1-weighted image with fat suppression, triangular fibrocartilage tear.

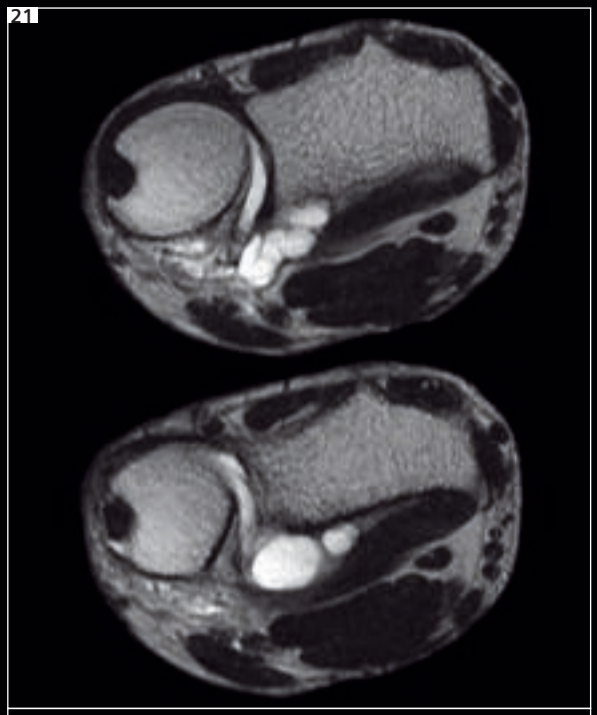

21 Axial T2-weighted image: synovial ganglion extending from the distal radioulnar joint (contrast in the joint!).

Acknowledgements

The author would like to thank Wanda Machado RT/MRI, Saint Mary's Regional Medical Center, Reno, NV, USA and Steve Sweet RT Director of Imaging Services and the whole MRI staff at Saint Mary's Regional Center for their skill, support and encouragement.

Isotropic MR Arthrography of the Shoulder Case Reports

Kunihiko Fukuda[1], Daichi Hayashi[1], Hiroki Funasaki[2]

[1]*Department of Radiology, The Jikei University School of Medicine, Tokyo, Japan*
[2]*Department of Orthopaedic Surgery, The Jikei University School of Medicine, Tokyo, Japan*

Case 1

18-year-old American football player with 2-year history of recurrent episodes of the left shoulder dislocation.

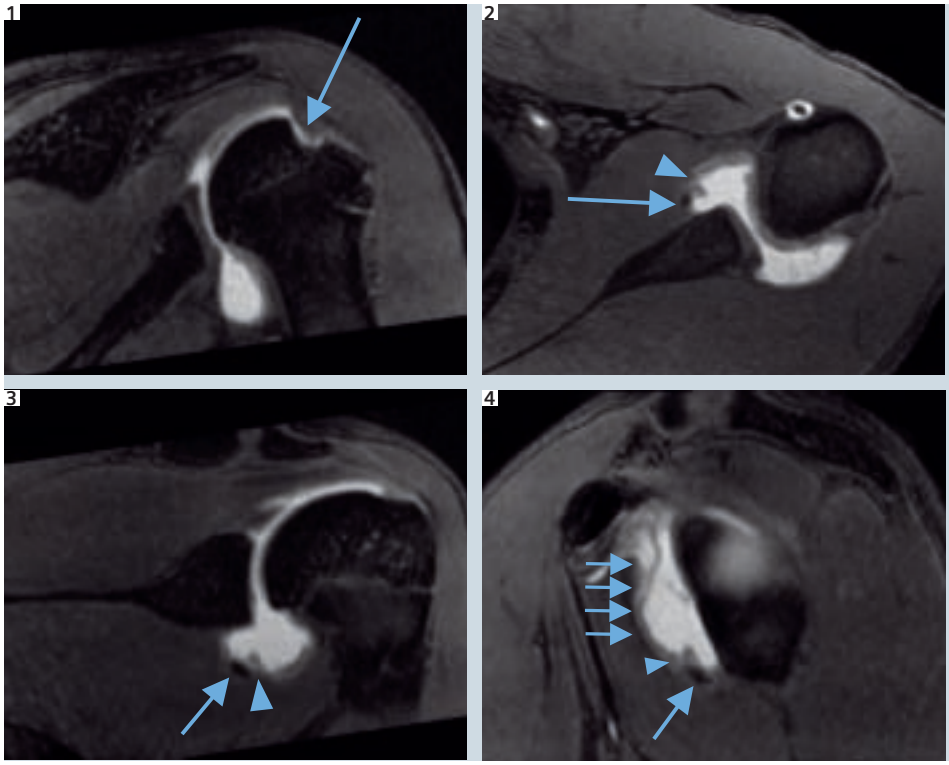

MRI findings

1 This steep oblique coronal image shows depression fracture of Hill-Sachs lesion in the postero-lateral aspect of the left humeral head (arrow).

2 3 4 Medial displacement of the antero-inferior glenoid labrum (arrows) and labro-AIGHL (Anterior Inferior GlenoHumeral Ligament) complex (arrow heads) are present. Anterior displacement of the MGHL (Medial GlenoHumeral Ligament) is also seen in the sagittal image (Fig. 4, double arrows).

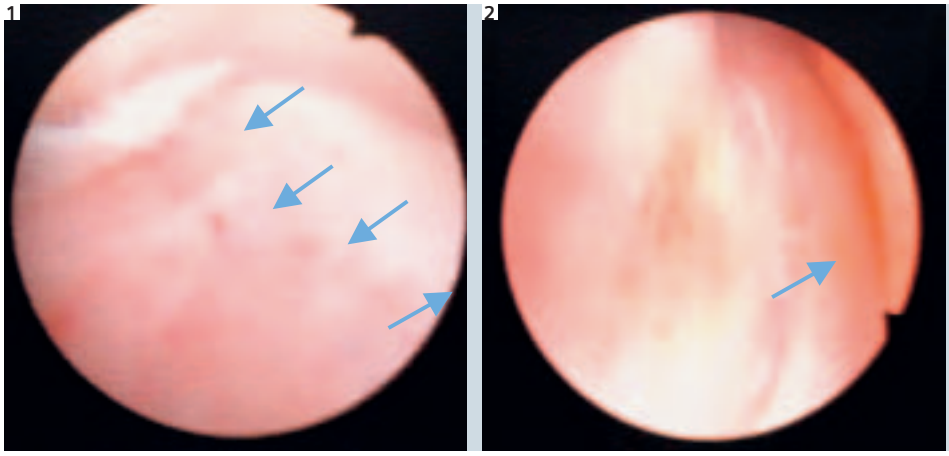

Arthroscopic findings

1 A large shallow impression of Hill-Sachs lesion is present on the postero-lateral aspect of the left humeral head (arrows).

2 Medial displacement of the labro-AIGHL complex (arrow) is noted on the glenoid margin, consistent with ALPSA (Anterior Labroligamentous Periosteal Sleeve Avulsion) lesion.

Case 2

43-year-old school teacher with 10-year history of recurrent episodes of the left shoulder dislocation.

1

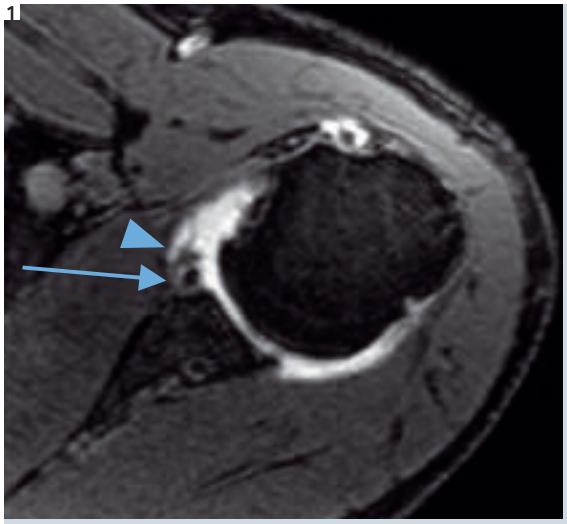

2

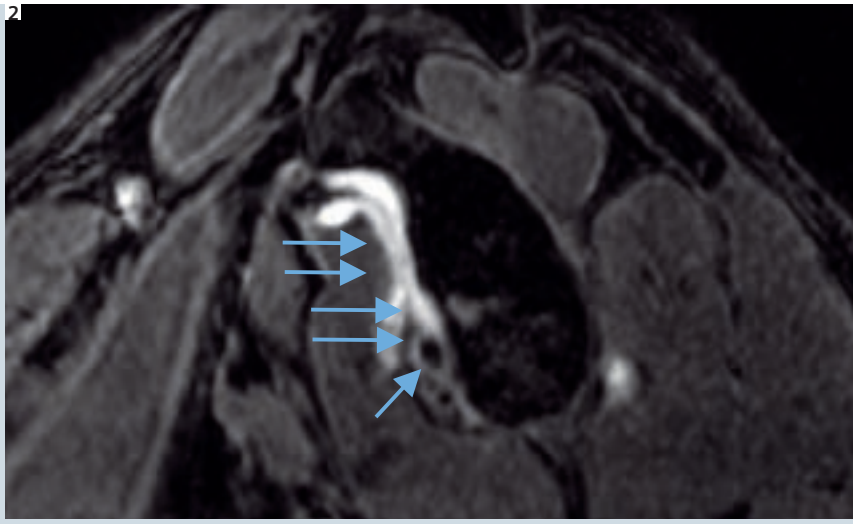

MRI findings

1 Bony fragment of the bony Bankart lesion is seen in the anterior glenoid margin (Figs. 1, 2, arrows). Labro-AIGHL (Anterior Inferior GlenoHumeral Ligament) complex is also displaced anteriorly together with the bony fragment (arrow head).

2 MGHL (Medial GlenoHumeral Ligament) is well depicted (double arrows)

1

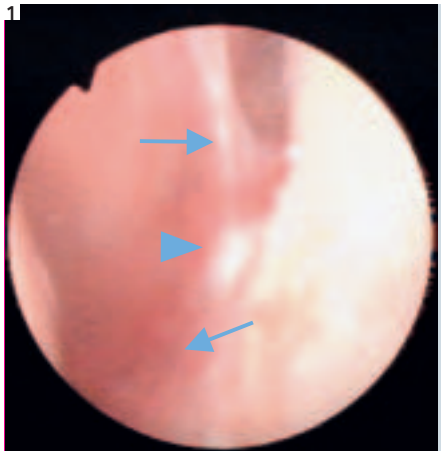

Arthroscopic findings

1 Detachment of labro-AIGHL complex (arrows) and a bony fragment (arrow head) from the glenoid margin is seen.

Sequences protocol	
3D VIBE	
TR/TE	*8.2/3.1 msec*
Flip angle	*12 deg.*
Band width	*150 Hz/pixel*
Fat Sat	*Water Excitation*
FoV	*205 x 205*
Matrix	*256 x 256*
Slice thickness	*0.8 mm*
Coil	*CP Body Array*
Acquisition time	*4:54 min.*

MR-Arthrography of the Hip

Stefan F. Werlen, M.D.

Klinik Sonnenhof, Radiology Dept., Bern, Switzerland

Introduction

This article describes the technique and findings of MR-Arthrography (MRA) of the hip joint, with special regard to the clinical setting of femoro-acetabular impingement.
MRA of the hip joint is a technique that uses intra-articular contrast medium, high field scanners and dedicated coils and sequences. With this technique only, one is able to detect subtle, but important changes of labrum, cartilage and bone of the hip joint. Today the direct MRA technique is widely used among musculoskeletal radiologists.

Examination Technique

Under fluoroscopic control, a 22-gauge spinal needle is introduced from ventral into the joint in the outer third of the head/neck-junction. Then 10 to 20 cc of diluted Gadolinium is injected.
All examinations are performed with a 1.5T Magnet (MAGNETOM Avanto, Siemens Medical Solutions, Erlangen, Germany). On the MR table a flex coil is positioned over the joint. After a short localizer in three planes the following sequences are used:
1. Axial T1-weighted sequence to assess bony structures and pathologies and also capsule configuration and thickness, as well as periarticular soft tissue changes (TR 650, TE 20, 200 mm field of view, 224 x 512 matrix, 4 mm slice thickness section thickness with a 0.2 mm section gap, 17 slices, 3 min).
2. Axial FLASH-sequence with a few thin slices, centered on the upper joint-space. This sequence is used to evaluate the version of the acetabulum and subcortical hypersclerosis and cystic changes of the acetabular rim (TR 550, TE 10, Flip angle 90°, 120 mm field of view, 256 x 256 matrix, 2 mm section thickness with a 0.1 mm section gap, 11 slices, 3:06 min).
3. Coronal-oblique protondensity-weighted (PDW) thin-slice sequence especially for the evaluation of the cartilage and its damages (TR 3200, TE 15, 120 mm field of view, 256 x 256 matrix, 2 mm section thickness with a 0.1 mm section gap, 23 slices, 5 min). This sequence is aligned perpendicular to the femoral neck and is marked on the axial T1-weighted sequence.
4. PDW sequence in sagittal direction also for cartilage assessment (TR 3200, TE 196 15, 120 mm field of view, 256 x 256 matrix, 2 mm section thickness with a 0.2 mm section gap, 23 slices, 5:37 min).
5. Radial PDW sequence is used in which all slices are oriented basically orthogonal to the acetabular rim and labrum. This sequence is based on a sagittal oblique localizer, which is marked on the PDW coronal sequence, and runs parallel to the sagittal oblique course of the acetabulum (TR 2000, TE 15, 260 mm field of view, 266 x 512 matrix, 4 mm section thickness, 16 slices, 4:43 min). In the center of the radial sequence, where the slices cross over, the signal wipes out. This produces a broad line without signal on the image, which affects the quality of the image. The more slices cross over, the broader the no signal line becomes. To reduce this artifact, this sequence is split into two sequences with 8 slices each. The whole examination, including the hip injection, lasts approximately 50 to 60 min.

Findings

In the impingement patients we found osseous changes, like retroversion of acetabulum and acetabular cysts. Osseous bumps and deformation of the femoral head/neck junction.
Often labral tears and ganglions are detected.
The PDW sequences showed nicely various cartilage defects and capsular thickening or scarring after surgical procedures.

References

1 Leunig M, Podeszwa D, Beck M, Werlen S, Ganz R, Magnetic resonance arthrography of labral disorders in hips with dysplasia and impingement., Clin Orthop 418, 74–80, Jan, 2004.
2 Locher S, Werlen S, Leunig M, Ganz R, [MR-Arthrography with radial sequences for visualization of early hip pathology not visible on plain radiographs], (Arthro-MRI mit radiarer Schnittsequenz zur Darstellung der praradiologischen Huftpathologie.), Z Orthop Ihre Grenzgeb 140: 1, 52–7, Jan–Feb 2002.
3 Magnetic Resonance Arthrography of the Hip in Femoroacetabular Impingement: Technique and Findings Stefan Werlen MD, Michael Leunig MD†, and Reinhold Ganz MD† Operative Techniques in Orthopaedics Volume 15, Issue 3 , July 2005, pages 191–203.
4 Werlen S, Porcellini B, Ungersböck A, Magnetic resonance Imaging of the hip joint. Seminars in Arthroplasty, Vol 8, Jan 1997.

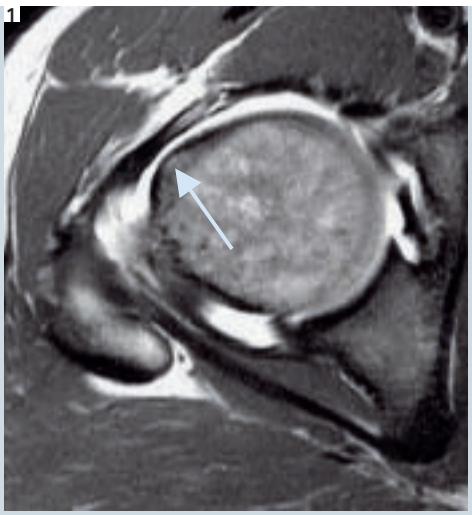

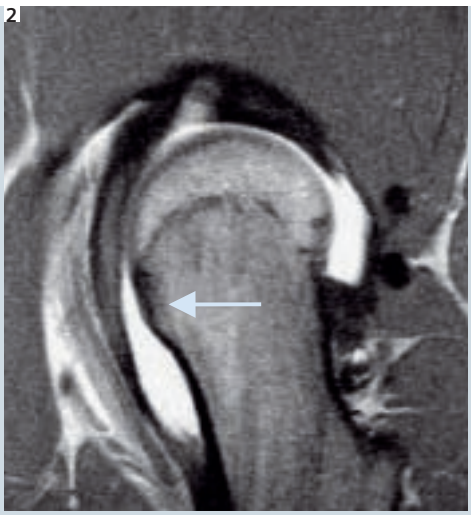

1 2 Osseus bump at the anterosuperior femoral neck, causing Cam Impingement.

3 Impingement cyst at the anterosuperior femoral neck.

4 White arrow indicating rupture of labral base.

5 Huge intra- and extracapsular labral ganglion.

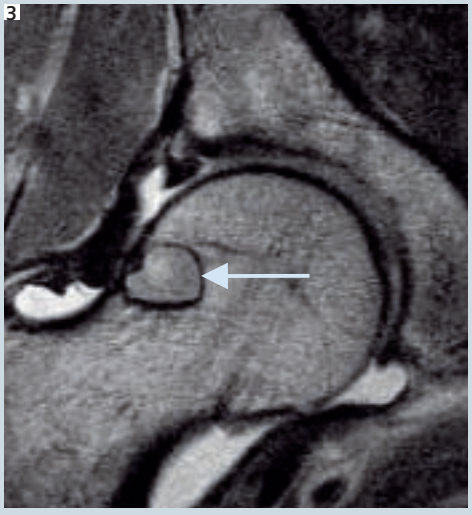

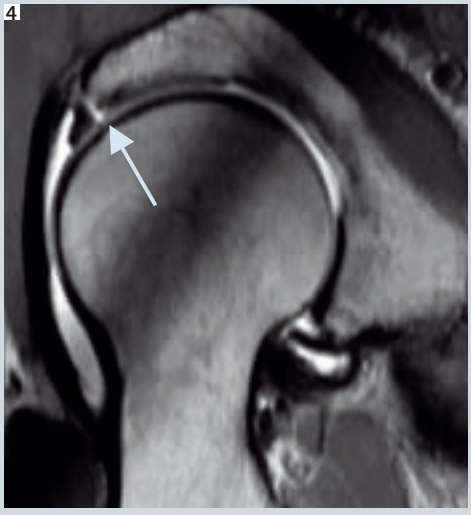

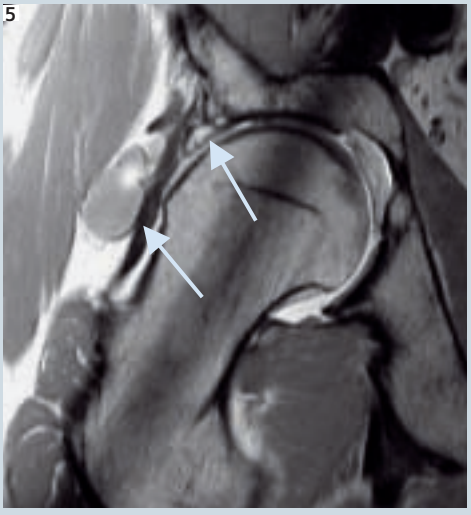

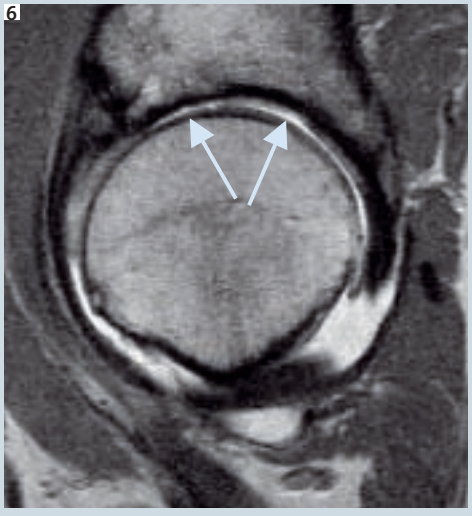

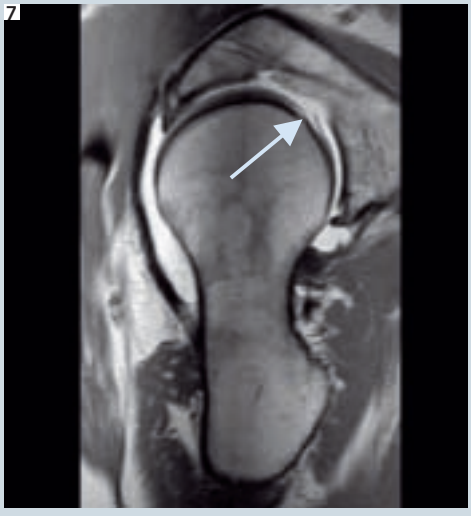

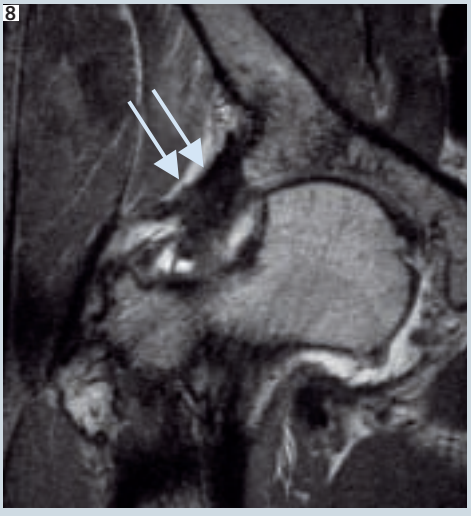

6 Focal cartilage ulcers at the acetabular joint surface.

7 Cartilage rupture and flap formation at the femoral head in pincer type impingement.

8 Extensive postoperative thickening and scarring of joint capsule.

Direct MR-Arthrography

Stefan F. Werlen, M.D.

Klinik Sonnenhof, Radiology Dept., Bern, Switzerland

Introduction

Direct MR-Arthrography is a widely used technique to diagnose intraarticular pathology. Unlike indirect methods as i.v. administration of Gadolinium, this method provides a fully distended capsule, which allows accurate distinction of intraarticular structures.

Technique

Puncture of the joints requires fluorocopic control except the knee. After proper disinfection and sterile coverage,the joint is punctured with a 22-gauge needle or a 22-gauge spinal needle and 1:200 diluted Gadolinium is injected. The amount of contrast injected ranges from 40 ml in the knee to 4–6 ml in the wrist.

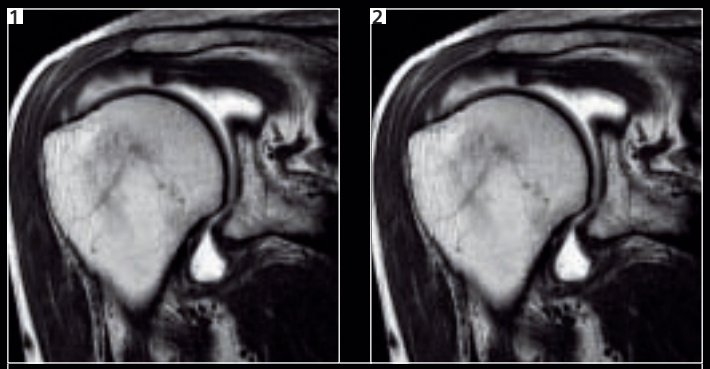

1 2 Coronal T1- and T2 FS-weighted sequences: delamination type undersurface partial tear of the supraspinatustendon.

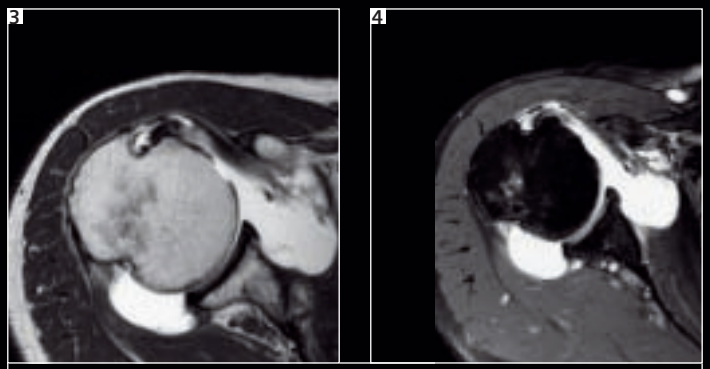

3 4 Axial T1-weighted and TrueFISP sequences: partial tear of the subscapularis tendon with subluxation of the biceps tendon, which shows severe degeneration.

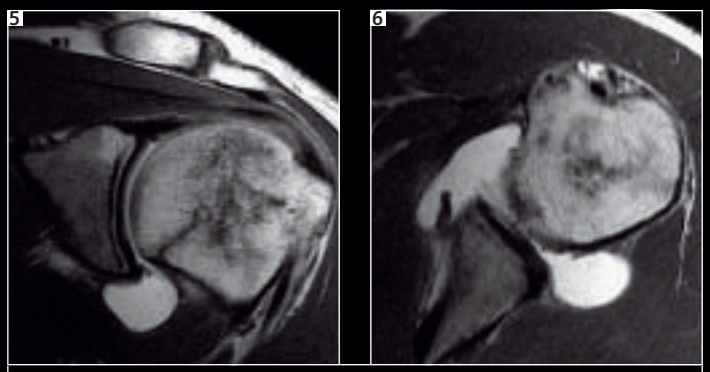

5 6 Coronal and axial T1-weighted sequences: ALPSA type lesion of anterior and inferior labrum after shoulder dislocation.

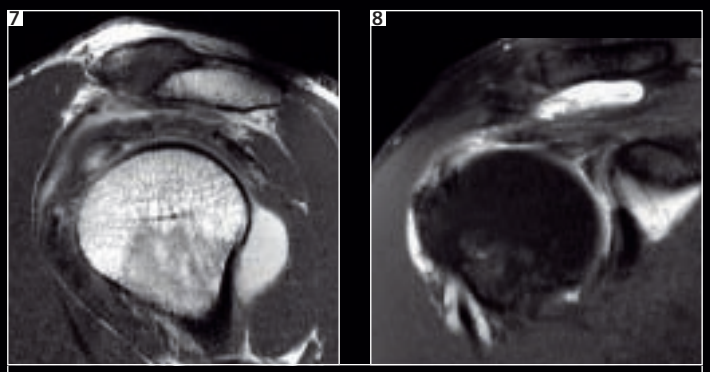

7 8 Sagittal T1-weighted and coronal T2 FS-weighted sequences: SLAP IV lesion with extension of the tear into the biceps tendon.

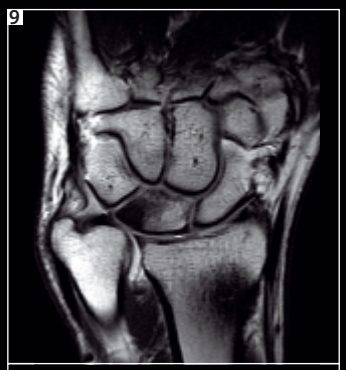

9 Coronal T1-weighted sequence: ulnar impaction syndrome with tear of the TFCC (triangular fibrocartilage complex).

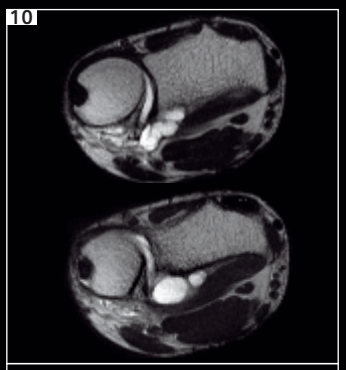

10 Axial T2-weighted sequence: synovial ganglion extending from the distal radioulnar joint (contrast in the joint!).

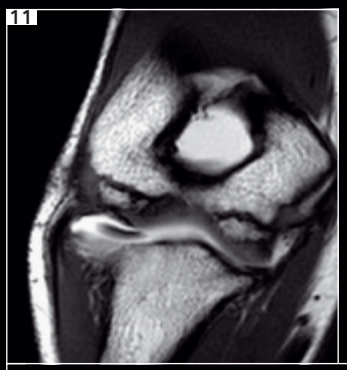

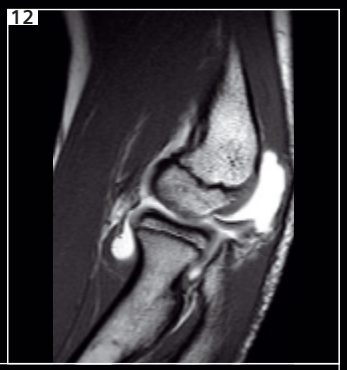

11 12 Coronal and sagittal T1-weighted sequences: cartilage flake from lesion of the capitellum humeri dislocated into the dorsal capsular recess.

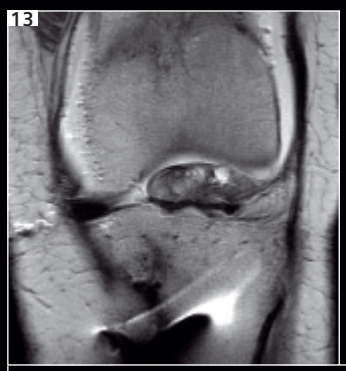

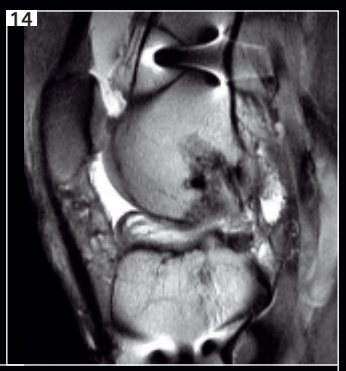

13 14 Coronal and sagittal protondensity-weighted sequence: cyclops lesion after anterior cruciate ligament replacement in the knee.

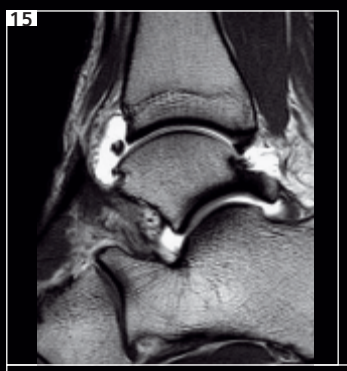

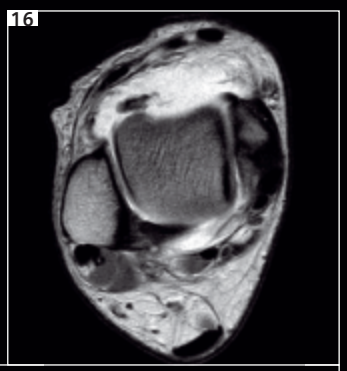

15 16 Sagittal T1-weighted and axial protondensity-weighted sequence: corpus liberum in the anterior capsular recess of tibiotalar joint.

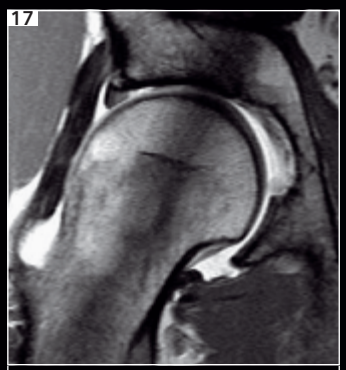

17 Radial protondensity-weighted (PDW) sequence: cartilage defect at the acetabular rim in impingement syndrome of the hip.

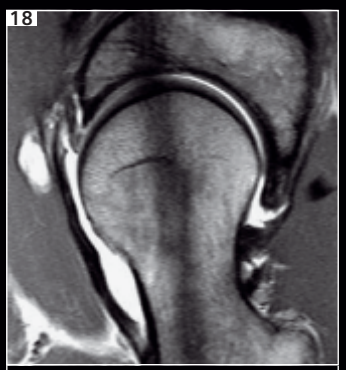

18 Radial PDW sequence: labral tear at base and extralabral ganglion formation in impingement syndrome of the hip.

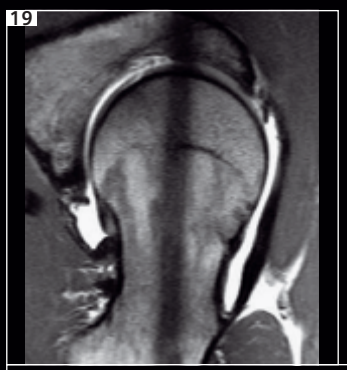

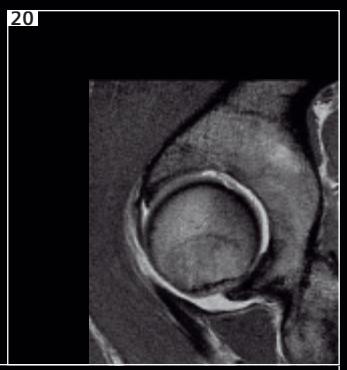

19 20 Radial PDW sequence: cartilage tear and flap formation in impingement syndrome of the hip.

Wrist Imaging with MAGNETOM Espree: Changing a Practice

Robert W. Prost, Ph.D.[1]; Bradley D. Bolster, Jr., Ph.D.[2]

[1]*Department of Radiology, Medical College of Wisconsin, Milwaukee, WI, USA*
[2]*Siemens Medical Solutions, USA*

Background

One of our long-standing areas of expertise at Froedtert hospital has been wrist imaging. MRI of the wrist is particularly useful in the diagnosis of pain and instability due to ligament injuries, bone edema and occult fracture.
Due to the scale of the anatomy involved, wrist MRI requires a large imaging matrix at small FoV, necessitating high signal-to-noise ratio (SNR). Originally we used single-turn solenoid coils which were built in the Biophysics department. These close-fitting coils produced excellent image quality at fields of view which were as small as the manufacturer's gradients could create (8 cm). While the image quality was excellent, the positioning was the source of both benefit and difficulty. In a superconducting 1.5T magnet, the solenoid coil had to be oriented with the axis of the coil perpendicular to that of the magnet bore. Therefore patients had to lie prone with their wrists superior to their heads. This placed the coil at or near magnet isocenter which resulted in outstanding image quality and excellent fat suppression. The patients paid a price for this in that their arms were overhead for the entire exam and the shoulder stress was not insubstantial. The prone position also contributed to claustrophobia.
Recently, a small general purpose transmit/receive birdcage coil became available from Mayo Clinic Medical Devices (Rochester, MN, USA) for Siemens MAGNETOM scanners with Tim (Total imaging matrix). The BC-10 has a 10 cm diameter, as its name suggests, and allows for comfortable wrist positioning in a natural hand position as opposed to the flattened position required with many wrist specific coils. It also allows for a more natural positioning of the arm inline with the body.

A Case Study

Our first patient for the BC-10 coil was a department employee we'll call Maddie. Maddie had a several year history of wrist pain with possible arthritic degeneration. Her job duties included extensive use of a keyboard, which aggravated the wrist pain. Her orthopedic surgeon had prescribed a wrist MRI. After six months of worsening wrist pain, Maddie still had not made an appointment for her test. Her reasons turned out to be two-fold. First,

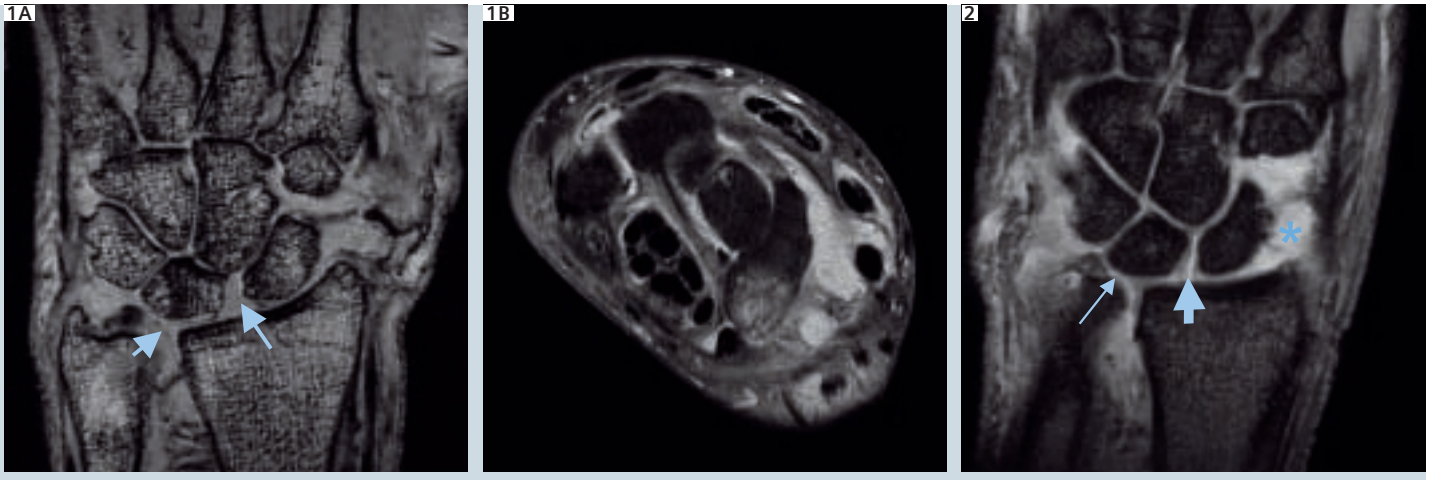

1 A coronal gradient echo image of Maddie's wrist demonstrating arthritic degeneration with a widened scapholunate space and possible triangular fibrocartilage (TFC) tear (A). Axial fat suppressed protondensity-weighted image demonstrating extensor tendon sheath effusion.

2 A 55-year-old male with wrist pain demonstrating both TFC (thin arrow) and lunotriquetral tears. Synovial hyperplasia (*) can also be well appreciated.
A scapholunate ligament defect is also questioned (thick arrow).

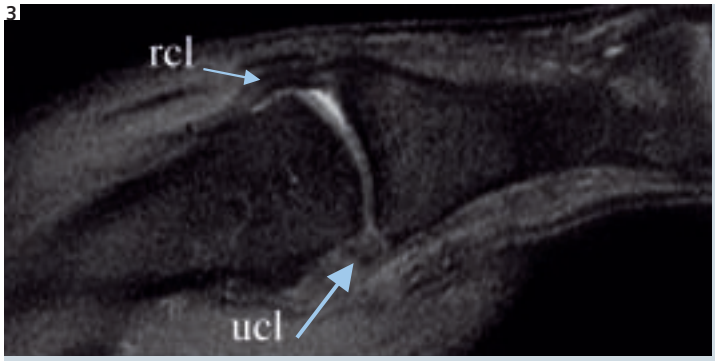

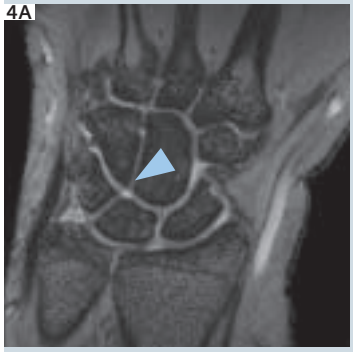

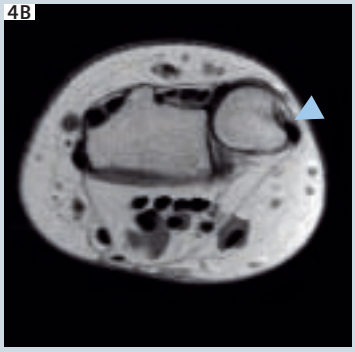

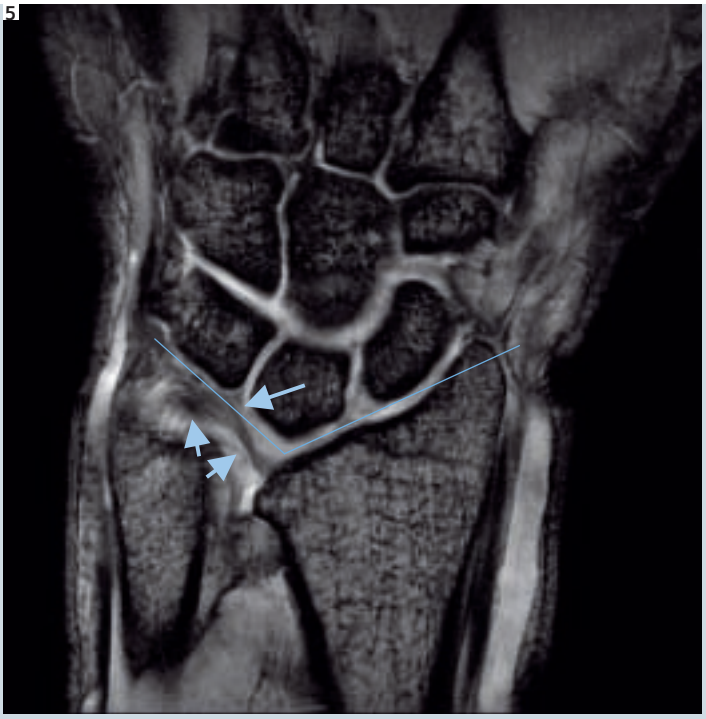

3 Coronal image of the thumb in an 18-year-old woman with a possible gamekeepers' injury. The tendons are intact and the patient was treated without surgery.

4 A 24-year-old woman imaged after a motor vehicle accident and referred for ongoing ulnar nerve pain and wrist instability. A scapholunate tear is demonstrated (large arrowhead) as well as a subluxation of the extensor carpi ulnaris (small arrowhead).

5 A 26-year-old woman with complaint of wrist pain. Madelung's deformity is well visualized in these coronal images with a characteristic V-shape proximal carpal row caused by a congenital underdevelopment of the head of the radius. The TFC (short arrows) and lunotriquetral ligament (long arrow) are well shown and intact.

she was claustrophobic and did not want to lie in the magnet, especially in the prone position. Second, she had a previous shoulder injury ipsilateral to the painful wrist. She was unable to lift her arm straight over her head and so did not want to endure what was certain to be a painful and unsettling exam.
The MAGNETOM Espree, combined with the BC-10 resulted in an optimal solution. Maddie was placed in the decubitus position with the affected wrist on the padded table surface. The coil was placed over the wrist, and sandbagged against her thigh. Once in the magnet, Maddie was able to lean back against the bore wall with a cushion behind her knees for the comfort of her back. Maddie did not suffer any claustrophobia as her head was entirely out of the magnet, despite her being only 5' 4" (1.64 m) tall. She also did not suffer any shoulder pain. The wrist was very close to isocenter, and the image quality was outstanding. As a result of the MRI, her pain has been discovered to be primarily arthritic in nature and she has avoided surgery.
In addition to wrist injuries, the BC-10 coil has also been used to image fingers as shown in Fig. 3. The very small fields of view which are achievable with this coil enable high resolution images of the small ligaments found in the fingers. Small FoV images are inherently more sensitive to motion than are large FoV images. The patient comfort achievable with the BC-10 coil in the decubitus position has improved patient comfort and cooperation which are key to obtaining motion-free images.

Discussion and Conclusions

In the last four months, we have scanned approximately 25 patients for wrist, finger, thumb and elbow indications. The decubitus position is used for nearly all of these patients. Image quality is equal to or better than that which we obtain with our solenoid coil. Patient scans can be completed in 30-45 minutes rather than the 45 minutes to 1 hour slots on the conventional scanners.
The BC-10 is a birdcage coil rather than phased array. As a result we are not able to use integrated Parallel Acqusition Technique (iPAT) in our sequences. This has not been a problem in wrist imaging. We image almost exclusively at an 8 cm FoV and our objectives are to achieve maximum signal-to-noise with maximum spatial resolution. With the huge improvement in patient comfort afforded by the combination of MAGNETOM Espree, BC-10 and decubitus position, the exam does not require further hastening.

Literature
1 Kocharian, A., Adkins, MC., Amrami, KK, et. al. Wrist: Improved MR Imaging with Optimized Transmit-Receive Coil Design. Radiology 2002; 223: 870–876.
2 Zlatkin, MB., Rosner, J. MR imaging of ligaments and triangular fibrocartilage complex of the wrist. Radiologic Clinics of North America. 44(4): 595–623, ix, 2006 Jul.

Water Excitation in Musculoskeletal Low-Field MR Imaging (0.2 Tesla)

Wallabh D. Upasani, M.D.; Priti Upasani, M.D., D.N.B., D.M.R.E.

Thane Scan Center, Mumbai, India

Introduction

MR imaging is an important component of musculoskeletal (MSK) imaging. With new developments in RF coils, high-field magnets and new techniques like cartilage mapping, MSK imaging is getting better.
For the low-field systems (0.2T) Water Excitation (WE) has proven to be very beneficial. This article will give the reader an insight into advantages and limitations of the water excitation technique on a 0.2T system.

Importance of fat suppression

While investigating shoulder joint pain, WE demonstrates the inferior acromial spur causing the impingement much better than the T2-weighted images due to suppression of bone marrow fat signal (Fig. 1).
Fat suppression also offers better contrast-to-noise ratio, which enables better detection of marrow lesions and facilitates post-contrast imaging. Also fat suppressed images show fewer artifacts as chemical shift artifacts decrease with fat suppression.
There are three basic techniques of fat suppression: (1) spectral fat suppression technique, also known as fat sat, (2) inversion recovery technique or STIR, and (3) water excitation technique or WE.

Low field fat saturation

Fat-water frequency (3.3 ppm) is too narrow (28 Hz) at low field compared to 1.5T systems (200 Hz), which makes fat suppression difficult at low field strength. Post-contrast T1-weighted fat suppressed imaging is a challenge on 0.2T systems and in that context the water excitation technique is clinically relevant.

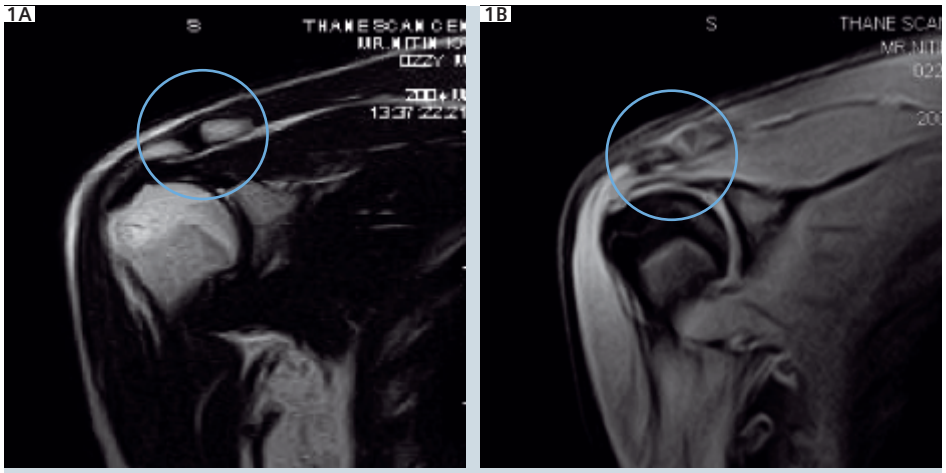

1 **(A) T2-weighted coronal image in a case of impingement.
(B) WE image shows the inferior acromial spur much better.**

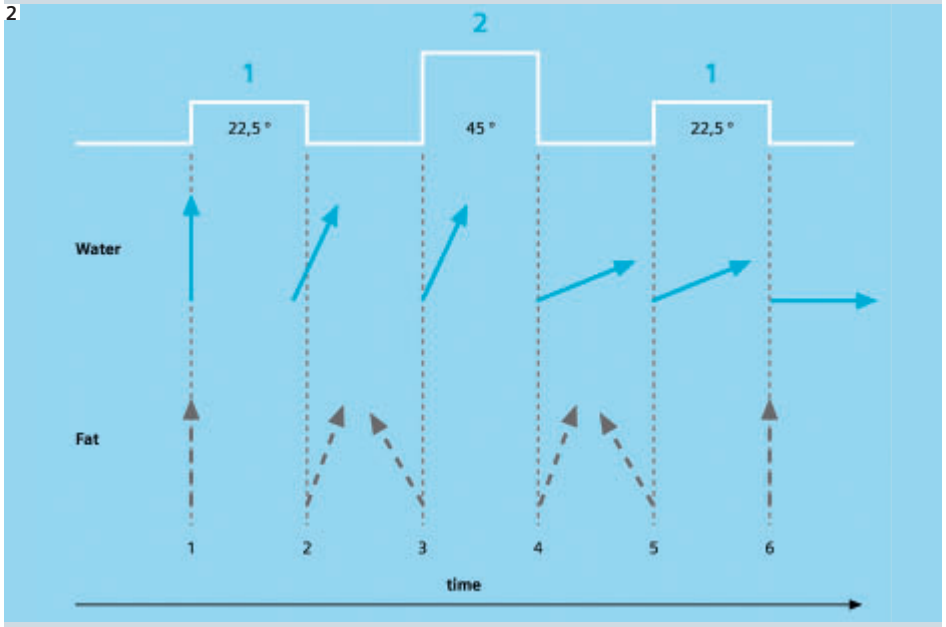

2 **Shows water and fat net magnetization after the (1-2-1) binomial pulse that is used in the WE technique. Note that fat net magnetization remains parallel to the main magnetic field and hence does not contribute to any signal resulting in fat suppressed images.**

Courtesy of Willhem Horger, Siemens Medical Solutions, Erlangen, Germany.

Principle of Water Excitation

Water Excitation utilizes binomial excitation pulses which effect only water protons leaving fat protons almost unexcited. At the end of the binomial pulse, the water net magnetization is rotated into the transverse plane (producing signal) while the fat net magnetization remains parallel to the main magnetic field, producing no signal. Fig. 2 shows water and fat net magnetization after the (1-2-1) binomial pulse that is used in the WE technique. Note that fat net magnetization remains parallel to the main magnetic field and hence does not contribute to any signal resulting in fat suppressed images.

Benefits of Water Excitation

1. WE is faster than STIR and allows more anatomical coverage. WE allows shorter TR and therefore shorter scan time as compared to STIR (Fig. 3).
2. WE offers better contrast-to-noise ratio, which enables better detection of lesions (Figs. 4 and 5). WE is of great utility in knee MRI where diagnosis of meniscal injury is in doubt. Better delineation of signal abnormality with WE increases the confidence level of diagnosing meniscal tear.
3. Post-contrast imaging: Post-contrast T1-weighted fat suppressed imaging is a challenge on 0.2T systems and in that context the Water Excitation technique is clinically relevant (Figs. 6, 7 and 8).

How do we perform WE on our MAGNETOM Concerto?

The prerequisite for obtaining water excitation images is performing multiple frequency offsets, for example -10 Hz, -5 Hz, 0 Hz, 5 Hz, 10 Hz, 15 Hz. The ideal frequency offset is the one which shows darkest marrow signal and relatively bright signal of the cartilage. The actual procedure is as follows:
1. After registration and positioning of the patient in the appropriate coil, activate the exam-card. *syngo* MR user interface is easy to use and helps transfer the measurement program in the exam queue with a single mouse-click. The localizer runs automatically and the first trial protocol opens up for positioning

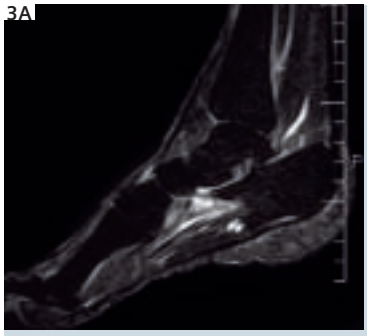

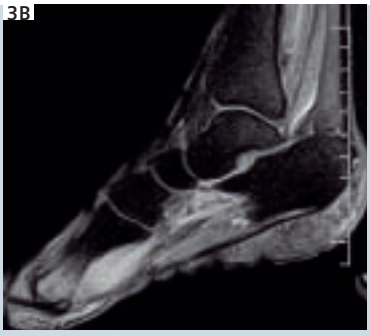

3 Comparison of STIR and WE techniques. (A) STIR sequence, TR 3390 ms, 13 slices, 4 mm thick, TA 8:54 min. (B) WE, TR 33 ms, 22 partitions, 4 mm thick, TA 4:47 min.

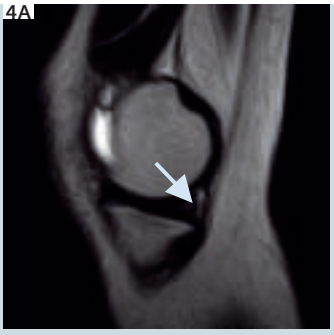

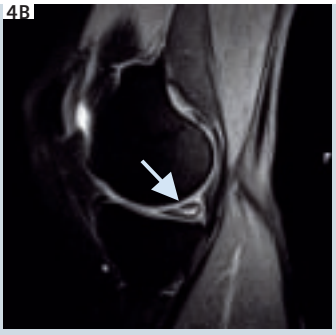

4 Abnormality in the posterior horn of medial meniscus is difficult to characterize in A (T2-weighted sagittal image). B (WE) optimally demonstrates the tear in the posterior horn of medial meniscus.

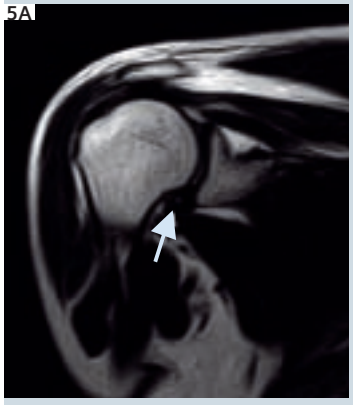

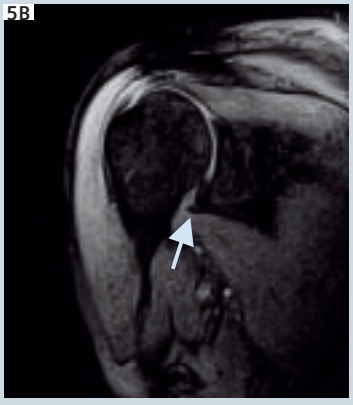

5 Inferior labral tear is not well appreciated in A (T2-weighted coronal image) but is well demonstrated in B (WE).

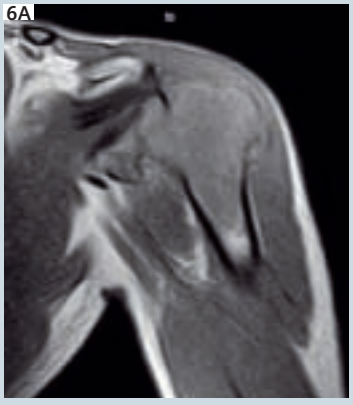

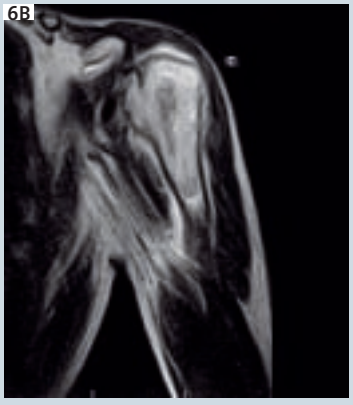

6 Marrow abnormality in the proximal end of the humerus is diffuse in A (T1-weighted coronal image). B (WE) depicts the aggressive nature of the lesion which turned out to be Osteosarcoma at surgery.

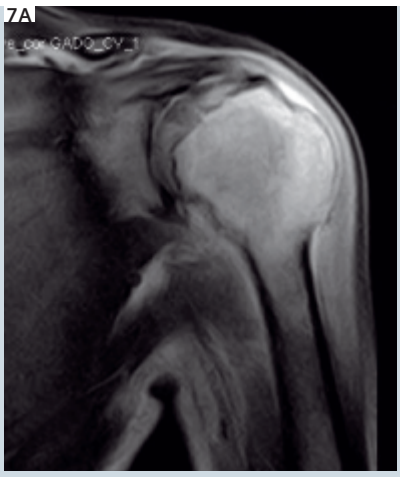

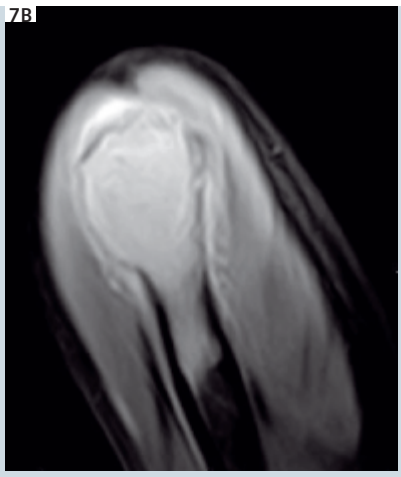

7 Post-contrast enhancement is much better in B (WE) due to fat suppression than in A (T1-weighted sagittal image).

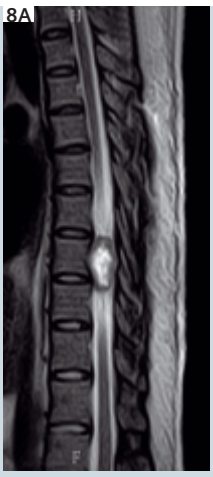

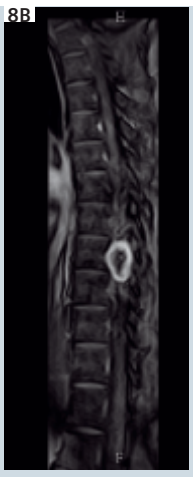

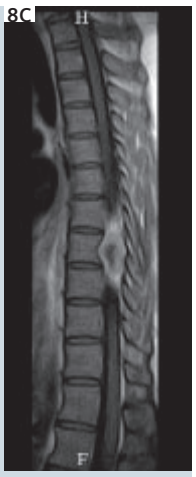

8 A (T2-weighted sagittal image) shows a focal lesion in the spinal canal in the dorsal spine. The enhancement of the lesion is much better highlighted in B (WE sagittal, post-contrast) than in C (T1-weighted sagittal, post-contrast) which turned out to be neural sheath tumor at surgery.

the volume to be scanned. The intuitive software copies the position, orientation and extend of slice group via copy reference to the final protocols.
2. After automatic adjustments, trial measurements 22 seconds each run automatically.
3. The entire program is optimized for workflow where the measurement queue stops with Pause – "check for best..."
4. This is the time when the operator needs to find the best frequency offset. The ideal frequency offset is the one which shows darkest marrow signal and shows relatively bright signal of the cartilage.
5. In the sequence card, part 2, the operator needs to key in the correct offset and apply the change (red circle in Fig. 9).
6. The final measurement will complete and generate a WE set of images.

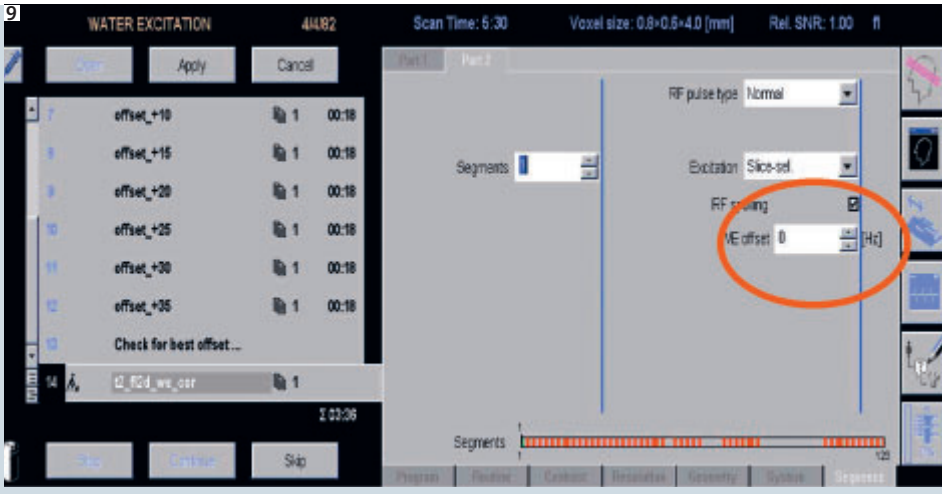

9 Showing where the operator needs to key in the correct frequency offset.

Challenges with WE on 0.2T

1. WE is more sensitive to flow artifacts, hence these artifacts are exaggerated. Appropriate sat bands when positioned reduce these artifacts.
2. If the correct frequency offset is not selected, fat suppression is not achieved and the measurement needs to be repeated.

Conclusion

WE technique is of great value to us at low-field especially post-contrast imaging. WE technique provides better coverage and is faster than STIR, which is beneficial to patients in acute pain. With WE the referring clinicians receive additional information to help manage their patients better.

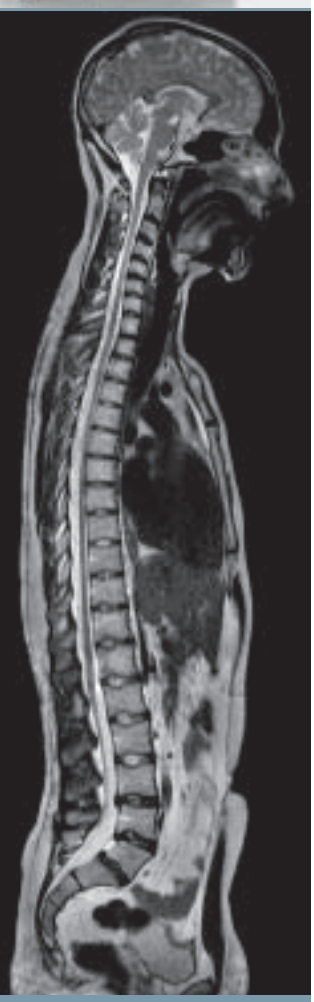

We see a way to seamlessly image up to 100 cm FoV within a single exam

Small footprint giant steps

We see a way to position up to 4 coils simultaneously for true multi channel imaging

Proven Outcomes in Magnetic Resonance.

Discover the changing face of midfield MRI with MAGNETOM® C!. Work that flows, image quality that convinces and patient comfort that satisfies. Distilled into the most compact C-shaped magnet with a pole diameter of only 137cm. High-field technology and superior workflow support deliver high diagnostic confidence in a cost-friendly package. MAGNETOM C! – small footprint, small investment, giant steps in quality health care.

www.siemens.com/medical

SIEMENS
medical

MR-Z884-10-7600

Results may vary. Data on file.

Application Hints for MR Orthopedic Imaging: The Knee Examination

Steve Rigsby, MR Internal Education Specialist

Siemens Medical Solutions USA

Introduction

Advancements in coil technology, sequences, and optimization of the spectral fat saturation process have improved MR image quality of the knee.

Coils

Depending upon the Siemens MAGNETOM system and configuration used, there are a variety of coils available. These include both radio frequency (RF) receive (Rx) only and RF transmit (Tx) and receive coils. These two RF options offer circular polarized (CP), multiple element array and Tim Matrix coils. All of these coil options have advantages for improving image quality in knee imaging, but we will focus on the use of *syngo* GRAPPA (iPAT) and its benefits. *syngo* GRAPPA uses multi-element coils, aligned in the phase encoding direction, which combines under-sampled phase encoding data from each coil's raw data before Fourier-Transform to produce the final reconstructed image. iPAT is utilized to optimize some of the sequences being discussed in the next section. It reduces scan time without loss of image resolution which increases exam throughput.

Table 1: iPAT Compatibility Chart

Coil Name	# of Channels	Sagittal iPAT	Coronal iPAT	Transverse iPAT
CP Extremity	1	no	no	no
Tim Body Matrix	6	yes	yes	yes
8-Channel knee coil (1.5T)	8	Yes (R to L only)	Yes (R to L only)	yes
3T CP Tx/Rx	1	no	no	no
8-Channel knee coil (3T)	8	Yes (R to L only)	Yes (R to L only)	yes

Application Hint: In order to use the iPAT (integrated Parallel Acquisition Technique) option a multi-element coil must be utilized. If you only have a CP coil and want to utilize this option, the Tim Body Matrix coil is a good alternative. There are simple rules to follow if using this option: Do not overlap the coil ends as stronger bending can result in damage to the coil electronics. Do not bend the coil crosswise. Use fixation material and cushions to avoid patient motion during the examination.

Coil examples for current MAGNETOM systems:
1. CP extremity coil,
2. Tim Body Matrix coil,
3. 1.5T 8-channel Rx Coil,
4. 3T CP Tx/Rx Coil,
5. 3T 8-channel Tx/Rx coil

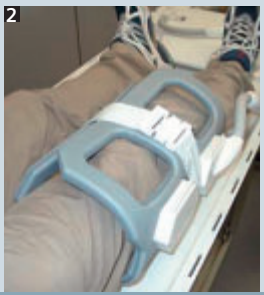

Sequences

Aside from the standard T1, T2, GRE and TIRM sequences, two sequences useful for orthopedic imaging are *syngo* SPACE (Sampling Perfection with Application optimized Contrasts using different flip angle Evolutions), and *syngo* BLADE. The first is a three dimensional scan allowing for very thin slice partitions. If isotropic resolution is used MPR (multi-planar reconstruction) can be performed to generate images of equal resolution in alternate image planes. The second is two-dimensional imaging but is used to compensate for patient motion and vascular flow motion related artifacts. *syngo* SPACE is a single slab 3D-TSE with variable flip angle over the echo train, using non-selective refocusing pulses, which allows for short echo spacing and ultra-high turbo factors. This sequence can be combined with an inversion recovery and restore pulses to offer T1, T2, PD, DarkFluid and Fluid contrast. Using iPAT with this sequence reduces the scan time and specific absorption rate (SAR) without loss of image resolution.
syngo BLADE is a motion insensitive multi-shot Turbo Spin Echo (TSE) se-

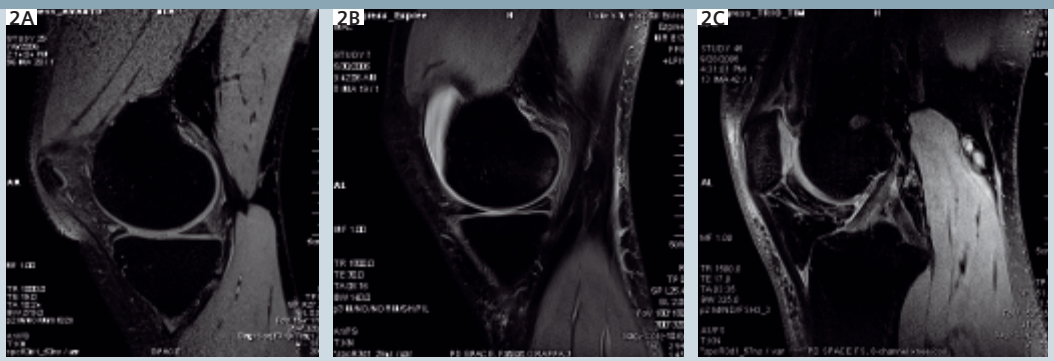

2 Examples of *syngo* SPACE (protondensity-weighted sagittal image with fat suppression) from A: MAGNETOM Espree, B: MAGNETOM Avanto C: MAGNETOM Trio, A Tim System. Each of these scans has 2 mm or less in-plane resolution.

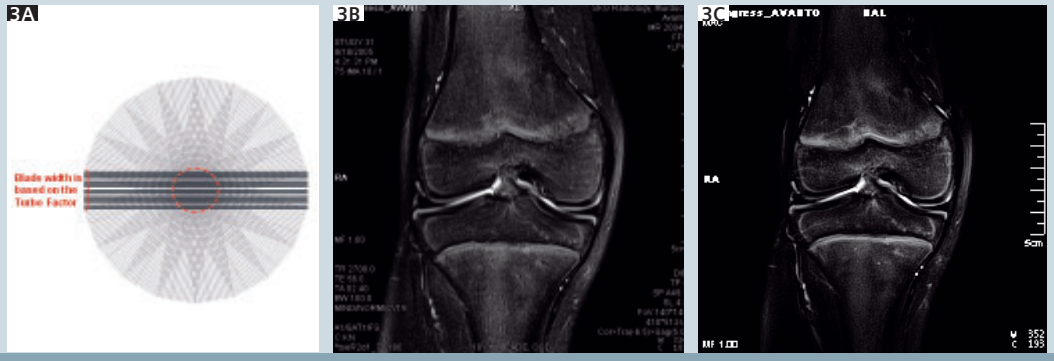

3 For *syngo* BLADE k-space is filled in a radial fashion. B: Without motion correction. C: With *syngo* BLADE.

quence with inter-shot motion correction for in-plane motion. K-space is filled in a radial fashion (see Fig. 3A). It can be used in any image plane. iPAT can be used to increase the accuracy of the motion correction due to broader blades, reduce SAR, and generate faster acquisitions.

Application Hint:
1. When using *syngo* BLADE with a CP or single channel coil ensure the "coil combine mode" within the protocol has the "sum of squares" option selected.
2. Since a radial filling is used with *syngo* BLADE, the phase encoding direction changes with every projection of this BLADE, and therefore wrap is a concern in the sagittal and coronal plane. To correct for this, use a slightly larger FoV as well as sat bands to minimize aliasing.

Optimization of Fat Saturation Process

When performing spectral fat saturation techniques with automatic frequency adjustments the results are not always optimal. This could be a result of the anatomy positioned far from iso-center. To correct or confirm the accuracy of the fat and water peak adjustments there is a simple pre-scan procedure to follow. On the selected protocol, choose the "confirm frequency adjustment" option on the "system>adjustment" tab. When the automatic adjustments are completed a pop-up will appear on the screen. This will give a graphic display of the water peak (default on the right) and the fat peak (default on the left).
The next step is to "float" the curser over the fat peak on the graphic display. If the number displayed in Hertz is the separation of fat from water for the field strength of the scanner, based on the chart (Table 2), the adjustment is correct. The scan can be started by selecting the continue icon. If the number displayed is not correct, for example 235 H difference on a 1.5T system, a manual adjustment of the frequency can be performed.
To perform this manual adjustment from this same graphical display, select the fat peak (left click). The system frequency will temporarily adjust to the center of the fat peak (a red line will display on the fat peak). The next step is to add the appropriate Hertz value (from chart above) to this temporary value. This will re-adjust the frequency to allow the spectral fat saturation RF pulse to suppress the fat peak. For example, based on the values seen in the graphical display above, the system frequency is 63.659134: Adding 220 H would now change the frequency to 63.659354. Select the "apply" icon and then the "continue" icon to start the scan. This process can be used for fat saturation throughout the body to improve this technique.
These application hints provided for coil selection, iPAT use, sequences and optimization of fat saturation can help to improve the knee examination image quality.

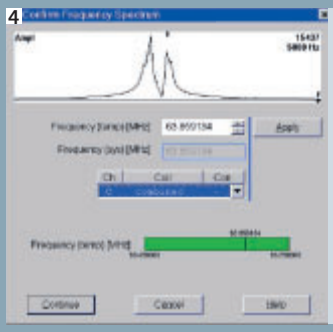

4 Graphical display of confirm frequency.

Table 2: Fat/Water separation

Field Strength	Freq. separation of fat and water
1.0T	145 H
1.5T	220 H
3.0T	440 H

Fat/water separation in Hertz per field strength.

MR Imaging of the Carpometacarpal Joint of the Thumb

Carola Stöcks

Radiologie München Nymphenburg, Munich, Germany

You can use either the knee coil or small flex coil for the examination of the carpometacarpal joint of the thumb.
The knee coil is the coil of choice. If contrast medium will be administered, it is advisable to perform vein puncture prior to positioning the patient.

Patient positioning

For this examination, the patient is placed in the prone position with the extremity to be examined extended on the patient table. **Note:** A head first/supine position should be registered, since the extremity to be examined is extended forward but not rotated.
Ideally, the hand to be examined is positioned outstretched (with the back of the hand pointing upward) in the knee coil. The respective arm and the shoulder are cushioned with foam pads to obtain the most horizontal position possible. The thumb should not be angled, but positioned in a straight line and cushioned/stabilized with foam wedges. To counteract involuntary fasciculations, it is recommended to place a sandbag on the hand prior to closing the coil. Some patients find it comfortable to have a foam rubber roll placed under their legs to help stabilize the body.

Slice positioning

After generating the first scout localizer of the hand, an extended transverse localizer is planned for across the carpometacarpal joint of the thumb (e.g. T2, 6

1 2 Knee coil positioning.

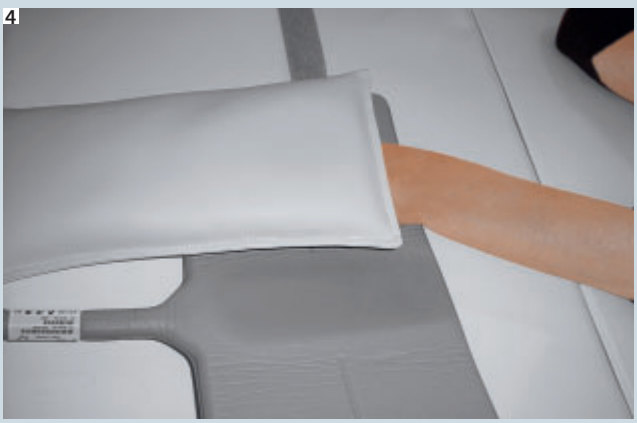

3 4 The examination can be performed with the small flex coil as well. Small flex coil positioning.

slices, 1 averaging, duration: approx. 6 s). This technique enables additional exact planning of the coronal (Fig. 2A) and sagittal slice positions (Fig. 3A), for evaluating the ulnar and radial collateral ligament (Fig. 2B) as well as the flexor and extensor tendons (Fig. 3B).
In addition, the FoV (field of view) should not exceed > 150 mm and the SNR (signal-to-noise ratio) should be 1.00 (max. 1.20 – min. 0.80).

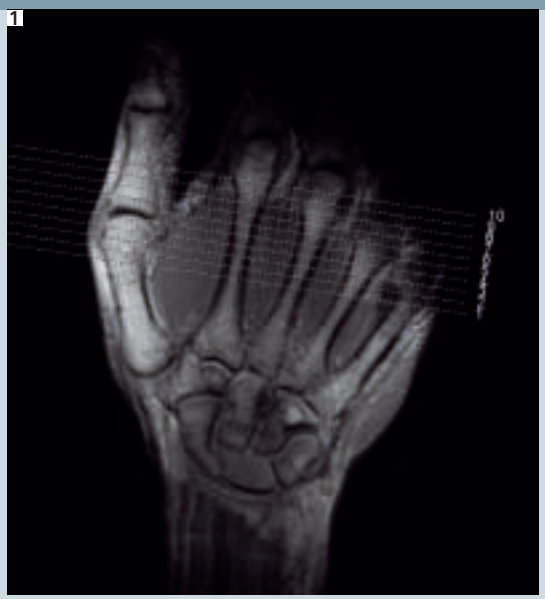

1 Coronal localizer with a transverse slice position through the basal joint of the thumb.

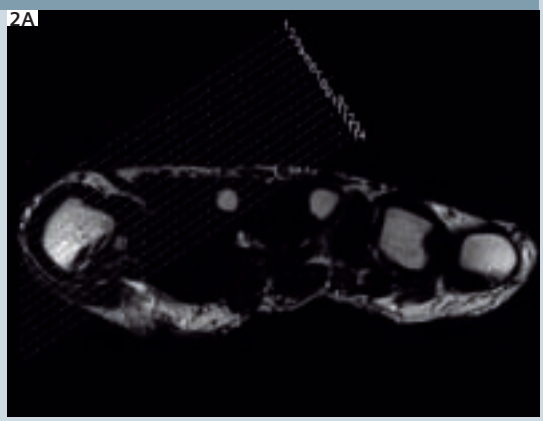

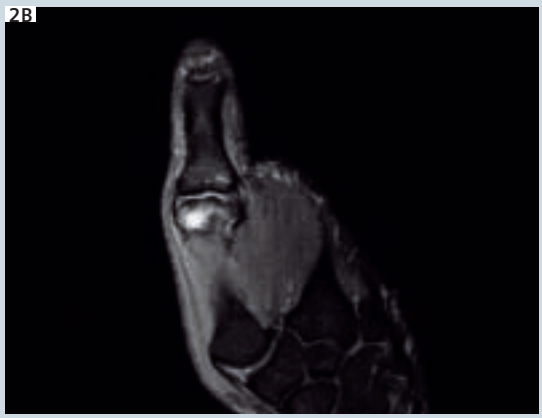

2 A: Planning a coronal slice position on a T2-weighted axial image.

B: Resulting coronal image of the basal joint of the thumb, displaying the radial and ulnar ligaments.

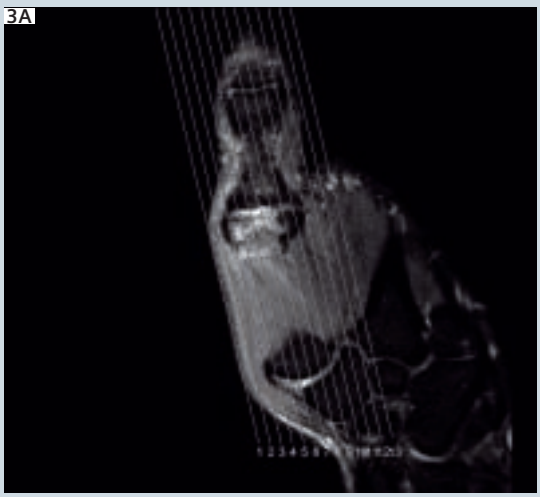

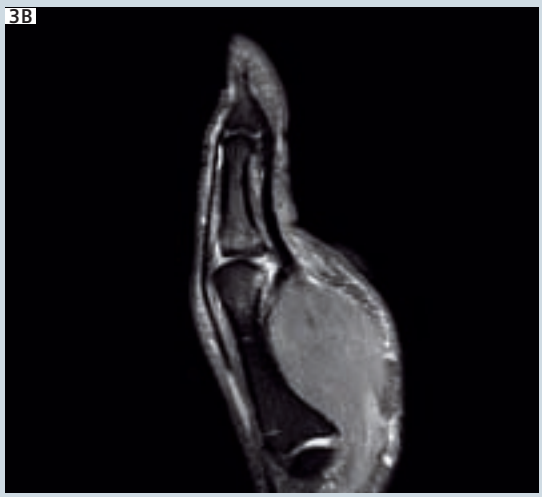

3 A: Planning of the sagittal slice position on a coronal image.

B: Resulting sagittal image of the thumb for evaluation of the flexor and extensor tendons.

MRI of the Forefoot

Martina Königstein

Radiologie München Nymphenburg, Munich, Germany

Forefoot imaging can be done with the 8-channel foot/ankle coil. Excellent image quality can also be achieved using alternative coils. This „How I do it?" describes the examination with the knee coil and the small flex coil. Dependent on the diagnostic question, it is determined whether contrast medium is administered to the patient or not. If yes, it is advisable to perform vein puncture prior to positioning the patient.

Patient positioning

The patient is positioned in the prone position (feet first/prone position) on the examination table.
For examinations in the prone position, the foot is optimally stabilized in either the knee coil or the small flex coil. The foot to be examined (sole of the foot points upward) is positioned in the knee coil, paded with foam wedges and stabilized from above with a sandbag before the coil is closed (photo 1+2, knee coil)

When the examination is performed with the small flex coil, a 45°-wedge is placed under the foot and a sandbag on the foot to stabilize it prior to wrapping the small Flex coil around the foot (photo 3+4 small flex coil)

Slice positioning

After generating the first scout localizer of the foot, an extended transverse and coronal localizer are planned across the metatarsal bones. (e.g., T2, 2x 5 slices,

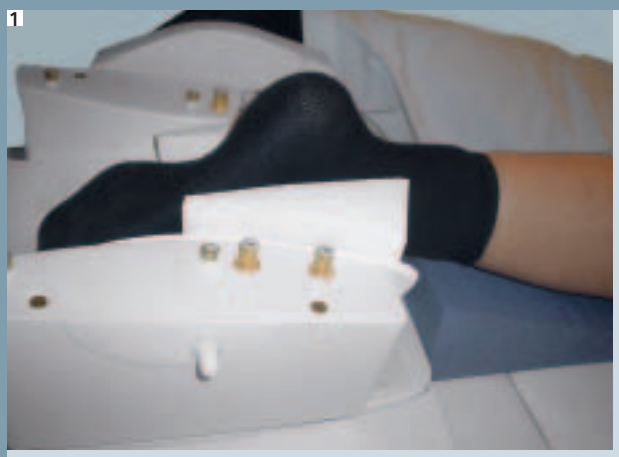

1 2 Knee coil positioning.

3 4 Small flex coil positioning.

1 averaging, duration: approx. 60 s; see Fig. 1).This technique allows for additional exact planning of the sagittal slice position (Fig. 2A) to evaluate the flexor and extensor tendons (Fig. 2B).
Furthermore, this technique also enables additional exact planning of the coronal plane (Fig. 3A) to check for incorrect positioning, fractures, and bone marrow edema (Fig. 3B).

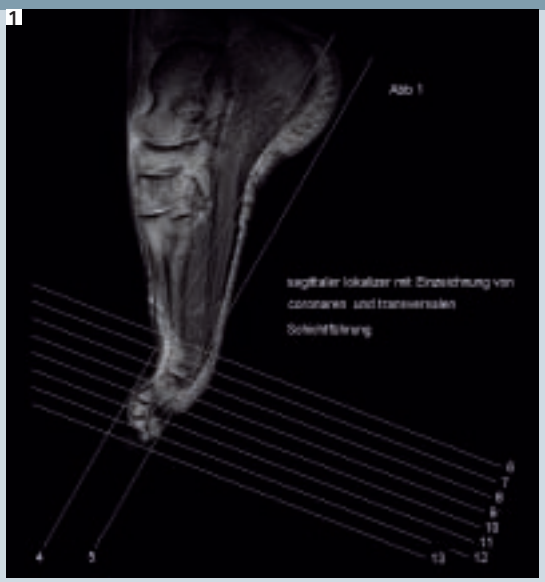

1 Sagittal localizer with coronal and transverse slice positions drawn in.

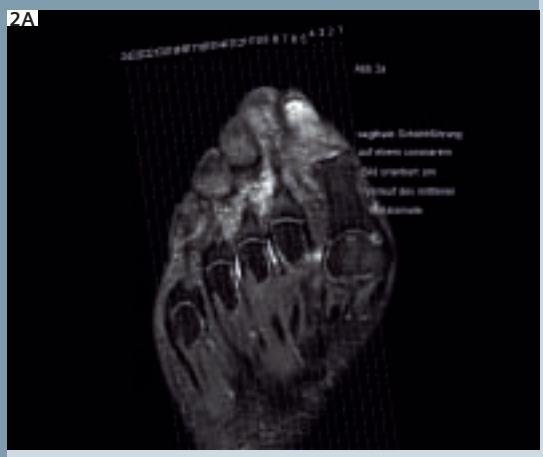

2 A: Sagittal slice position on a coronal image orientated along the course of the medium metatarsale.

B: Resulting sagittal image des ersten Strahls to evaluate the flexor and extensor tendons.

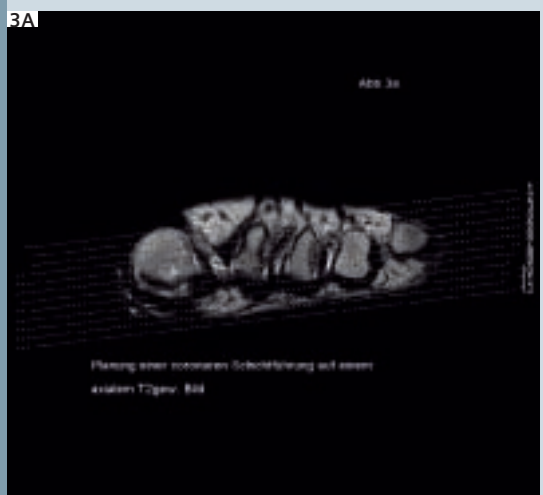

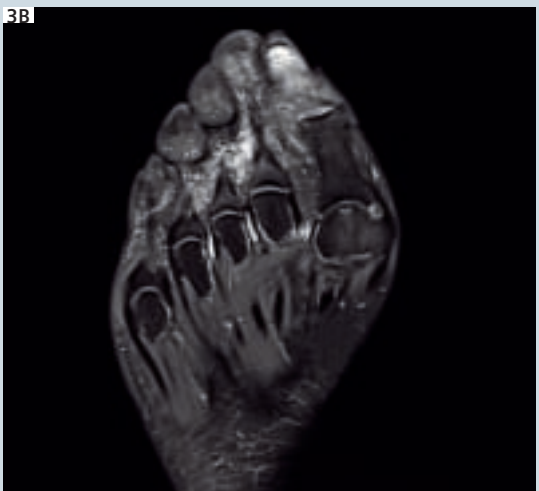

3 A: Planning coronal slice positioning on an axial T2-weighted image.

B: Resulting coronal image for evaluating the basal joint of the large toe.

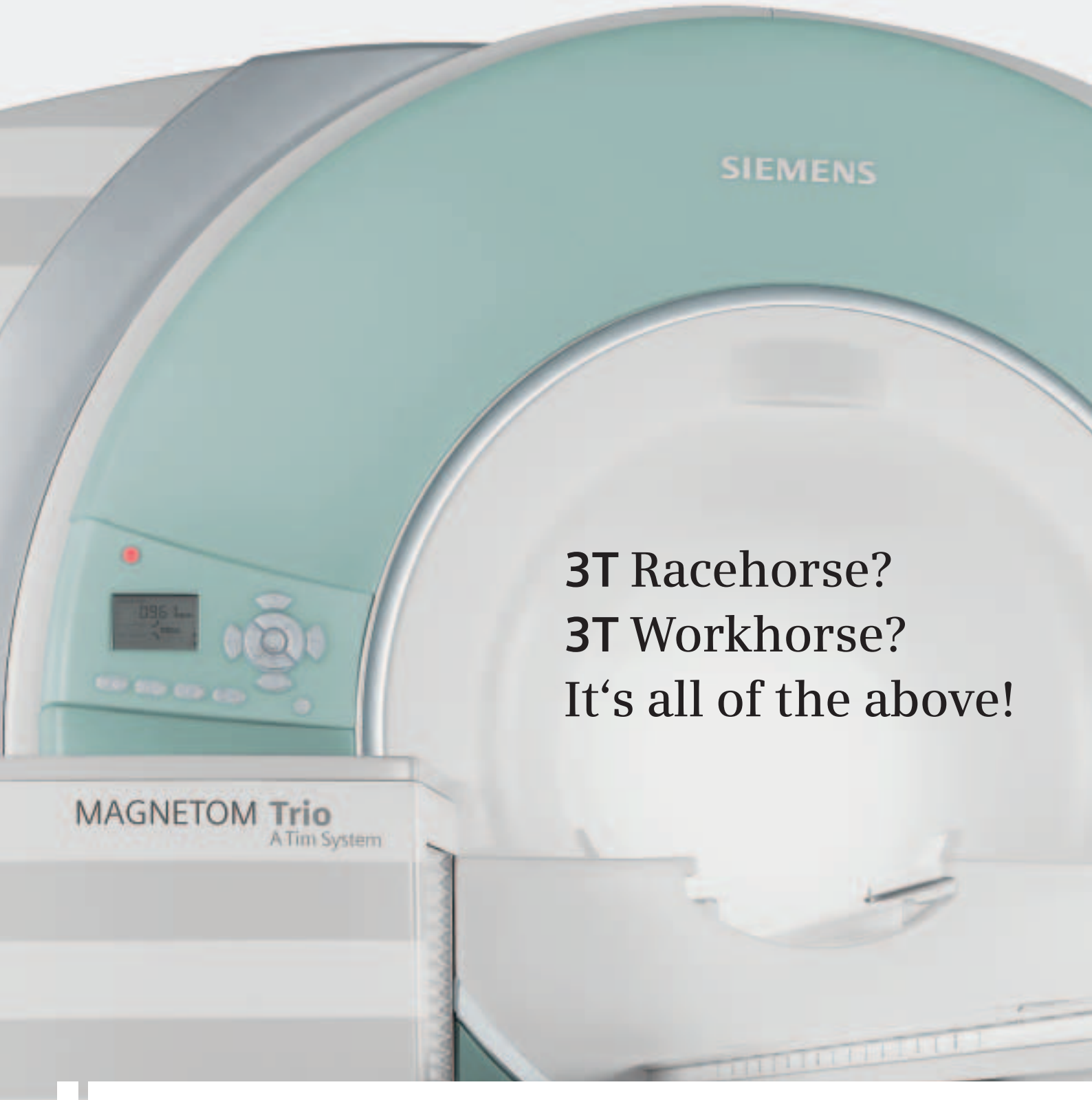

3T Racehorse?
3T Workhorse?
It‘s all of the above!

Proven Outcomes in Clinical 3T MRI.

It’s time to think differently about 3T. MAGNETOM Trio™ is the only 3T with the power of Tim®, Total imaging matrix technology. For 3T that works hard and works fast. Tim makes 3T simple to use for all clinical applications and all body parts. Available with up to 102 seamlessly integrated coils and up to 32 RF channels for ultra-fast scan times and high image resolution. MAGNETOM Trio. From the most routine to the most challenging. It’s time to let it take you to the next level.

www.siemens.com/mr

SIEMENS
medical

MR-Z1007-1-7600

syngo REVEAL Images

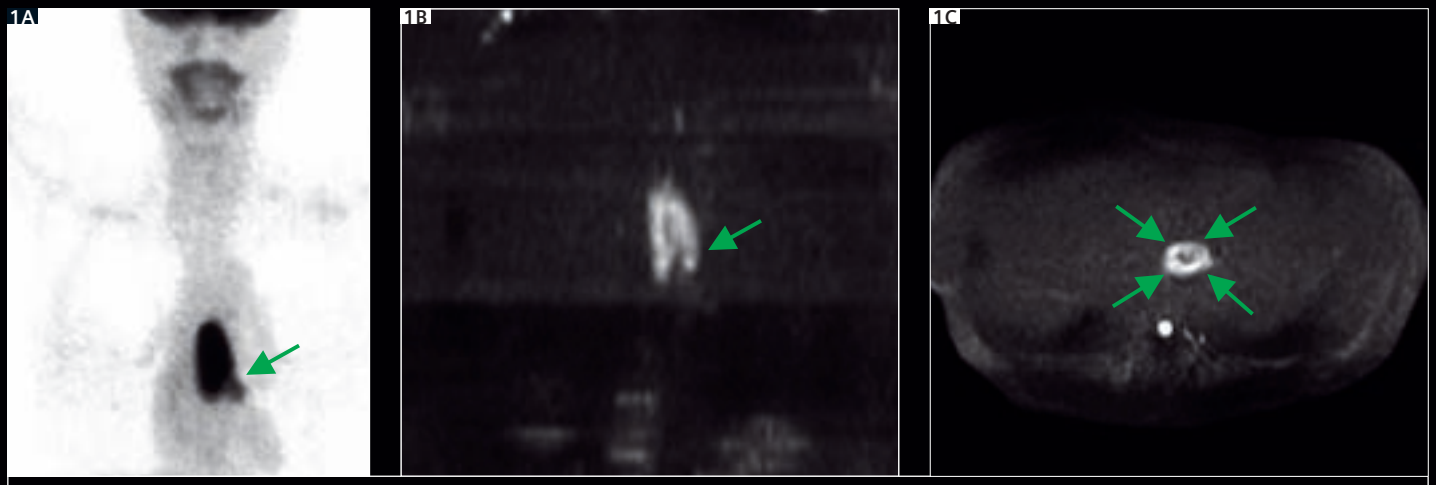

1 **Esophageal carcinoma. 1A: PET image. 1B: Coronal *syngo* REVEAL image. 1C: Axial *syngo* REVEAL image.**
Courtesy of Department of Diagnostic Radiology, Hong Kong Sanatorium and Hospital, Hong Kong.

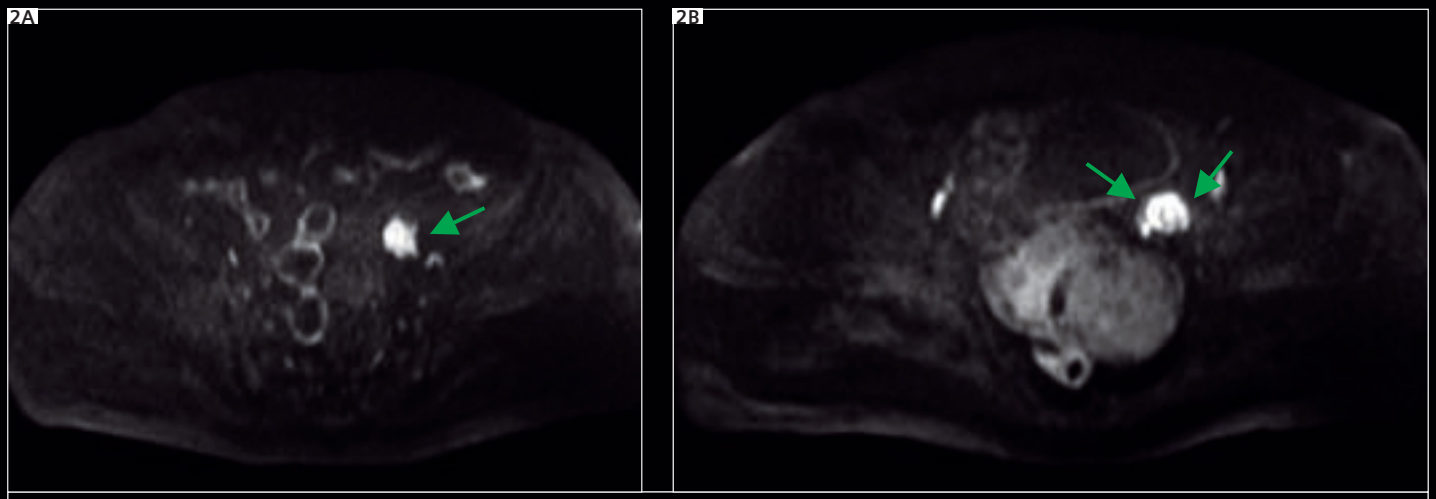

2 **Axial *syngo* REVEAL images of the ureter. Transitional cell carcinoma.**
Courtesy of Department of Diagnostic Radiology, Hong Kong Sanatorium and Hospital, Hong Kong.

MRI with MR Fistulogram for Perianal Fistula: A Successful Combination

Anil Kumar Bhaya, M.D.; Nanda Kumar, BSc (Radiography)

Department of Radiology and Imaging, Apollo Hospitals, Dhaka, Bangladesh

Introduction

Perianal fistula commonly occurs in an otherwise healthy patient, typically, middle-aged men. Most experts believe that it occurs as result of anal gland obstruction, secondary abscess formation and subsequent external decompression through one of several fairly predictable routes. The internal origin of the fistula usually begins from the middle of the anal canal at the dentate line.

Fistulae may be classified [1] surgically as:

1. Intersphincteric (70%)
2. Transsphincteric (25%)
3. Suprasphincteric (5%)
4. Extrasphincteric or Supralevator (< 1%)

Is Imaging Required?

In the early stages of perianal inflammation, the localized perianal abscess can be successfully drained without guidance. Perianal fistula occurs in the chronic phase of perianal abscess. If a surgeon can define the fistulous track from the external to the internal openings with a probe, the fistula can be cured by deroofing it internally (fistulotomy).

However, 5 –15% of fistulas have a complicated course and require a road map before the proper surgical approach can be devised (Figs. 1, 2).

The goals of imaging include defining the presence and cause of any secondary tracks and to gauge the extent of sphincteric involvement by the fistula to best plan surgery and prevent relapse [2] (Figs. 3, 4 , 5).

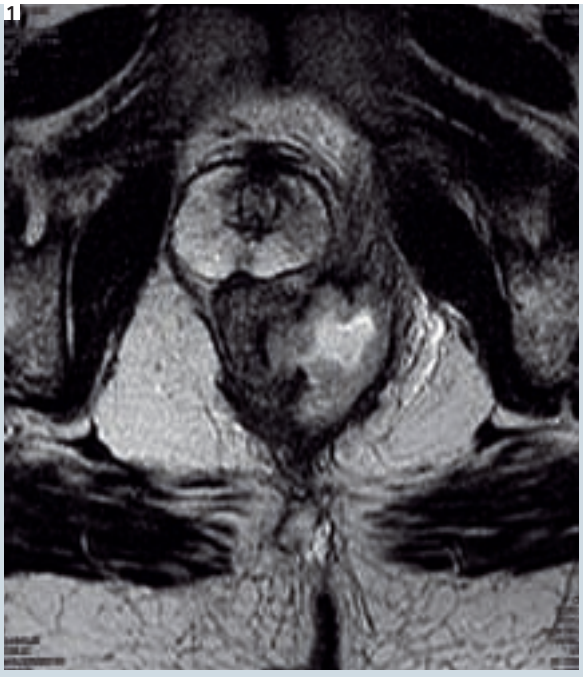

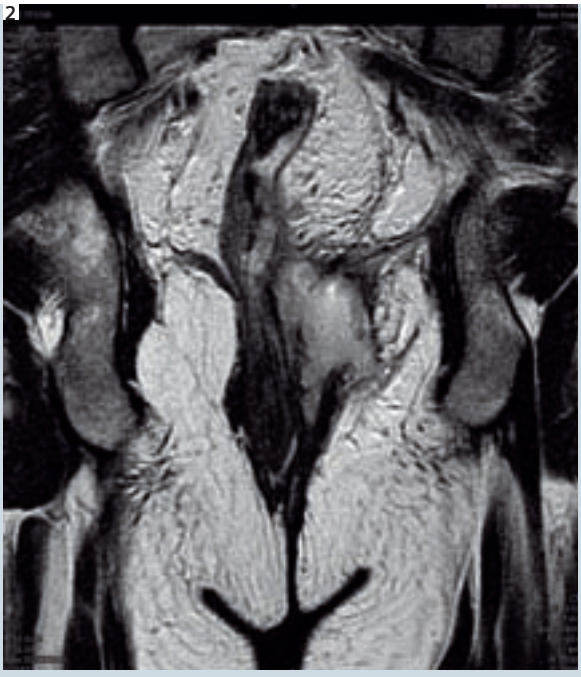

1 High-resolution axial T2-weighted TSE image shows a large abscess with transphincteric extension.

2 Coronal T2-weighted TSE image in the same patient as Fig.6 shows grade 5 complex fistula. The patient had no external opening and had a healed scar from prior perianal abscess drainage. The MRI information helped to decide on the appropriate therapy

3

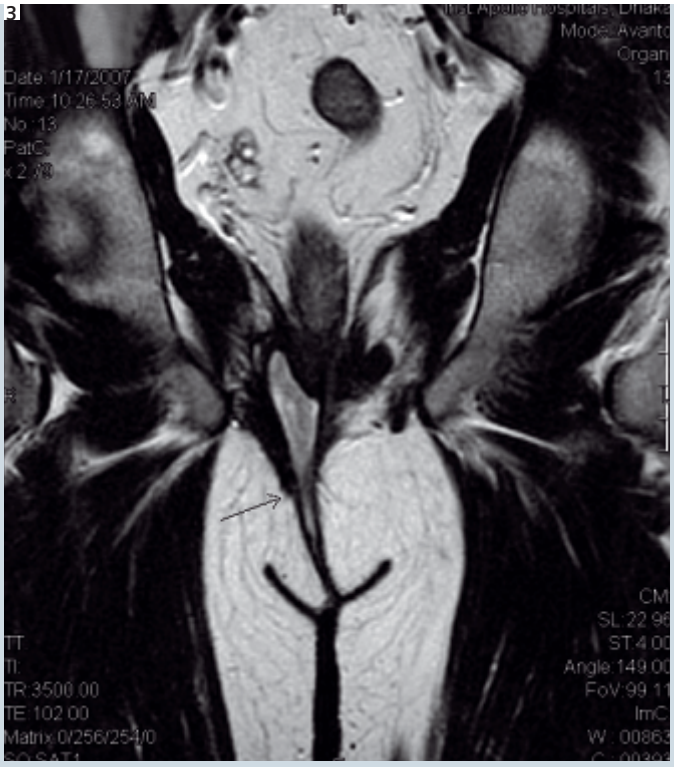

4

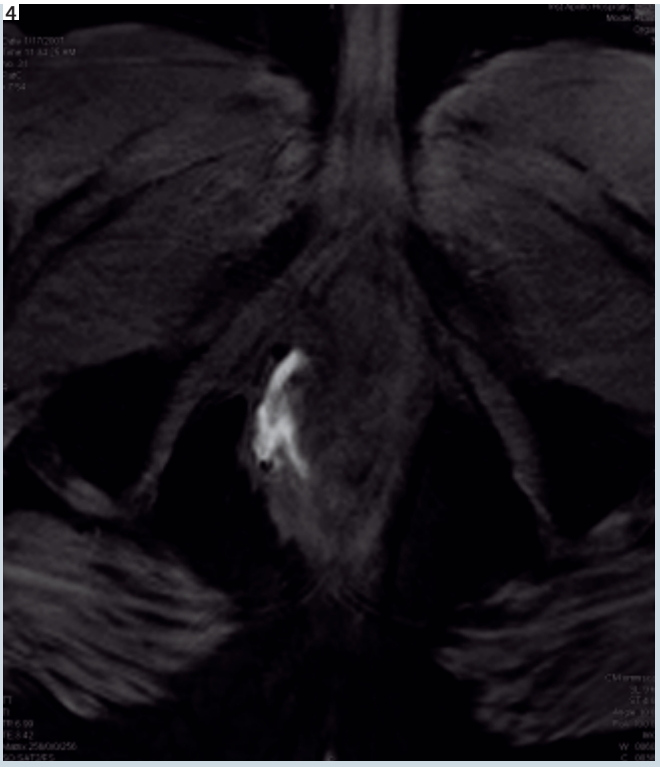

5

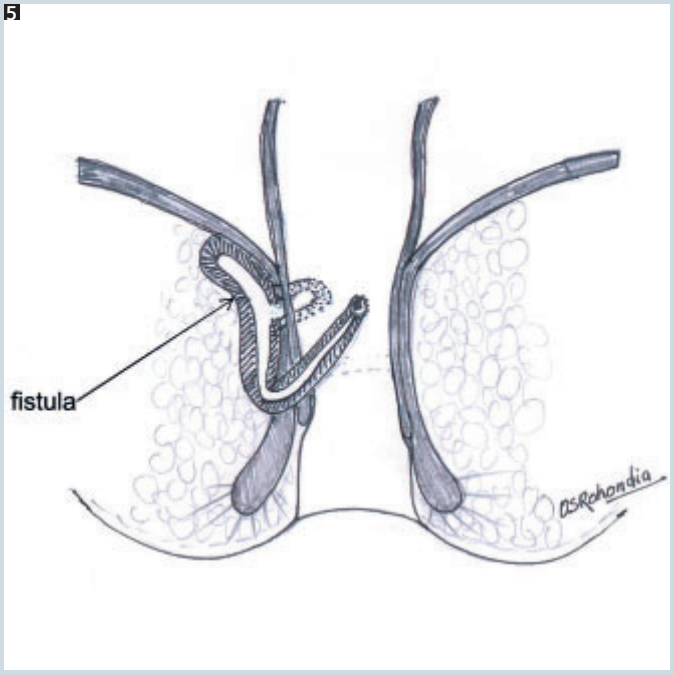

3 **High-resolution coronal T2-weighted TSE image in this patient with recurrent fistula operated 5 times earlier reveals presumably simple intersphincteric fluid intensity well defined fistula.**

4 **MR Fistulogram after injection of dilute gadolinium using 3D VIBE sequence reveals medial transsphincteric ramification of the fistula.**

5 **The findings were surgically confirmed and this image is the surgeon's perspective of the complex fistulous tract in the lithotomy position.**

Courtesy of Dr. O.P. Rohandia, Apollo Hospitals, Dhaka, Bangladesh.

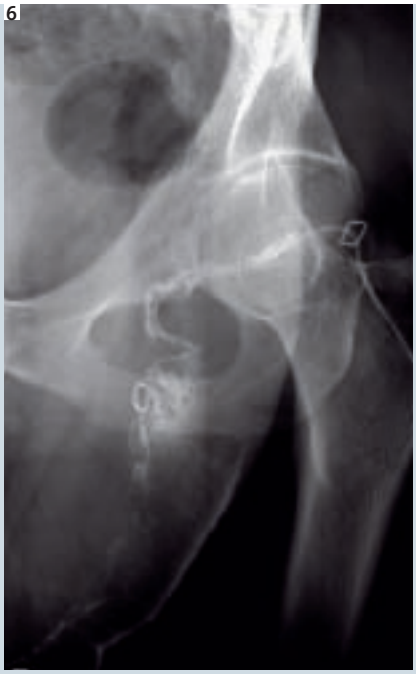

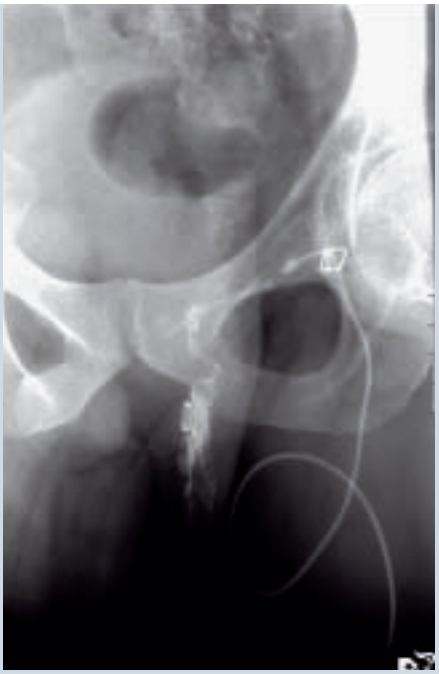

6 X-Ray Fistulogram in a male patient with recent history of perianal abscess drainage reveals an irregular fistulous tract. However, the exact anatomical relationships are difficult to ascertain.

7 Delayed protondensity-weighted axial MR image after MR Fistulography shows well delineated tract with transphincteric extension. The internal opening was not appreciated by examination under anesthesia and confirmed by injection of Gentian Violet at surgery. Due to the information delivered by MR Fistulography the surgeon treated this successfully by excision and seton.

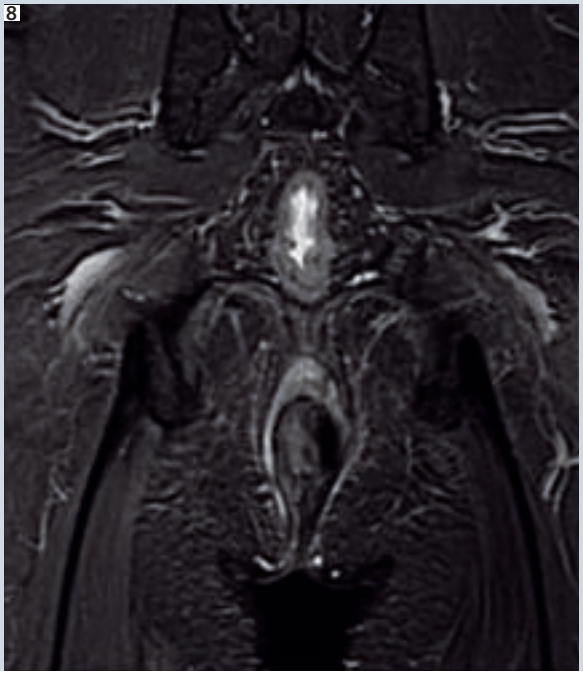

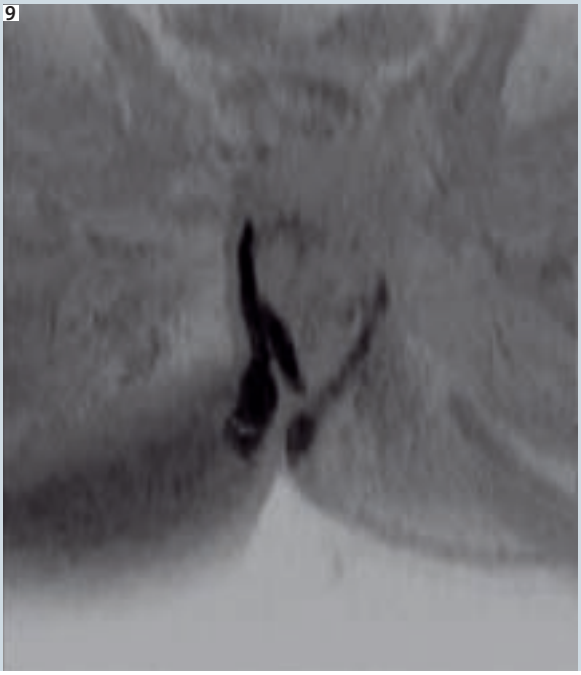

8 Coronal T1-weighted TIRM sequence shows intersphincteric tract. Inverted U-shape.

9 MR Fistulogram (inverse image) confirms horseshoe fistula and also delineated secondary tract.

MR Imaging Techniques

Although direct sinogram, CT scan and endoanal ultrasound have been used to assess the fistula, all of those techniques have had their limitations. For example, although the direct sinogram may delineate the track, it can be very difficult to correlate the track route with the local anatomic musculature and spaces necessary for pre-operative planning (Figs. 6, 7).

Endosonography has also been reported to be no more accurate than examination under anesthesia. MR imaging has become the method of choice due to its orthogonal display of the perineum and lower pelvis along with its superior contrast resolution, allowing faithful reproduction of the anatomy and pathology of the tracks. Compared to the body coil, the quadrature phased array and the Body Matrix coils afford better contrast and spatial resolution both with 2D and 3D sequences. However, the results of fistula imaging with endoanal coil have been disappointing. Investigators in a large study in which endoanal MRI was compared with body coil MRI found a surgical concordance rate of 68% for endoanal MRI as compared to 96% for body coil MRI [3]. In addition to conventional and turbo spin echo sequences, fat suppressed dynamic gadolinium enhanced imaging has been performed and found useful especially with digital subtraction [4]. MR fistulography with instillation of saline can facilitate the detection of fistula tracks, but the technique is cumbersome and depends on the existence of an external opening [5].

Our Experience

All our studies were performed on a 1.5T unit (MAGNETOM Avanto, Siemens Medical Solutions, Erlangen, Germany) with 32x8 channel Tim technology, using Body- and Spine Matrix coil combination. No special bowel preparation was used although the patients were advised to keep their perianal regions clean for cannulation.

Table 1: Routine protocol

Sequence	FoV	SL./gap	Matrix	Average	Sat
T1 TIRM Cor (Scout)	350	5/10%	320/80	1	Superior
T2 TSE Cor	210	4/10%	256/100	1	Superior
T1 TSE Cor	210	4/10%	256/100	1	Superior
T1 TSE Tra	210	4/10%	320/80	2	Parallel
T1 TIRM Tra	210	4/10%	320/80	1	Parallel
T2 TSE Sag	210	3/10%	320/80	2	Superior
T1 VIBE Fs Tra	210	2.5/20%	256/100	1	Parallel
T1 VIBE Fs Cor	210	2.5/20%	256/100	1	Superior
T1 VIBE Fs Tra (Post-Con)	210	2.5/20%	256/100	1	Parallel
T1 VIBE Fs Cor (Post-Con)	210	2.5/20%	256/100	1	Superior

Following a routine protocol in supine position (see Table 1) the patient is placed in prone position and the site of fistula opening is cleaned well with alcohol and povidone-iodine (Win - Medicare) solution. For cannulation we use an infant feeding tube or butterfly cannula without the needle and with the tube cut in bevelled fashion to facilitate easy and non-traumatic entry. If there is resistance at the opening, we usually use mosquito forceps to widen it. The tip of the cannula is dipped in xylocaine gel for lubrication and local anesthetic effect. Prepared solution (1 ml Gadolinium, Omniscan, Amersham Health, Cork, Ireland) mixed in 20 ml of sterile normal saline) is gradually injected through the cannula (all air in the syringe is evacuated prior to the injection). As soon as reflow occurs or there is flow through secondary track and opening, we close the opening with sterile gauze and clean any contrast refluxed on the skin surface. After this the Body Matrix coil is placed on the pelvis covering the region of interest and isocentred within the magnet (Figs. 8, 9).

Conclusion

Our experience shows that phased array Body Matrix coils afford sufficient image contrast and resolution for accurate assessment of perianal fistulas. We also believe that a combination of the above with MR Fistulography enhances the diagnostic yield of the examination and also reduces the false positive diagnosis of fistulous tracks by distinguishing from the healed partially fibrotic but T2 hyperintense tracks. We also found that this technique may better define the internal opening for surgical planning.

References

1 www.surgical-tutor.org.uk.

2 Beets-Tan RGH, Beets GL, Geerard Vanderhoop, AG, Kessels AGH, Vliegan RFA, Baeten CGMI, Van Engelshoven JMA. Preoperative MR imaging of anal fistulas: does it really help the surgeon? Radiology 2001; 218: 75–84.

3 Halligan S, Bartram CI. MR imaging of fistula in ano: are endorectal coils the gold standard? AJR 1998; 171: 407-412.

4 Schaefar O, Lohrmann C, Langer M. Digital subtraction MR fistulography: now diagnostic tool for the detection of fistula in ano. AJR 2003; 181: 1611–1613.

5 Komatsu S et al. Circ J 2005: 69(1): 72–77.

5 Myhr GE, Myrvold HE, Nilseti G, Thoresen JE, Rinck PA. Perianal fistulas: use of MR imaging for diagnosis. Radiology 1994; 191: 545–549.

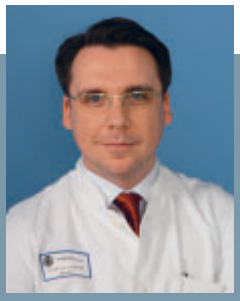

"*syngo* TimCT – this innovative fascinating MRI technique will set future trends concerning workflow and scan efficiency. Current oncologic staging strategies will experience substantial changes beneficial for the patient."

Arnd-Oliver Schaefer M.D.
University Hospital Freiburg, Germany

Metamorphosis of MRI:
How a Caterpillar Transforms into a Butterfly
Seamless Move-During-Scan with *syngo* TimCT

O. Schaefer[1], T. Baumann[1], G. Pache[1], U. Ludwig[2], M. Langer[1]

[1]*Department of Radiology, University Hospital Freiburg, Germany*
[2] *Department of Radiology, Medical Physics, University Hospital Freiburg, Germany*

Introduction

In the past, motion has been considered as one of the most dangerous threats to high quality MR imaging. Recently, with the technical advancements of modern MR scanners, several investigators have accepted the challenge of turning this drawback into an opportunity and introduced imaging during continuous patient movement. The idea behind these efforts was to enlarge the scan region in order to create an overview of wide parts of the human body. Besides the desire to depict systemic diseases in one examination, economic issues are pushing more and more to the forefront. Continuously moving table MRI has the potential to simplify current imaging strategies and can further strengthen the role of MRI as a "one-stop-shop" modality. In this context the research group around Fautz [1] invented Sliding Multislice (SMS) as a novel technique for the temporally and spatially seamless acquisition of axial slices during continuous table movement. Currently, we are the promoters of this technique in daily clinical routine for staging of rectal cancer, inflammatory bowel disease (IBD) and other systemic malignancies like lymphoma or multiple myeloma. In our opinion the metamorphosis of MRI has just begun: The caterpillar – stationary MRI – is transforming into an iridescent butterfly – Sliding Multislice, which will be part of the upcoming *syngo* TimCT (Continuous Table move with Tim) package.

How does this fascinating technique work?

During SMS, the patient is moved continuously through a fixed measuring range located around the isocenter of the magnet. This active scan region is divided into N segments along the z-axis, with N representing the number of slices being simultaneously recorded within a given TR (Fig. 1A). The thickness of the segments equals the slice distance of the final images. Furthermore, each segment is assigned to a different part of k-space, which is recorded while a certain slice is located in that segment. While all slices in the scan region are excited during the same TR, the full k-space data for each single slice is collected as it moves through the whole measuring range (Fig. 1B). For different slices the various parts of k-space are assembled along the same spatial trajectory in the scan region, but with a slight temporal shift. This spatial trajectory is arranged in such a manner that the central parts of k-space are acquired in a small area around the isocenter of the magnet. Further improvement of the signal-to-noise ratio is accomplished by automatically activating and deactivating the receiver coils according to the current patient position. In contrast to other move-during-scan techniques or multi-step MRI, the effect of z-dependent acquisition characteristics is identical for all slices. SMS can be employed to acquire standard T1- and T2-weighted sequences.

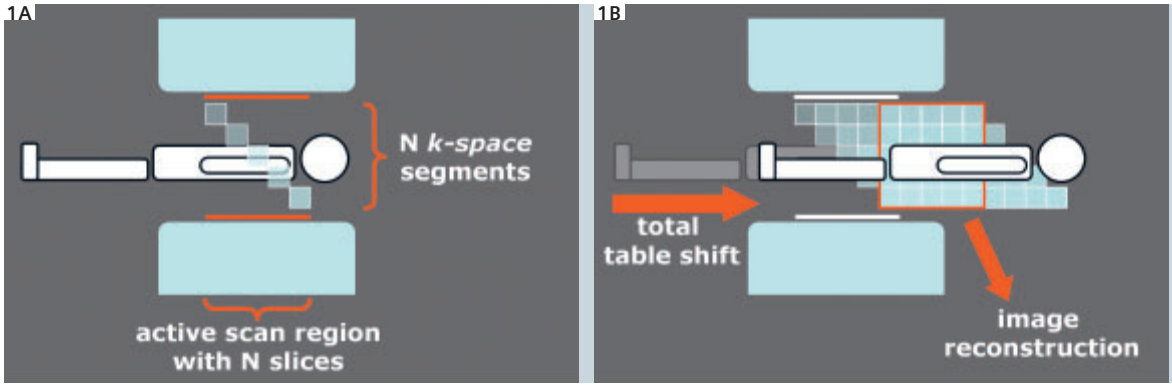

1 **A: Exemplary k-space trajectory demonstrates acquisition strategy in SMS.**

B: Continuous table movement allows for seamless acquisition with SMS.

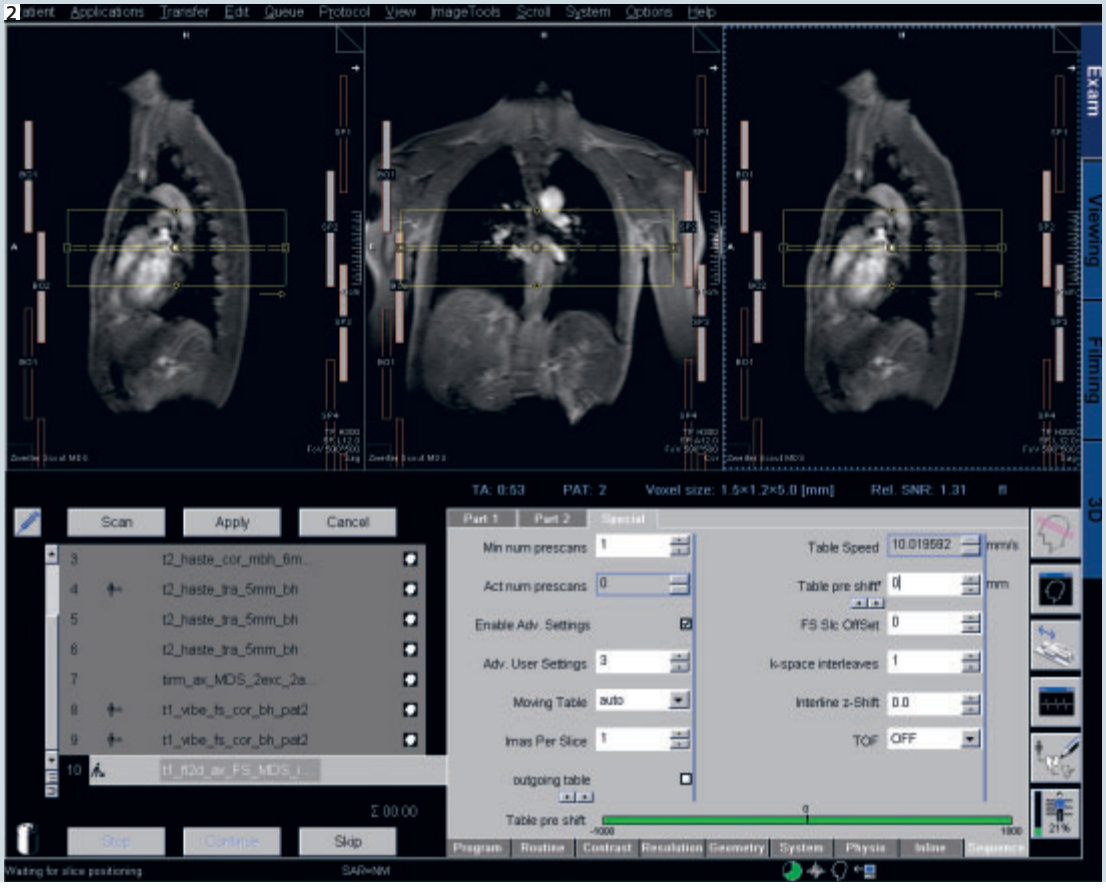

2 Planning of the axial *syngo* TimCT-FLASH 2D sequence. The scout consists of sagittal and coronal slices. The default table speed is 10 mm/s. During a breath-hold phase of 25 seconds the upper abdomen can be imaged with high quality. Therefore, the table preshift has to be adjusted accurately prior to the scan. An important prerequisite for an unimpaired sequence run is the selection of at most 4 coil elements which ensures automatic coil switching.

How do we perform continuous table move "SMS"?

From a user's point of view, SMS can be easily integrated into a standard imaging protocol for staging of rectal cancer, evaluation of recurrent Crohn's disease and whole-body imaging. Regardless of the desired scan region, a second localizer has to be performed to cover total abdomen, lungs, and head if necessary. Currently, we are able to select or to combine a free-breathing TIRM and a T1-weighted FLASH 2D or a contrast-enhanced breath-hold T1-weighted, fat-saturated FLASH 2D sequence. During a 25-second breath-hold phase the liver or alternatively the whole intestine can be imaged without motion-related artifacts. Due to motion-correction techniques [2], no disturbing artifacts occur during free-breathing imaging. The table preshift has to be adjusted. An important feature of SMS is automatic dynamic coil switching which requires selection of a maximum of 4 coils prior to the SMS run (Fig. 2).

Rectal cancer staging

For abdominal rectal cancer staging we routinely perform contrast agent based *syngo* TimCT-FLASH 2D as an adjunct to high-resolution pelvic MRI. The imaging parameters are summarized in Table 1. As the majority of colorectal liver metastases are hypovascularized, we administer 20 ml of Gd-BOPTA (Multihance) 60 s prior to scanning to assure depiction of the liver in a portal-dominant phase. The total imaging time accounts for 1 minute.

Hydro-MRI for IBD

For the evaluation of recurrent Crohn's disease we routinely acquire TimCT-FLASH 2D as part of our Hydro-MRI protocol. The imaging parameters are summarized in Table 1. Axial contrast-enhanced FLASH 2D sequence of a standard multistage technique requires 6 breath-hold phases of 20 seconds each, whereas the SMS technique necessitates only one single breath-hold phase of 25 seconds.

What have we achieved so far?

So far, we have examined more than 600 patients using the upcoming *syngo* TimCT technique.

Rectal cancer

To date, high-resolution pelvic MRI is considered the method of choice for local staging of rectal cancer. MRI is the only imaging modality which allows prediction of the circumferential resection margin (CRM) [3]. Current staging strategies normally consist of a combination of pelvic MRI with a CT of thorax and abdomen. Ideally, it would be desirable to combine the excellent soft-tissue contrast of MRI with the large volume coverage of multi-detector CT (MDCT) within one examination and this is now possible with SMS [4].
To asses the image quality of our approach, we compared SMS to a stationary breath-hold FLASH sequence of the upper abdomen. SMS obtained images of the liver and retroperitoneal area with an excellent image quality, which is of exceptional importance since the liver as

well as periaortic and iliac lymph nodes are major sites of distant tumor spread in patients with rectal cancer. Although the intestinal region was affected by motion artefacts, images of diagnostic quality could be achieved. Additionally, SMS was compared to MDCT for lesion detection (Fig. 3). From our rectal cancer surveillance program we selected 27 paired SMS and abdominal CT examinations. SMS could achieve equivalent sensitivities for nodal and hepatic manifestations of the disease in conjunction with high agreement between both methods and two independent observers on a per-lesion basis. SMS did not miss any case of hepatic involvement and correctly described all cases with a solitary hepatic metastasis, which is of great importance when a second curative approach is considered. To further improve the anatomic coverage and the diagnostic value of SMS, we now additionally perform a free-breathing TIRM-sequence through the thorax and abdomen. This approach enables us to detect pulmonary nodules as small as 5 mm. Meanwhile, abdominal SMS is widely accepted by our surgeons and oncologists and has replaced abdominal CT for staging of patients with rectal cancer at our institution.

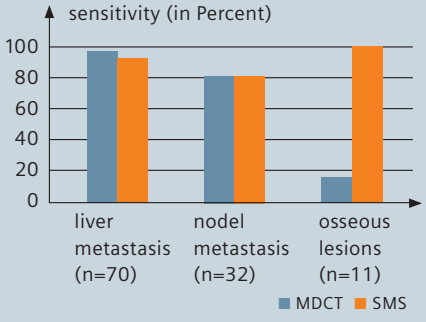

Sensitivities of SMS-FLASH 2D and MDCT for liver metastasis, malignant nodes, and bone lesions.

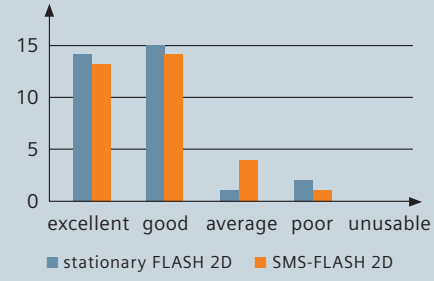

Image quality rating of the standard multistage FLASH 2D and the SMS-FLASH 2D sequence

Table 1: Sequence parameters

Parameters	*syngo* TimCT-FLASH 2D	*syngo* TimCT-TIRM*
TR [ms]	102	3568
TE [ms]	2,03	101,22
slice thickness [mm]	5,0	6,0
matrix	320 x 224	320 x 200
FoV read [mm²]	350 x 263	400 x 250
pixel bandwidth[Hz/pixel]	300	445
flip angle [°]	70	60
voxel size [mm³]	1,4 x 1,1 x 5,0	1,6 x 1,1 x 6,0
parallel imaging	*syngo* GRAPPA, factor 2	
acquisition time [min]	1	4

* WIP – Works in Progress. The information is preliminary. The sequence is under development and not commercially available in the U.S., and its future availability cannot be ensured.

Crohn's disease

Hydro-MRI is an upcoming imaging modality for the evaluation of patients with recurrent Crohn's disease [5]. It offers non-invasive detection of bowel wall pathology and extra-intestinal complications of the disease which makes the procedure particularly applicable for the predominantly young patient population that often requires repeated examinations during the course of the disease. Hydro-MR imaging protocols normally consist of several multi-step sequences in the axial and coronal plane using a breath-hold technique to cover the entire intestine which is laborious, time consuming and implies high patient compliance. After oral administration of 2000 ml of a 0.5% diluted methylcellulose solution we perform Hydro-MRI. To evaluate SMS for Hydro-MRI we analysed 32 patients with known Crohn's disease for lesion site and extra-intestinal disease complications. Crohn-associated lesions were found in more than 90% of the patients. Regarding lesion detectability, we found an excellent correlation between standard multistage and SMS FLASH-2D. Compared to the standard multistage technique, SMS reduces total examination time by 4.5 minutes without any loss in image quality. *syngo* TimCT allows a complete Hydro-MRI protocol in just 10 minutes. Performing SMS instead of a standard multistage sequence is time-efficient, improves workflow and thereby increases patient comfort without loss of diagnostic accuracy.

What conclusions can be drawn?

- The attributes of *syngo* TimCT are scan efficiency and image quality.
- *syngo* TimCT for oncology permits fast one-stop-shop imaging.
- *syngo* TimCT for recurrent Crohn's disease markedly reduces examination time.

References

1 Fautz HP, Kannengiesser SA. Sliding Multislice (SMS): a newtechnique for minimum FOV usage in axial continuously moving- table acquisitions. Magn Reson Med 2006; 55: 363–370.

2 Fautz HP, Honal M, Saueressig U, Schaefer O, Kannengiesser SA. Artifact reduction in moving-table acquisitions using parallel imaging and multiple averages. Magn Reson Med 2007; 57: 226–232.

3 MERCURY Study Group. Diagnostic accuracy of preoperative magnetic resonance imaging in predicting curative resection of rectal cancer: prospective observational study. BMJ 2006 [Epub].

4 Schaefer O, Langer M. Detection of recurrent rectal cancer with CT - MRI -PET/CT. Eur Radiol 2007 [Ahead of Print].

5 Mackalski BA, Bernstein CN. New diagnostic imaging tools for inflammatory bowel disease. Gut 2006; 55: 733–41.

Image Gallery *syngo* TimCT

Despite the free-breathing and extremely short examination time from head to toe, diagnostically sufficient image quality is constantly obtained.

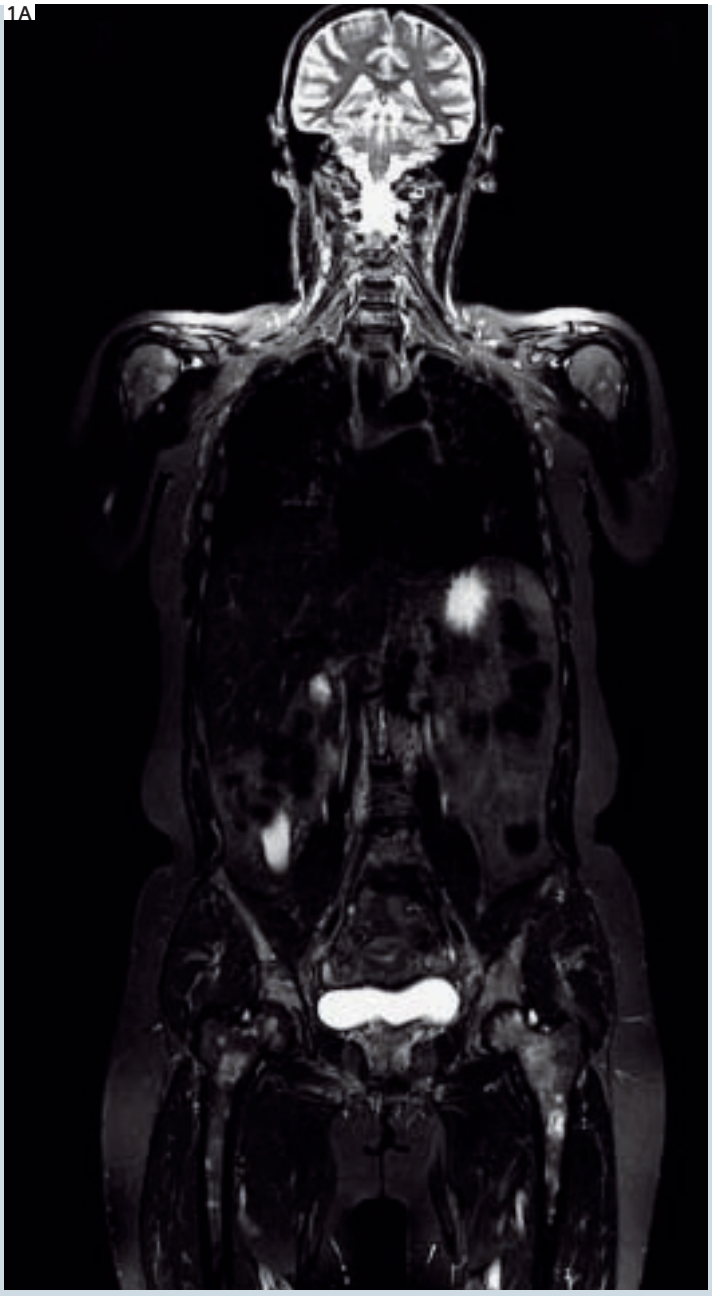

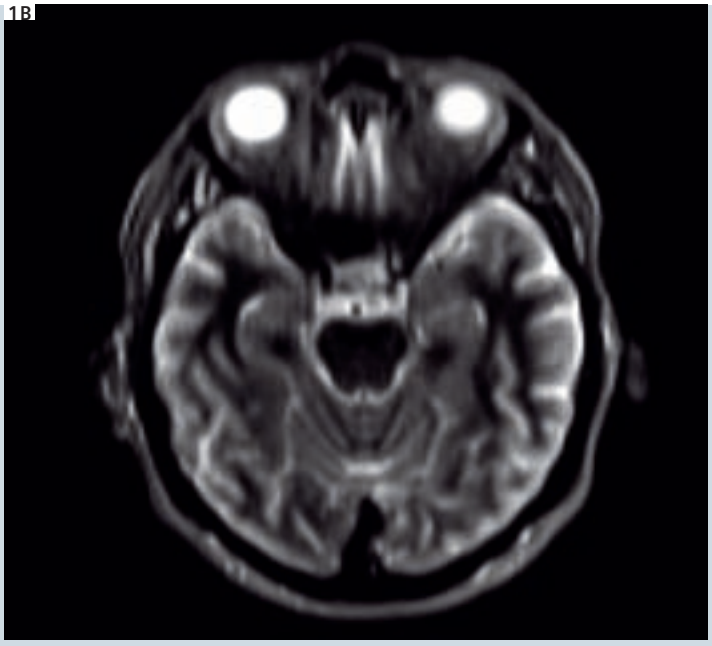

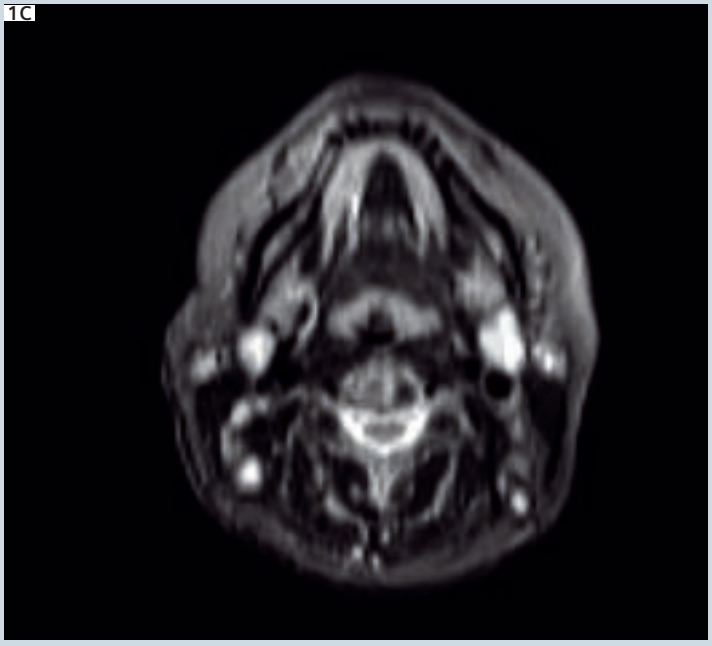

1 Whole-body MRI. Female with disseminated breast cancer.

B–I: *syngo* TimCT-TIRM* sequence generated during free-breathing in a 4 minute scan. Despite the free-breathing and extremely short examination time from head to toe, diagnostically sufficient image quality is constantly obtained.

C: Pathologic cervical nodes.

D, E: Lymphangiosis carcinomatosa of the lungs.

G–I: Extensive bone marrow infiltration.

* WIP – Works in Progress. The information is preliminary. The sequence is under development and not commercially available in the U.S., and its future availability cannot be ensured.

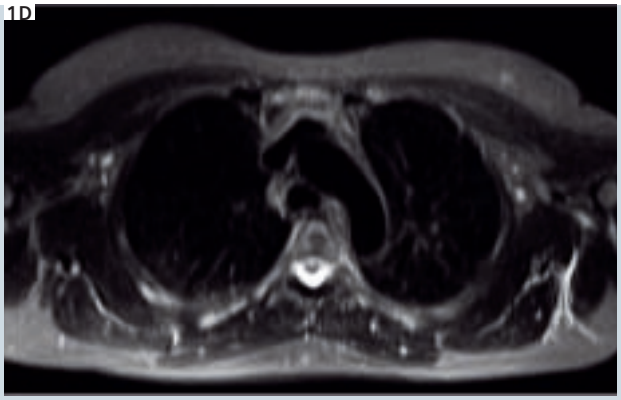
1D

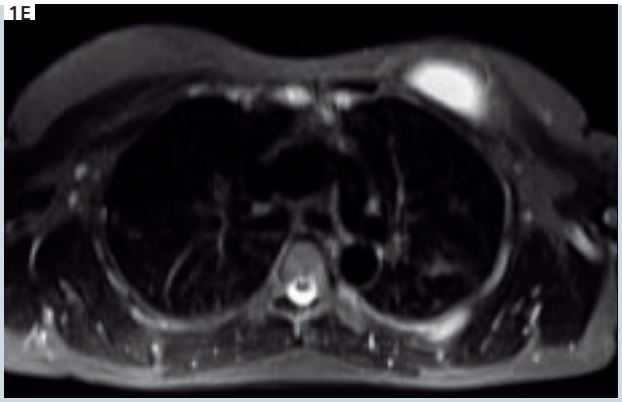
1E

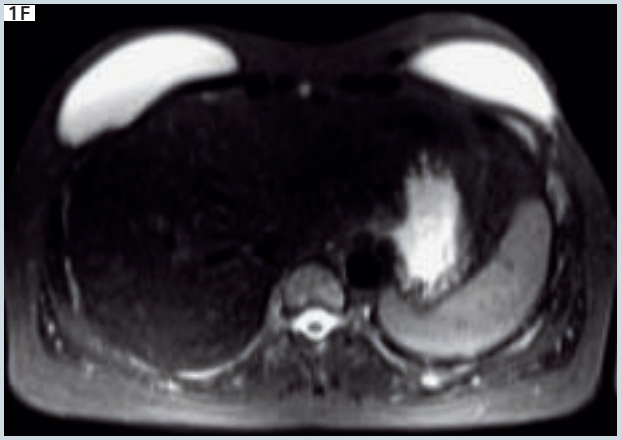
1F

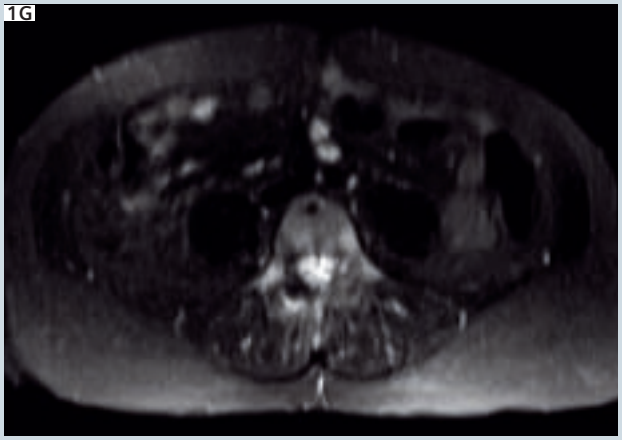
1G

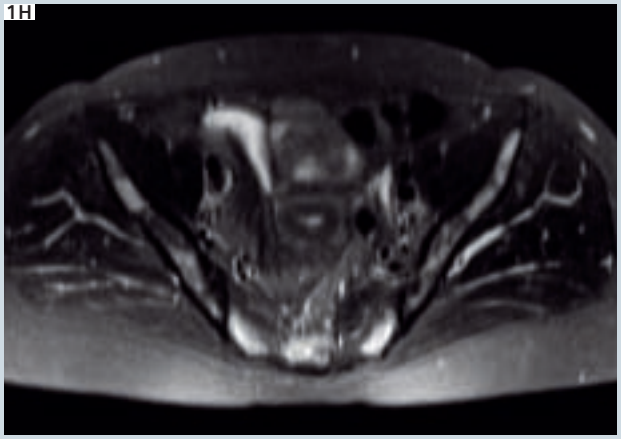
1H

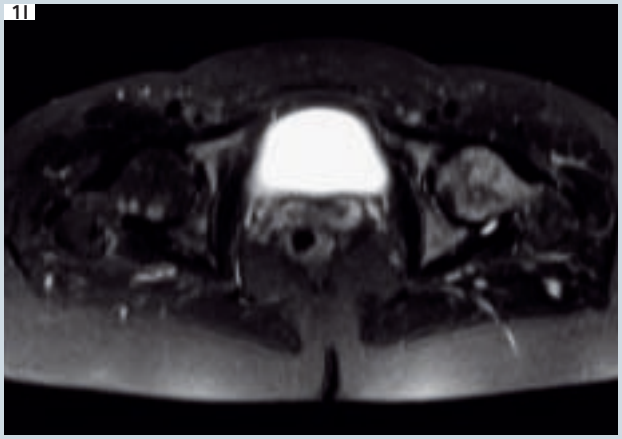
1I

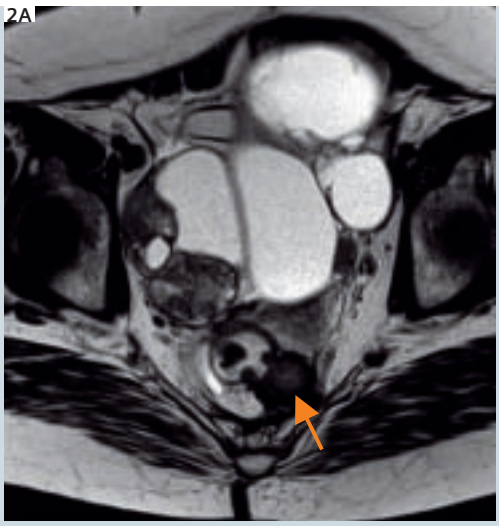

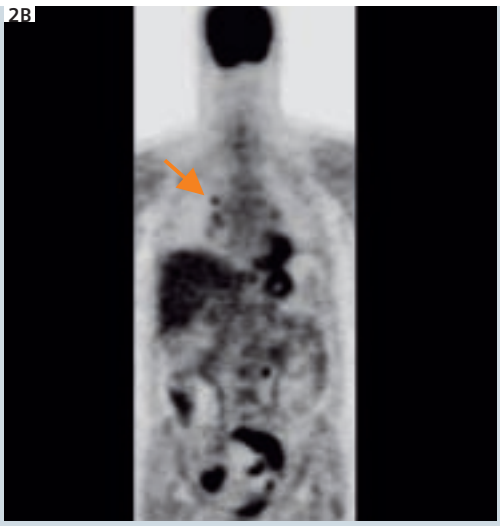

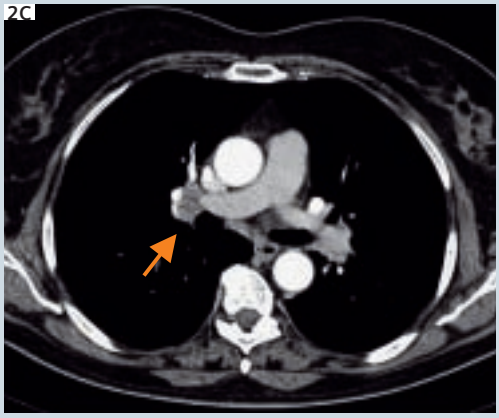

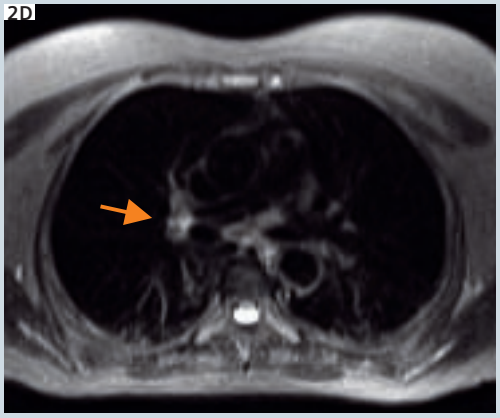

2 Female with recurrent rectal and ovarian cancer.

A: Axial T2-weighted TSE image derived from our high-resolution pelvic MRI protocol. Besides the large ovarian cancer an anastomotic rectal cancer recurrency growing into the presacral scar can be observed (arrow).

B: PET image reveals hypermetabolic hilar nodes (arrows).

C, D: MSCT and corresponding TimCT-TIRM* image from moving-table staging as part of our one-stop-shop workup for rectal cancer. Both imaging modalities clearly depict the suspicious hilar nodes.

* WIP – Works in Progress. The information is preliminary. The sequence is under development and not commercially available in the U.S., and its future availability cannot be ensured.

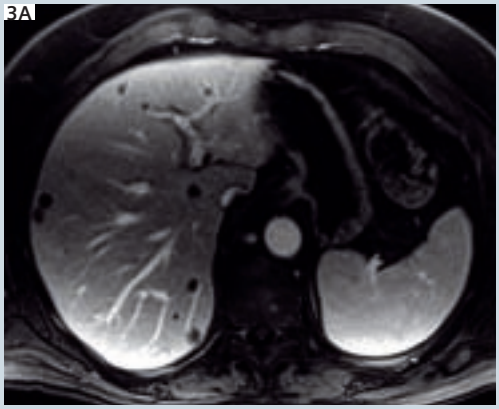

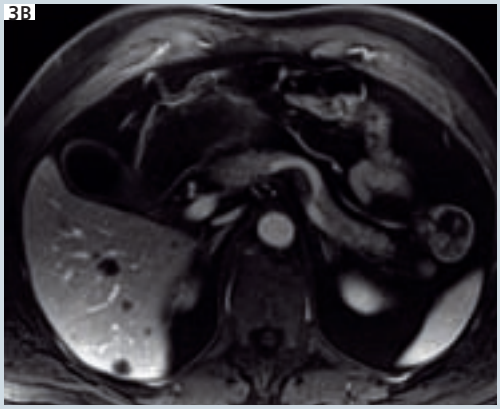

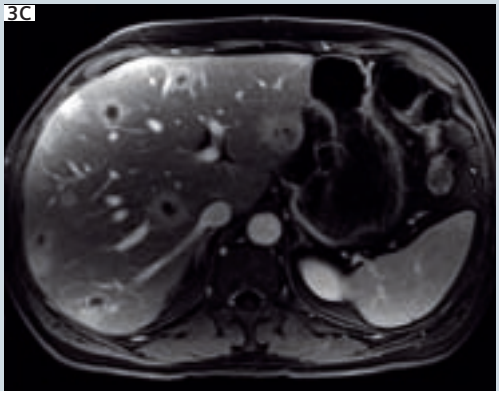

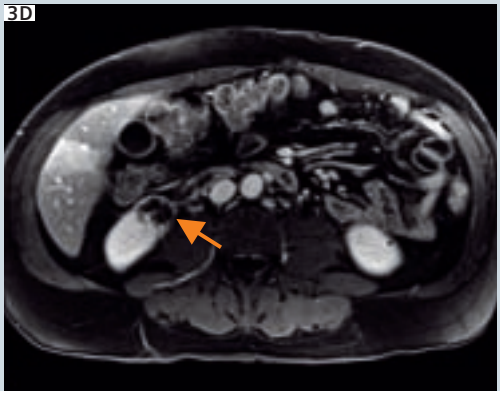

3 Rectal cancer patients examined with *syngo* TimCT-FLASH 2D for abdominal tumor staging.

A, B: *syngo* TimCT images show mulitple hypovascular liver metastases.

C, D: Besides metastatic spread to the liver a solitary renal metastasis can be detected with *syngo* TimCT (arrow).

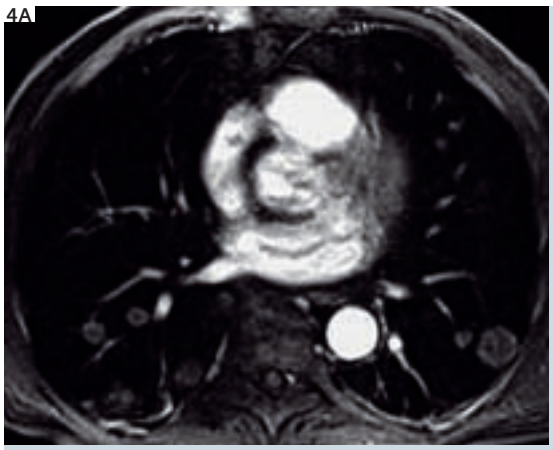

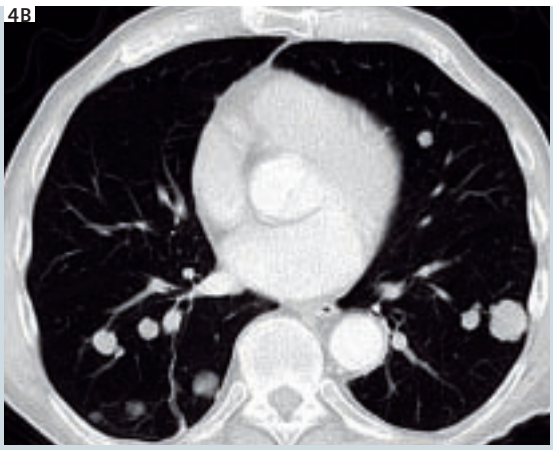

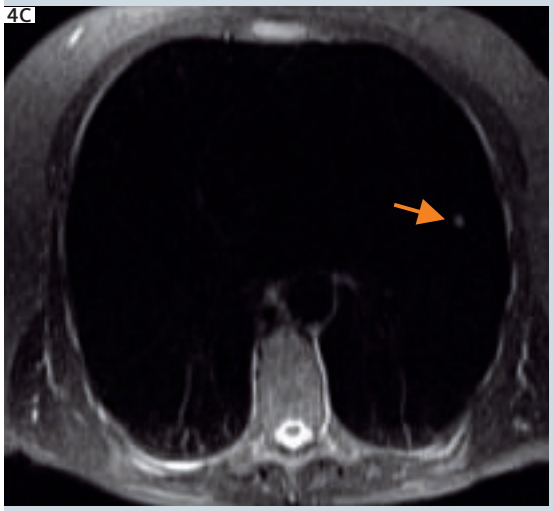

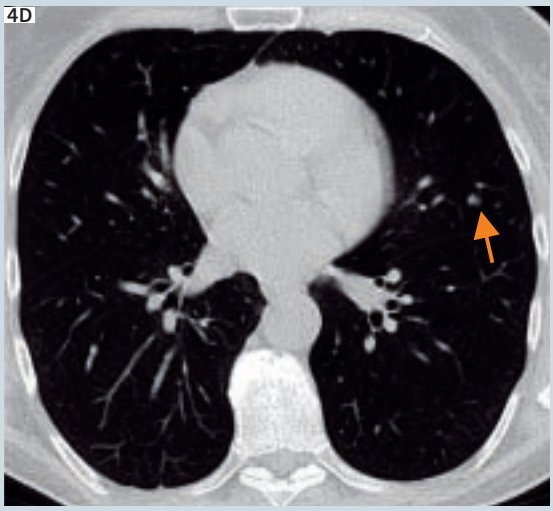

4 Whole-body staging of rectal cancer patients with *syngo* TimCT.

Comparison of MSCT (B, D), TimCT-FLASH 2D (A) and TimCT–TIRM* (C). Even small lung nodules (arrows) can be detected with *syngo* TimCT MRI as confirmed by MSCT.

* WIP – Works in Progress. The information is preliminary. The sequence is under development and not commercially available in the U.S., and its future availability cannot be ensured.

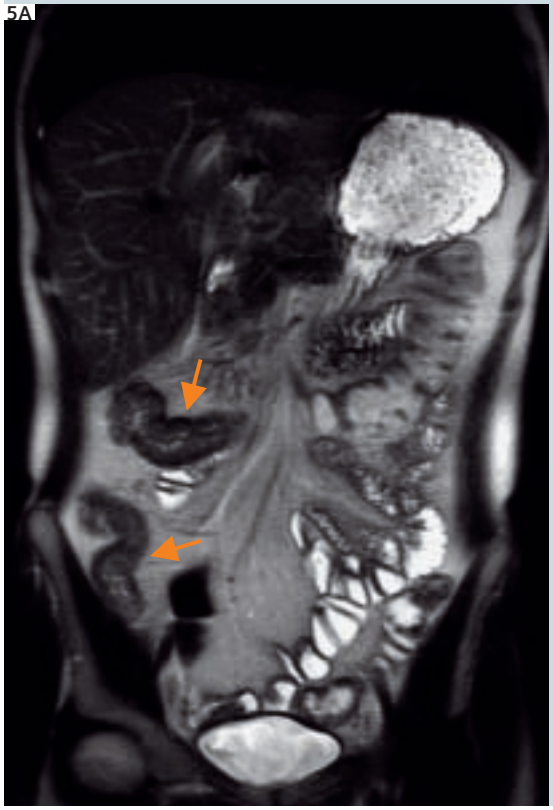

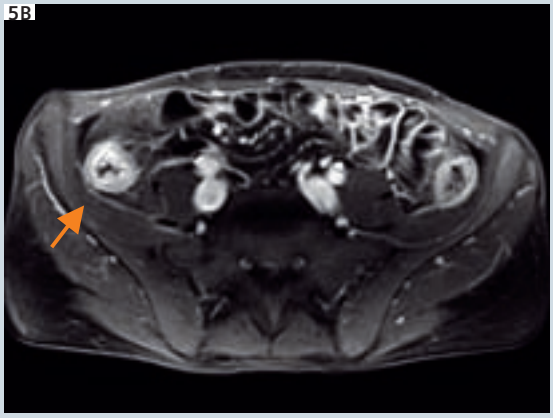

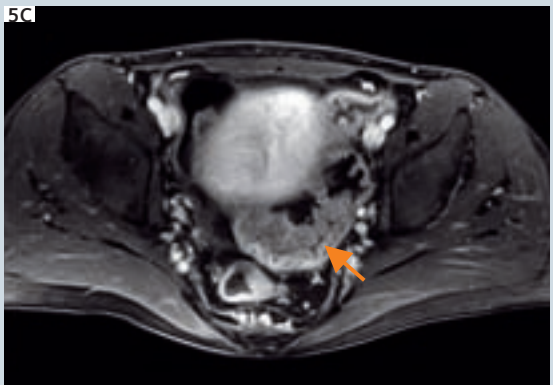

5 Hydro-MRI with TimCT-FLASH 2D. Male with recurrent Crohn's disease.

A: Coronal HASTE image. Inflammation of the terminal ileum and transverse colon (arrows).

B, C: Axial TimCT-FLASH 2D. 1 minute scan through abdomen and pelvis performed with one 25 second breath-hold phase. Inflammation of the caecum (arrow) and rectosigmoid colon (arrow).

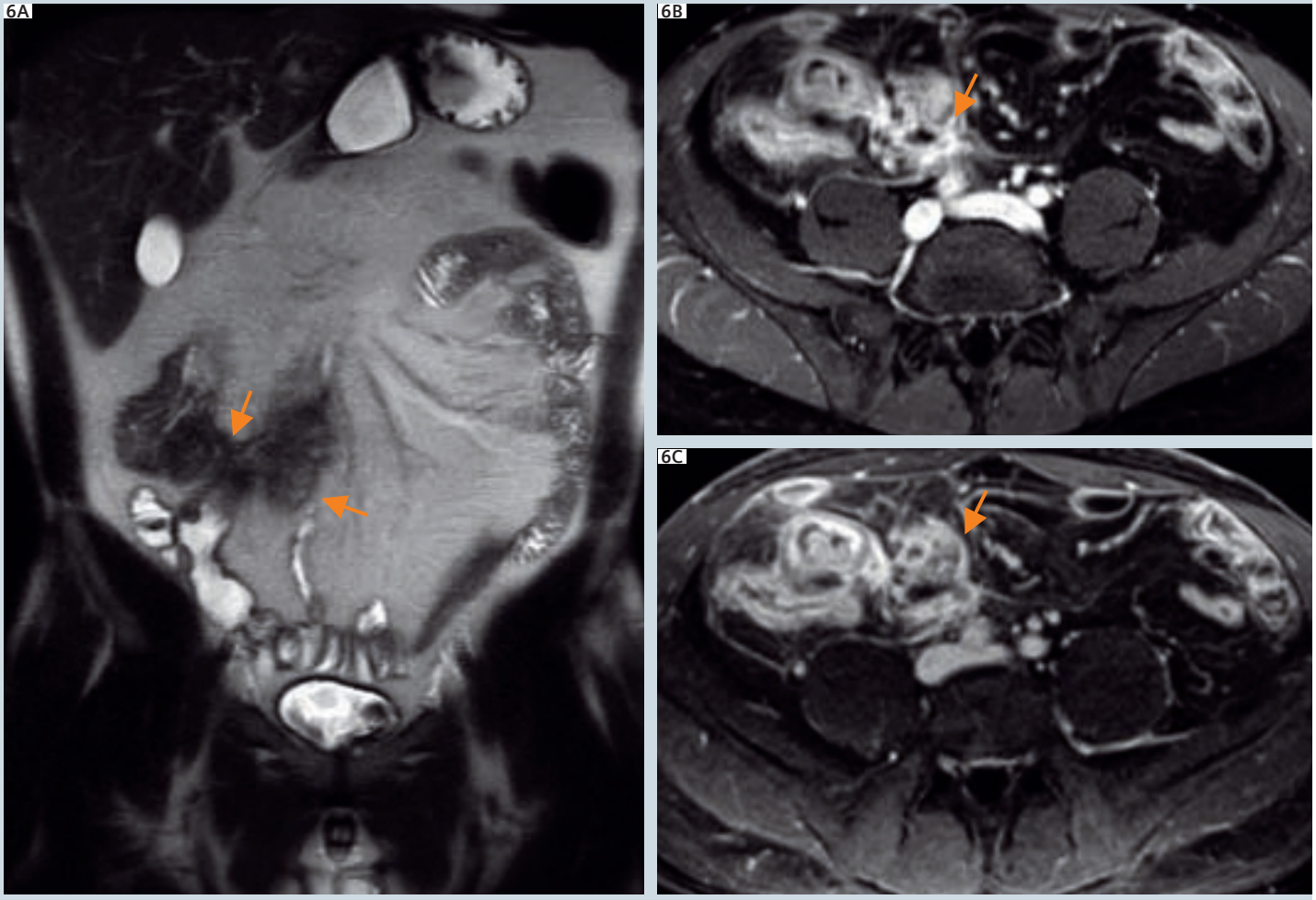

6 Hydro-MRI with TimCT-FLASH 2D. Male with recurrent Crohn's disease.

A: Coronal HASTE image. Mesenteric fistula with small abscesses.

B: Axial FLASH 2D derived from a standard breath-hold protocol. Crohn's disease of terminal ileum and caecum with mesenteric fistula (arrow).

C: Axial TimCT FLASH 2D 1 minute scan through abdomen and pelvis performed with one 25 second breath-hold phase. Crohn's disease of terminal ileum and caecum with mesenteric fistula (arrow).

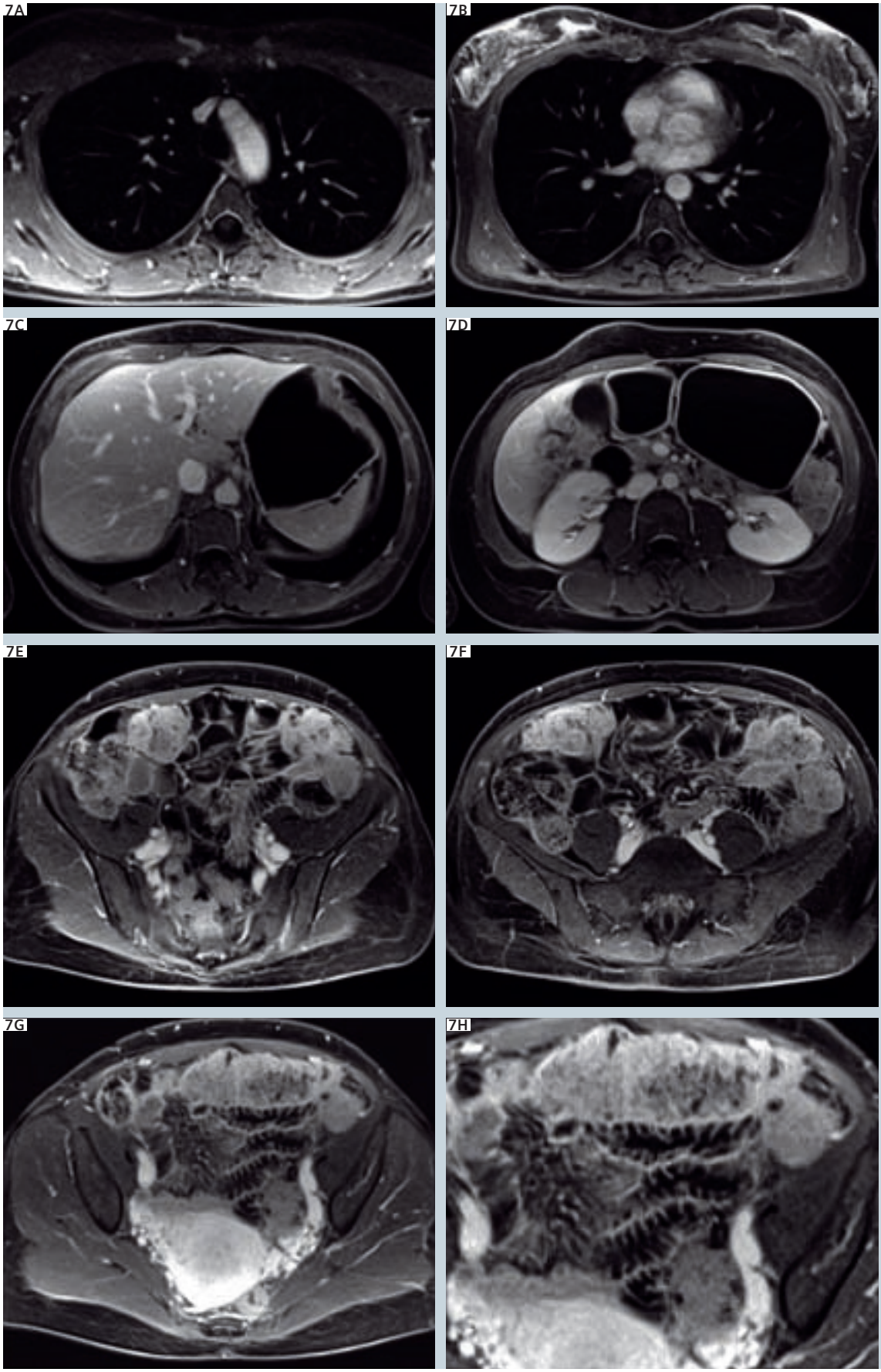

7 Contrast-enhanced TimCT-FLASH 2D. Female with celiac disease (CD).

2 minute scan through thorax, abdomen and pelvis recorded with three 20 second breath-hold phases during Hydro-MRI.

E–H: Increased number of folds in parts of the ileum.

Pushing the Boundaries of MR with Siemens MAGNETOM 7T

John Grinstead, Ph.D.; Siemens Medical Solutions USA, Inc.

Introduction

There has been a continual push towards higher and higher magnetic field strengths in MR, motivated primarily by the approximately linear increase in signal-to-noise ratio (SNR) with magnetic field strength. In the 1990s, 3 Tesla research systems were pushing the boundaries of the time. The engineering challenges at 3 Tesla led to technical improvements in areas such as RF technology. After considerable engineering efforts, 3 Tesla scanners made the transition to true clinical systems. Today, the technology is pushing forward again, this time to 7 Tesla. More challenges exist at 7 Tesla. These challenges are also opportunities to push innovation in MR technology even further, which will benefit all field strengths.

The MAGNETOM 7T System

7 Tesla MR systems are investigational devices and are not available for clinical use or diagnosis, but only for clinical research purposes.
Siemens is taking its expertise in RF technology and high-quality gradients and applying it to 7T. The MAGNETOM 7T offers 32 independent RF channels, and uses the proven fast and reliable whole-body MAGNETOM Avanto gradients. In addition, all Siemens 7T systems use the same advanced applications software platform as on our clinical systems.
The MAGNETOM 7T comes with a Siemens-approved CP transmit-receive head coil. The improvement in image quality due to a higher signal-to-noise ratio at 7T compared to a comparable transmit-receive coil on the 3T MAGNETOM Trio, A Tim System, is shown in Fig. 1. Of course, the Tim Trio is capable of much better SNR by using, for example, the 12-element receive-only Head Matrix coil, which is standard on the Trio, A Tim System. Multi-channel RF coils with higher SNR are also available at 7T. We used the CP coils because it allows a fair direct comparison, as for both field strengths the coil geometry is similar.
Whole-body 7T magnets are large unshielded magnets with a 2.4 meter outer diameter and 3.4 meter length, compared to standard 1.5T systems that have a 2 meter outer diameter and a 1.2 meter length. Because the magnets are unshielded, unlike modern clinical magnets, passive iron shielding is needed in the scanner room walls to minimize the floor

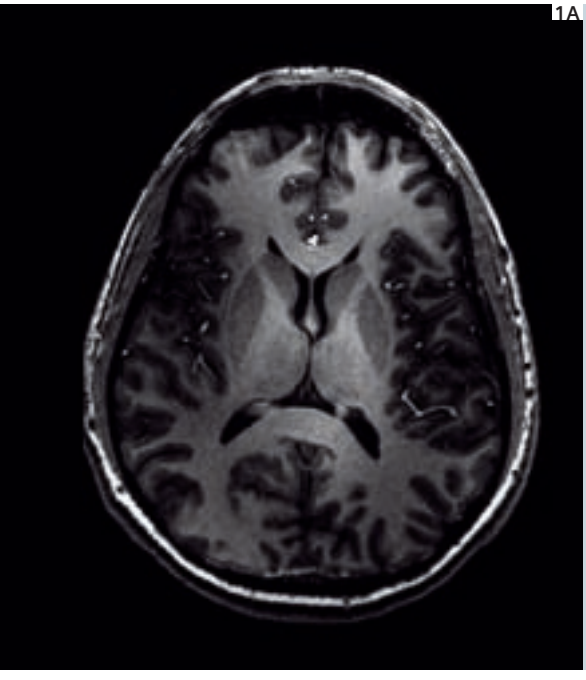

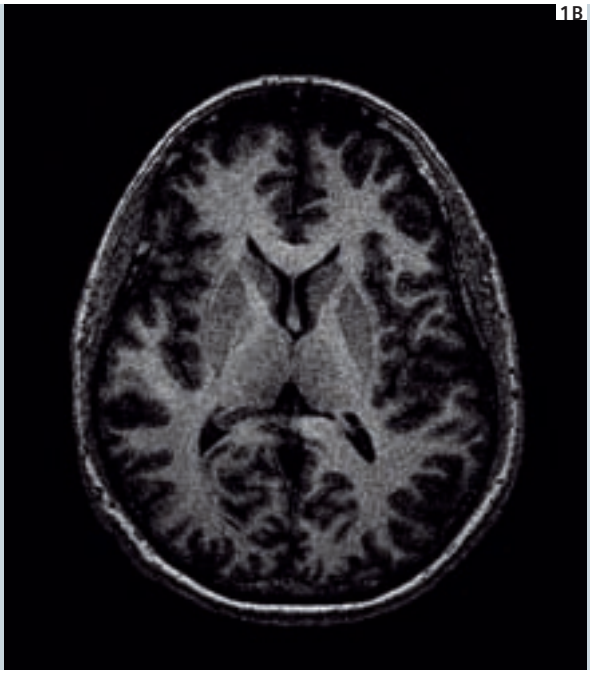

1 Comparison using transmit-receive volume coils at 7T (A) and 3T (B) for a T1-weighted MPRAGE sequence at 1 x 1 x 2 mm resolution.

Courtesy of W. Rooney and C. Springer, Oregon Health and Science University, Portland, OR, USA.

space footprint by restricting the 5 gauss line which is considered the safe boundary for the general public, such as those with cardiac pacemakers. This can require between 200 and 400 metric tons of iron, and the associated construction costs are significant.
Partly because of this, and also because the majority of 7T studies to date involve neuro applications, a head-only 7T system is also available. The first such 7T system has already been installed at the Center for Imaging in Biomedicine in Lausanne, Switzerland. This is an actively shielded head-only magnet that does not require iron shielding. It also has head-only gradients that are approximately twice as powerful and fast as whole-body gradients (80 mT/m, 400 T/m/s), which is possible because of the reduced size of the gradients for head-only applications.

7 Tesla RF Coil Technology

Siemens is a proven leader in RF technology with its Total imaging matrix (Tim) technology, currently offering 32 independent RF channels with a scalable Open Architecture. This expertise, combined with strong collaborations with leading research institutions across the world, is an essential element for success to get the most out of the greater MR signal at 7T. Coil design is more challenging at ultra high field due to dielectric effects. Multiple coil designs are being explored at several institutions. A few examples of multi-channel RF coils built by industrial and academic partners are shown in Fig. 2.

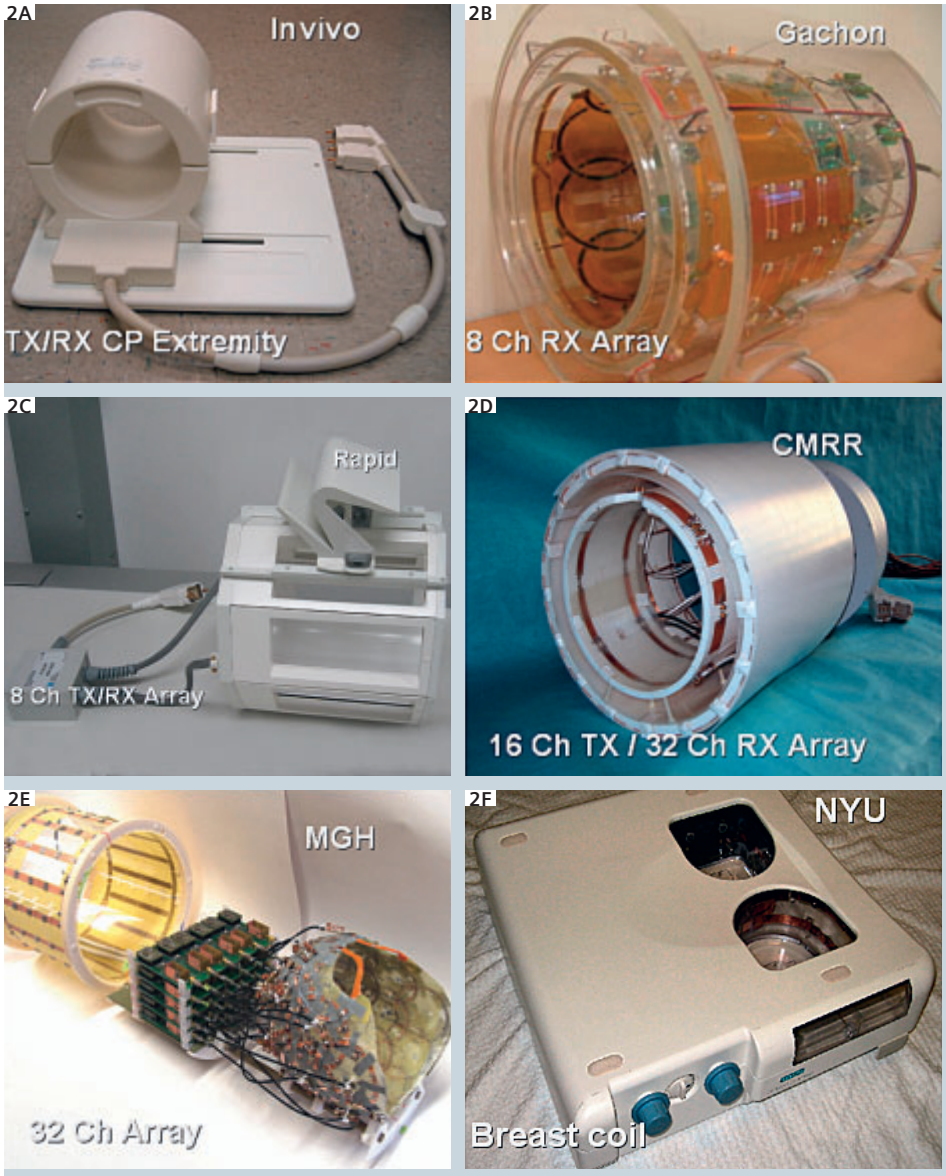

2 **A few examples of RF coils built by industrial and academic partners:**
A: CP Transmit/receive (TX/RX) extremity coil, Invivo
B: 8-channel RX array, Gachon Medical School, Seoul, Korea
C: 8-channel TX/RX array, Rapid Medical
D: 16-channel TX / 32 RX array, Center for MR Research, Minneapolis, MN, USA
E: 32-channel RX array, MGH Martinos Center, Boston, MA, USA
F: Breast coil, New York University, New York City, NY, USA

Signal and Contrast Improvements at 7 Tesla

As already mentioned, the primary reason to go up to 7 Tesla is to get more MR signal. The extra signal can be traded for a reduced imaging time by either reduced averaging or the use of integrated Parallel Imaging (iPAT) with high PAT factors. The extra signal can also be used to acquire exceptionally high resolution images in a scan time not possible at lower field strengths. Fig. 3 shows extremely high resolution ex vivo imaging of the temporal lobe (100 µm isotropic voxels), visualizing the entorhinal cortex islands related to the development of Alzheimer's disease. Fig. 4 is an in vivo coronal T1-weighted MPRAGE acquisition with 0.45 x 0.45 x 1 mm resolution, acquired with a 32-channel phased array coil, showing fine anatomical detail. Orthopedic imaging can also benefit from increased resolution and is being actively developed at 7T. Fig. 5 shows an image of the knee acquired with 0.35 x 0.35 x 4 mm voxels. The basis of the functional MRI (fMRI) signal is blood-oxygenation level dependent (BOLD) contrast, which generally increases quadratically with the magnetic field. This

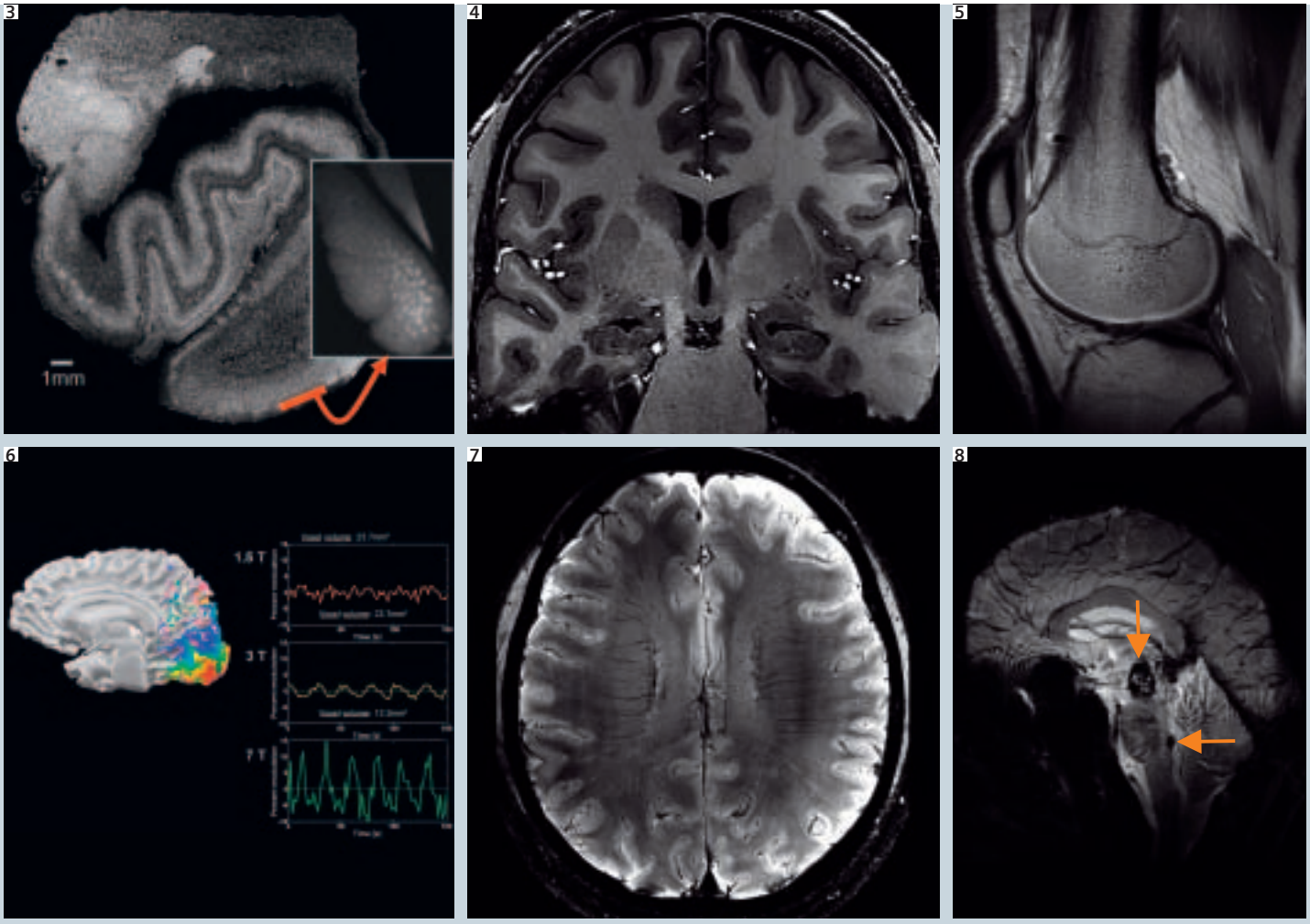

3 **Ex vivo images of the temporal lobe with 100 µm isotropic resolution, visualizing the entorhinal cortex islands related to the development of Alzheimer's disease.**

Courtesy of B. Fischl, L. Wald et al., MGH Martinos Center, Boston, MA, USA.

4 **A coronal T1-weighted MPRAGE image with 0.45 x 0.45 x 1 mm resolution, acquired with a 32-channel phased array coil.**

Courtesy of G. Wiggins, C. Wiggins, L. Wald et al., MGH Martinos Center, Boston, MA, USA.

5 **Knee image acquired at 0.35 x 0.35 x 4 mm resolution.**

Courtesy of M. Ladd, Erwin-Hahn-Institute for Magnetic Resonance, Essen, Germany.

6 **The plots show the increased BOLD (Blood Oxygen Level Dependent) signal change with field strength in a region of the occipital cortex throughout a series of fMRI measurements.**

Courtesy of H. Scheich, A. Brechmann, J. Stadler, Institute for Neuro-Biology, Magdeburg, Germany.

means the BOLD related signal change at 7T can be more than 5 times as much as 3T. Fig. 6 compares BOLD signal plots for a region of interest in the occipital cortex for optimized protocols at 1.5, 3, and 7 Tesla, showing a strong increase in the BOLD response with field strength. The higher magnetic susceptibility differences between venous blood and tissue can also be used for venous anatomical imaging. Fig. 7 depicts small veins in the corpus callosum and white matter; Fig. 8 shows a lower venous anomaly and cavernoma. Figure 9 is an extremely high resolution T2*-weighted gradient echo image with 0.22 x 0.22 x 1 mm voxels at two different zoom levels, showing a very high level of detail and many tiny blood vessels penetrating the cortex. This amount of resolution and venous sensitivity makes it possible to use gradient echo imaging to see microvascular changes in the initial stage of Multiple Sclerosis lesion development in vivo, which has not been seen at lower field strengths (Fig. 10). One can now see the small veins around which these lesions develop.

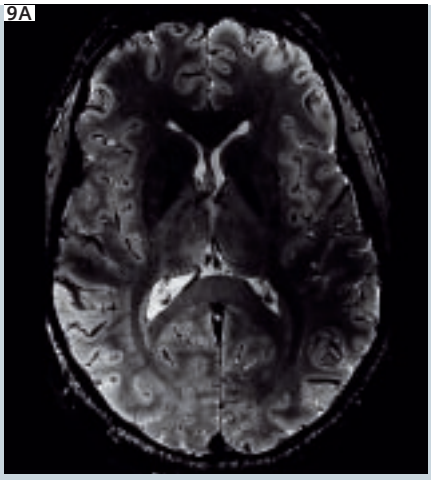

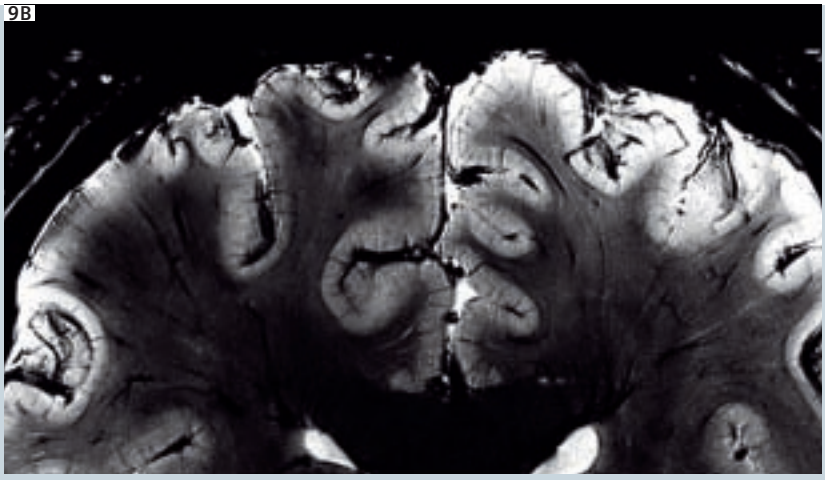

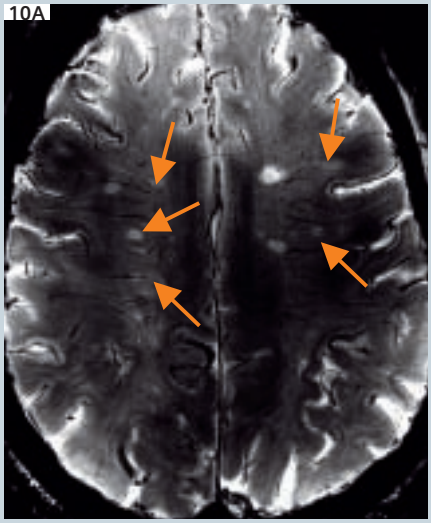

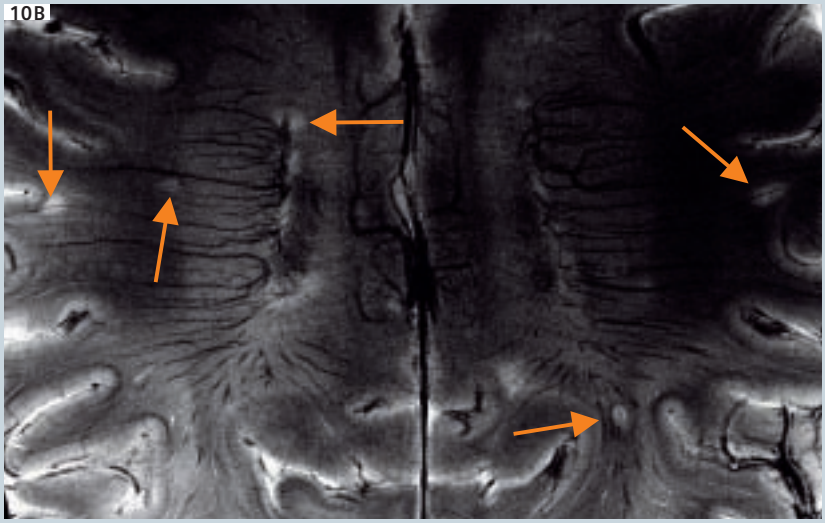

7 **Depiction of the veins in the corpus callosum and white matter.**

Courtesy of Z. Cho, Gachon Medical School, Seoul, Korea.

8 **Lower venous anomaly and cavernoma.**

Courtesy of M. Ladd, R. Forsting, Erwin-Hahn-Institute for Magnetic Resonance, Essen, Germany.

9 **High-resolution T2*-weighted gradient echo image with 0.22 x 0.22 x 1 mm voxels at two different zoom levels, showing many tiny blood vessels penetrating the cortex.**

Courtesy of G. Wiggins, C. Wiggins, L. Wald et al., MGH Martinos Center, Boston, MA, USA.

10 **(A) Microvascular changes in the initial stage of Multiple Sclerosis lesion development. (B) The small veins around which the lesions develop are visible.**

Courtesy of Y. Ge, R. Grossman, New York University, School of Medicine, New York City, USA.

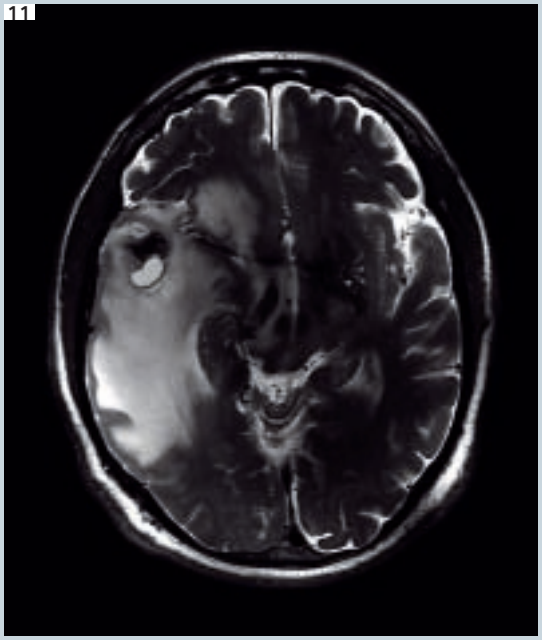

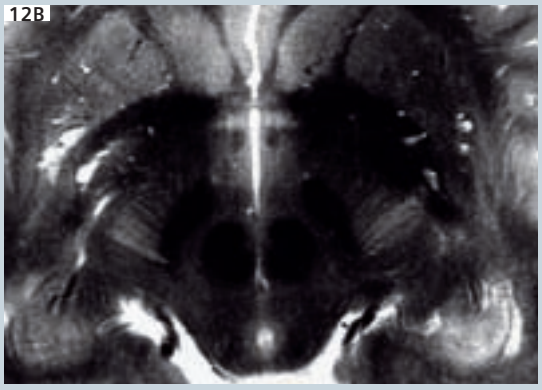

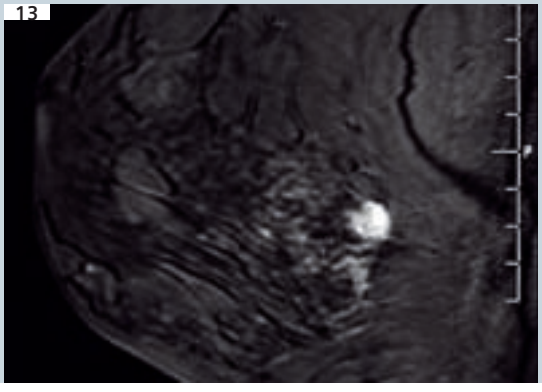

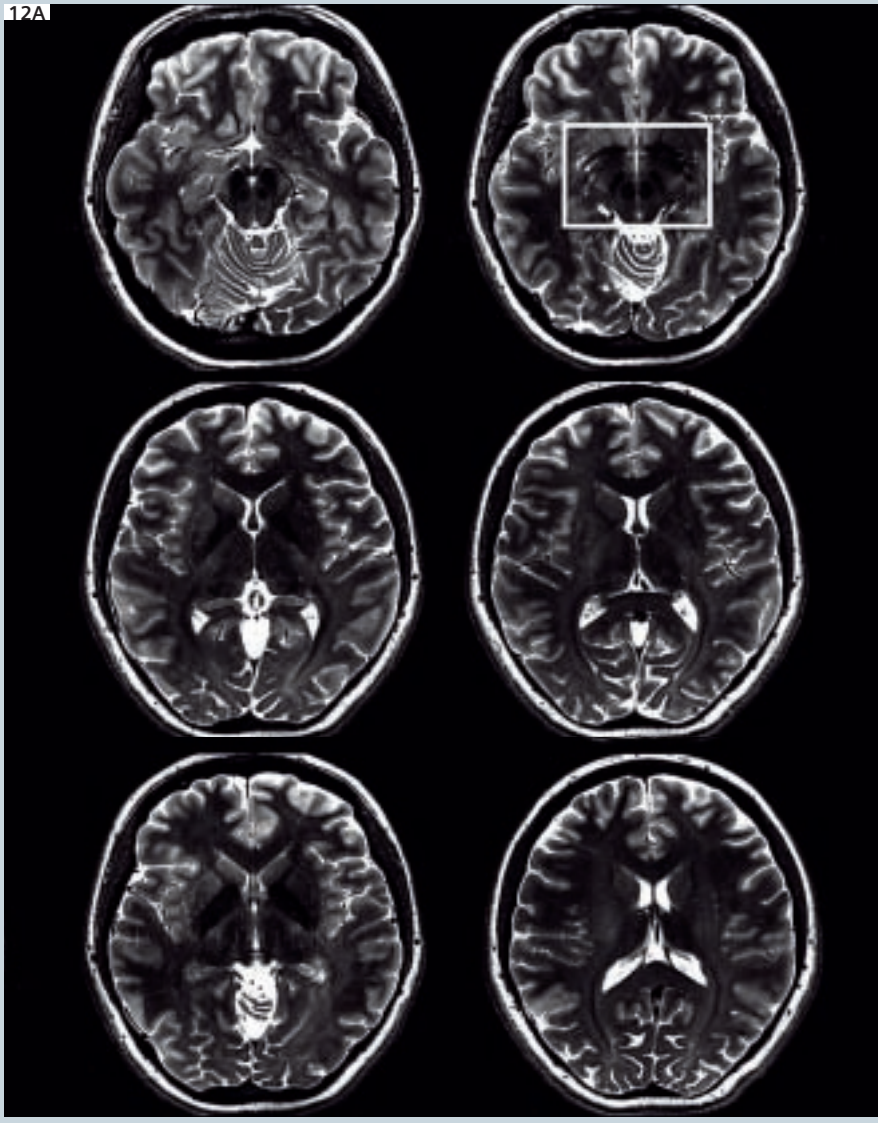

11 **T2-weighted image of glioblastoma using an 8-channel coil.**

Courtesy of M. Ladd, Erwin-Hahn-Institute for Magnetic Resonance, Essen, Germany.

12 **(A) Several slices from a T2-weighted turbo spin echo sequence. The zoomed section (B) shows high contrast between deep brain structures that have high iron content.**

Courtesy of E. Auerbach, C. Snyder, Gözübüyük, G. Adriany, T. Vaughan, K. Ugurbil, Center for MR Research, Minneapolis, MN, USA.

13 **Breast lesion post-contrast.**

Courtesy of R. Lee, L. Moy, New York University, School of Medicine, New York City, USA.

Fig. 11 is a T2-weighted image using an 8-channel coil demonstrating excellent contrast and resolution in examining glioblastoma. Fig. 12 contains several slices from a high resolution T2-weighted turbo spin echo using a 32-channel head coil with PAT factor of 2, 1024 x 1024 matrix, and 0.18 x 0.18 x 2 mm voxels. The zoomed section shows the high contrast of deep brain structures having relatively high iron content caused by the increased iron susceptibility effects at 7T.

Contrast agents have stronger effects at higher field due to both increased magnetic susceptibility and increased T1. This allows the use of smaller contrast doses or potentially can increase the lesion conspicuity post-injection. Fig. 13 shows initial results in the breast with good tumor contrast in the glandular tissues.

Conclusion

Development on 7 Tesla systems is progressing rapidly, and the user base is constantly growing with more than 10 MAGNETOM 7T systems already in operation. Although the siting, magnet size, engineering challenges, and associated costs are significant, the benefits of higher MR signal and contrast are allowing us to begin to see things not seen before. Technical advances at 7 Tesla should also benefit lower field strengths, and keep them at the forefront of MR research, making it worth the investment in applications and hardware development.

Parallel Transmission (pTX) Technology*

MR Imaging with an 8-Channel RF Transmit Array

Franz X. Hebrank[1], Lawrence L. Wald[2], Vijayanand Alagappan[2], Elfar Adalsteinsson[3], Kawin Setsompop[3], Adam Zelinski[3], Ulrich Fontius[4], Juergen Nistler[4], Franz Schmitt[4]

[1]*Siemens Medical Solutions, Charlestown, MA, USA*
[2]*Massachusetts General Hospital (MGH) Martinos Center, Charlestown, MA, USA*
[3]*Massachusetts Institute of Technology (MIT), Cambridge, MA, USA*
[4]*Siemens Medical Solutions, Erlangen, Germany*

Introduction

In recent years there has been a trend towards higher field strength in MR imaging. Nowadays 3 Tesla is already routinely used for clinical imaging, and there is a tendency to move towards even higher field strengths for human imaging, like 7T. But besides the many potential advantages of ultra-high field MRI, there are also some methodological challenges like the destructive interference of transmit RF fields within a typical volume coil [1, 2]. These effects arise when the RF wavelength reaches the dimension of the human head or body and can lead to center brightening in the head at 7T (Fig.1) and shading in abdominal imaging at 3T. The spatial variations of the B_1 field lead to reduced tissue contrast and inhomogeneous image intensity. Several methods have been explored to compensate for these spatial variations of the transmit field. These methods include the application of shaped 2D and 3D RF pulses [3] or "RF shimming", where the channels of the transmitting coil are driven with tunable global RF-phase and amplitude in order to optimize the homogeneity of the resulting B_1 field [4, 5, 6].
So far 2D and 3D RF pulses were not practical in clinical MR imaging, since the duration of the pulses is too long for normal sequences. Parallel transmission (pTX) techniques have demonstrated the feasibility of accelerating time consuming 2D and 3D excitation pulses, to accommodate clinical sequences [3, 4, 7]. Another challenge linked to the design of tailored 2D and 3D RF pulses and RF shimming is the need for a transmit coil with preferably highly decoupled elements. On current coil designs this requirement is often reduced to a high degree of decoupling between next neighboring elements. This article describes the design and setup of a parallel Transmission (pTX) prototype Siemens MAGNETOM Trio, A Tim System equipped with an 8-channel transmit array. This prototype MR system was used in combination with two different TX coils to acquire phantom and in vivo images with 1 to 8 fold accelerated 2D and 3D RF pulses.

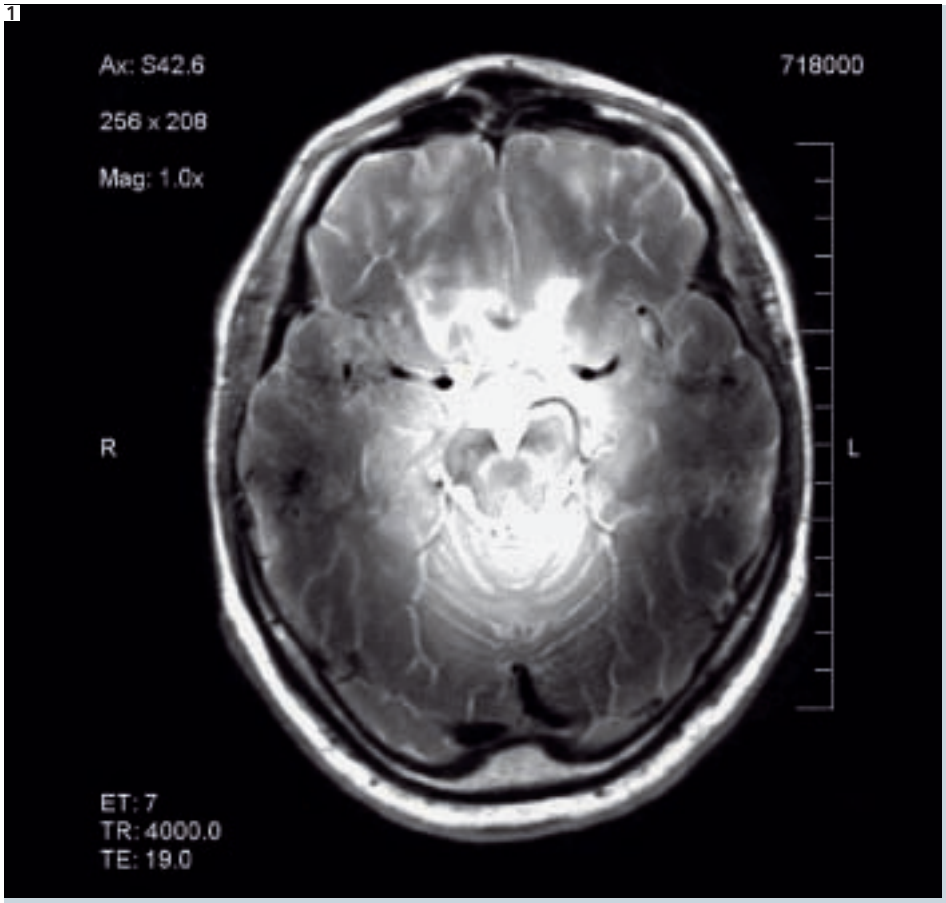

1 Center brightening in the head at 7T.

2

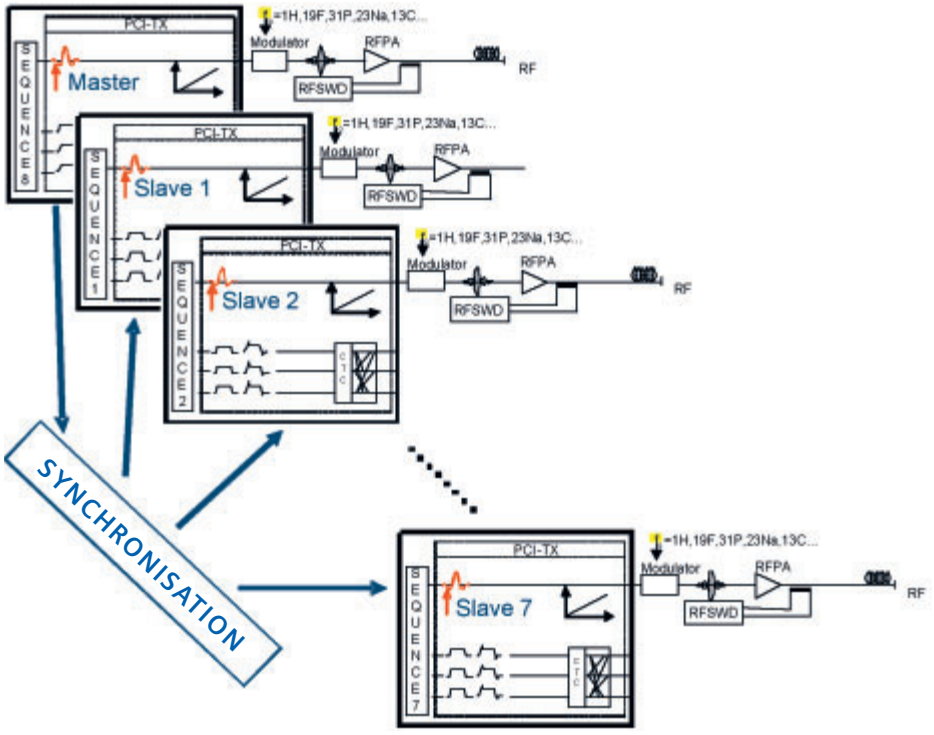

2 Block diagram of the Transmit Array system.

3 SAR simulations in the head.

4 Transmit only 8-channel. head coil.

Experimental Setup

System setup

A prototype 8-channel transmit array in a master-slave configuration was used, with one measurement control unit acting as the "master" controlling the other 7 "slaves" [8]. The transmit array was attached to a 3T MAGNETOM Trio, A Tim System, hence the primary console of the scanner was determined as the master (Fig. 2). Cloning the standard Siemens measurement control unit (MPCU) for all 7 slaves enables to run 8 independent sequences with individual RF shapes and characteristics, individual B_0 eddy current compensation and 3 additional gradient channels per unit, which can be used for gradient array [9] or dynamic shimming applications. Each of the 8 independent RF pulses is amplified by a separate 8 kW Dressler RF amplifier. For safety reasons, each channel includes its own independent RF power monitor (SAR supervision) which will switch off the RF in each channel if the SAR limit in any of the channels is exceeded. Moreover, the SAR settings can be configured for each channel individually limiting the peak power and the average power within the 6 minutes and 10 seconds time interval according to the IEC 60601-2-33 standard.

SAR calculation and safety concept

To ensure the safe operation and fulfillment of the IEC limits for SAR of the system in human imaging, the power limits were calculated before starting with the in vivo experiments. For this purpose a commercial program was used, which applies the Finite Integration Technique (FIT). The simulations were performed for the 8-channel head coil and the 8-channel body coil. The worst case SAR was calculated by summation of the E-field magnitude of all coil elements for all voxels in the human model. These worst case E-fields and the knowledge of the tissue properties were used to calculate the 10 g averaged local SAR and the whole-body SAR (Fig. 3). The calculated whole-body SAR was scaled down until the local SAR limits were fulfilled. These new whole-body SAR limits were divided by the number of transmit channels and were applied to the SAR supervision of each channel. With this concept the RF safety concerning whole-body and local SAR limits is guaranteed, even if one or more of the amplifiers will fail.

Transmit coils

Two different 8-channel coils were used for parallel transmission:
The first coil is a pTX only head coil (Fig. 4), which was used for the RF excitation in combination with the body coil receiving the RF signals [10]. This TX only coil was designed as a degenerated birdcage coil (DBC) [11], which basically can be used in two mode configurations, using either the eight "loop mode" basis set or the orthogonal birdcage modes as driven by an 8 x 8 Butler matrix [12]. The Butler matrix has 8 coaxial inputs and 8 coaxial outputs, which can therefore produce

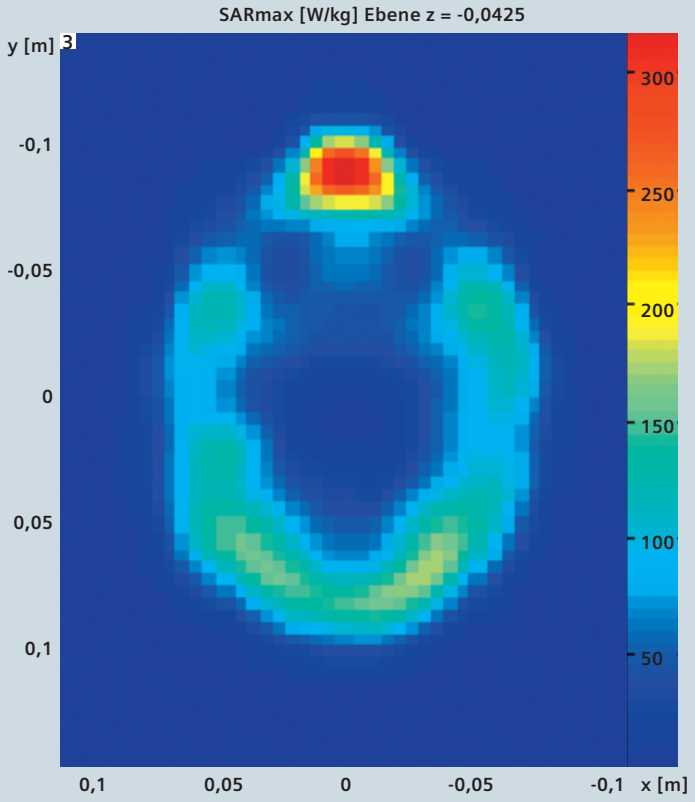

3

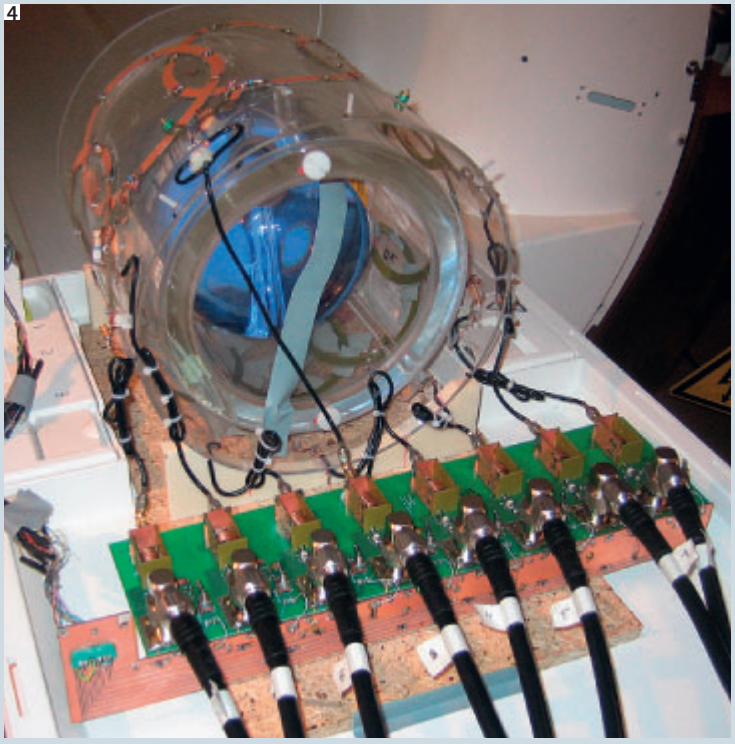

4

8 independent modes. The big advantage of using the modes of a birdcage coil excited by a Butler matrix is that they form naturally decoupled orthogonal modes which do not require additional decoupling strategies. This decoupling is essential for a parallel transmission methodology, since – similar to a parallel receive array – the capability of a transmit array to accelerate the spatially tailored excitation pulses depends on the spatially differing B_1 profiles of the individual array elements.

The second coil used for the experiments is an 8-channel TX/RX body coil, which also allowed the insertion of a Butler matrix into the TX and the RX path to generate orthogonal modes [13].

With both coils in a first step the magnitude and phase profiles of the transmitted B_1 field have been measured. To avoid an interference with the receive coil profile this measurement was performed for both 8-channel coils using the uniform standard CP mode of the scanner body coil for RF reception. The amplitude and phase of these B_1 fields were then used for the calculation of the RF pulse shapes as described in the next section.

RF pulse design

Different RF waveforms in the low flip angle domain were calculated based on the formalism used by Grissom et al. [14]. For excitation we used two types of gradient trajectories [3]:

The first trajectory consisted of a 2D excitation with a spiral trajectory in (k_x, k_y) and no encoding in z-direction. This 2D trajectory can be used to excite a high resolution target profile in the 2D plane. With this pulse design accelerations of integer factors of 2 through 8 can be utilized by successively increasing separation between the turns in the k-space trajectory. At a gradient amplitude of 35 mT/m and a slew rate of 150 T/m/s the duration of these 2D pulses could be reduced from 9.47 ms in the unaccelerated case (R =1) to 2.42 ms for R = 4, 1.64 ms for R = 6 and only 1.26 ms for R = 8 respectively. Therefore the R = 8 accelerated pulse was 7.5 times shorter than the unaccelerated pulse, which will make their application in clinical pulse sequences possible.

The second trajectory consisted of a 3D k-space excitation using a set of line segments or "spokes" in the k_z direction placed at regular intervals in the (k_x, k_y) plane [3, 15, 16, 17]. Using a sinc-like RF waveform during the transversal of each spoke achieves a sharp slice selection in z but with low resolution control of the in-plane magnetization profile. Two versions of these trajectories were designed and tested: one with 4 spokes with a pulse length of 3.42 ms and one with 1 spoke with a pulse length of 1.2 ms. With such a trajectory it is possible to achieve a uniform excitation across the phantom despite the nonuniform nature of the 8 individual excitation profiles.

Image examples

Phantom measurements

The 2D trajectory in combination with the 8-channel pTX head coil was used to excite a high-resolution spatial pattern of letters in the (x, y) plane. The resolution for this experiment was set to 5 mm with a FoV of 180 mm. Fig. 5 shows the image using an acceleration factor of R = 4. The high resolution "Tim TX" logo (Fig. 6) was also acquired using the 2D trajectory with an acceleration of R = 4. For this image parallel transmit and parallel receive have been used simultaneously by employing the 8-channel TX/RX body coil for excitation and the standard Siemens 12-channel Head Matrix coil for reception of the data. Fig. 7 shows as an example the image of a phantom using the 3D homogenous excitation with 4 spokes and an acceleration factor of R = 4. For this measurement the RF pulse duration was 3.42 ms.

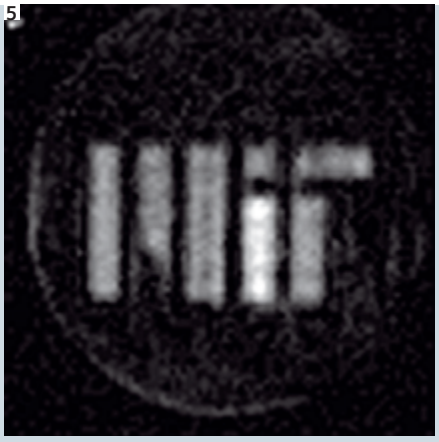

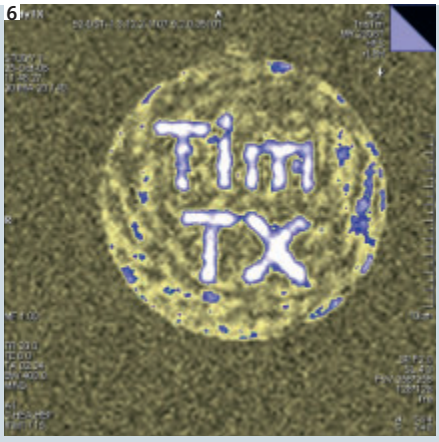

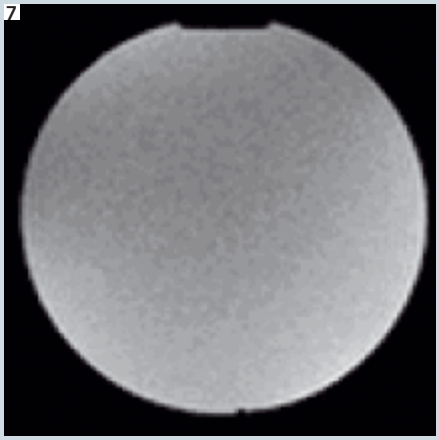

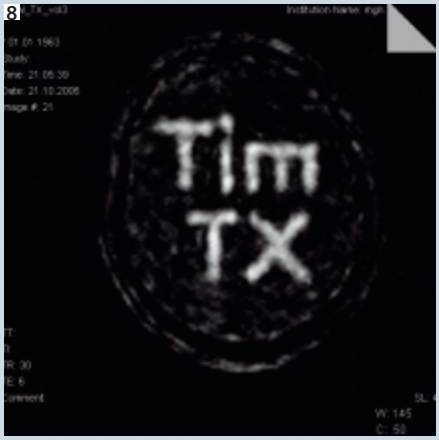

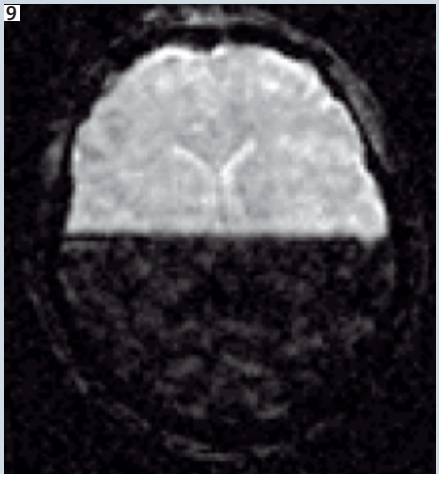

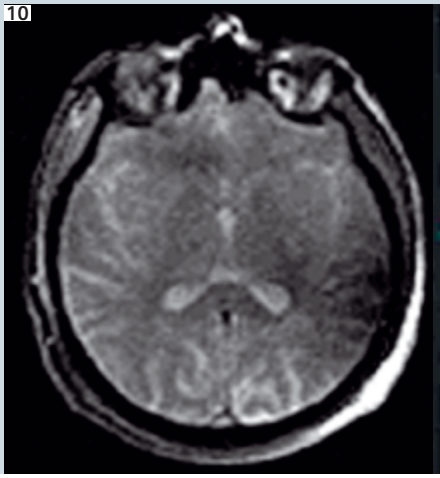

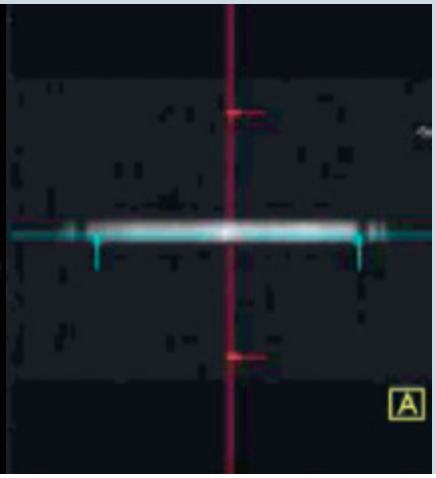

5 MIT logo excitation using a 2D trajectory and the TX head coil, R = 4.

6 "Tim TX logo", 2D excitation with body coil, acquisition with 12-channel Head Matrix coil, R = 4.

7 3D homogenous excitation using the 4 spokes trajectory.

8 "Tim TX" logo in the human head acquired with the TX head coil using an acceleration of 4.

9 "Half brain" excitation with the TX head coil, R = 4.

10 3D excitation of a homogenous slice in the brain using the TX/RX body coil for excitation.

11 3D excitation of a homogeneous slice in the human torso using the TX/RX body coil for excitation.

In vivo measurements

Using the TX only head coil for excitation and the 2D trajectory with an acceleration factor R = 4 the "Tim TX" logo could also be excited in the human brain (Fig. 8). Moreover with this coil/pulse configuration we were also able to excite only one half of the subject's brain (Fig. 9) using an acceleration factor of R = 4. Excitation of homogeneous brightness profiles in the head (Fig. 10) and the torso (Fig. 11) were obtained with the TX 8-channel body coil using the 3D pulses with a 4 spokes design as described above.

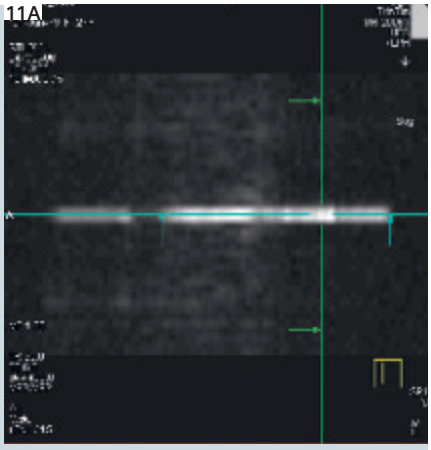

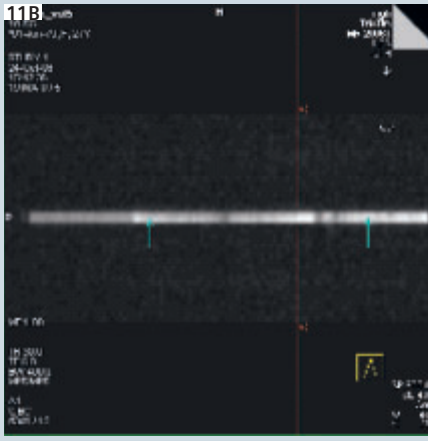

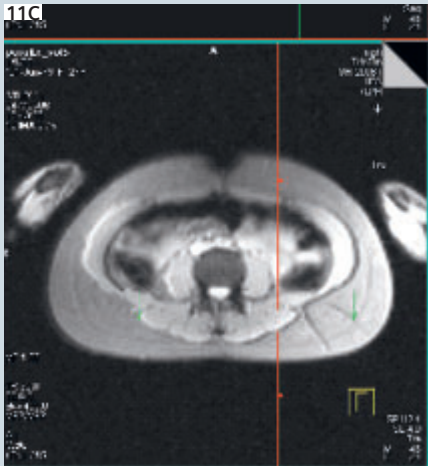

Conclusion

We have developed a new setup of a parallel Transmission (pTX) prototype Siemens MAGNETOM Trio, A Tim System equipped with an 8-channel transmit array. This new scanner was successfully tested in combination with two different 8-channel coils and two different RF pulse designs. With this combination of modified software and hardware we were able to acquire phantom and in vivo images with homogeneous signal distribution and high resolution spatial patterns. First results with the pTX array are very promising and raise the possibility of performing highly homogeneous head and whole-body imaging not only at 3T but furthermore at ultra high field strength like 7T, where destructive interference of transmit RF fields can lead to clinically compromised image quality. Moreover the design of 2D trajectories in combination with acceleration factors of up to 8 also raise the possibility to use these 2D pulses in clinical sequences, where the duration of the RF pulse is crucial.

* WIP – Works in Progress. The information is preliminary. The sequence is under development and not commercially available in the U.S., and its future availability cannot be ensured.

References

1 Hoult DI, Phil D. Sensitivity and power deposition in a high-field imaging experiment. J Magn Reson Imaging 2000; 12(1): 46–67.

2 Collins CM, Liu W, Schreiber W, Yang QX, Smith MB. Central brightening due to constructive interference with, without, and despite dielectric resonance. J Magn Reson Imaging 2005; 21(2): 192–196.

3 Setsompop K, Wald LL, Alagappan V, Gagoski B, Hebrank F, Fontius F, Schmitt F, Adalsteinsson E. Parallel RF Transmission with Eight Channels at 3 Tesla. Magn Reson Med 2006; 56(5): 1163–1171.

4 Katscher U, Bornert P, Leussler C, van den Brink JS. Transmit SENSE. Magn Reson Med 2003; 49(1): 144–150.

5 Vaughan, J.T., DelaBarre, L., Snyder, C., Adriany, G., Collins, C., Van de Moortele, P-F., Moeller, S., Ritter J., Strupp, J., Andersen, P., Tian, J., Smith, M., Ugurbil, K., RF Image Optimization at 7T & 9.4T, 2005, ISMRM. Miami Beach, Florida, USA. p. 953.

6 Adriany, G., Van de Moortele, P-F., Wiesinger, F., Moeller, S., Strupp, J., Andersen, P., Snyder, C., Zhang, X., Chen, W., Pruessmann, K.P., Boesiger, P., Vaughan, J.T., Ugurbil, K., Transmit and receive transmission line arrays for 7 Tesla parallel imaging. Magn Reson Med, 2005. 53(2): p. 434–445

7 Zhu Y. Parallel excitation with an array of transmit coils. Magn Reson Med 2004; 51(4): 775–784.

8 Fontius U., et al., A Flexible 8-Channel RF Transmit Array System for Parallel Excitation, 2006, ISMRM, Seattle, Washington, USA, p. 127

9 Parker DL, Hadley JR. Multiple-Region Gradient Arrays for Extended Field of View, Increased Performance, and Reduced Nerve Stimulation in Magnetic Resonance Imaging, Magn Reson Med, 2006; 56 (6): 1251–1260.

10 Alagappan V, Nistler J, Adalsteinsson E, Setsompop K, Fontius U, Vester M, Wiggins GC, Hebrank F, Renz W, Schmitt F, Wald LL. A degenerate Mode Band-Pass Birdcage for Accelerated Parallel excitation. Submitted for Magn Reson Med.

11 Lin FH, Kwong KK, Huang IJ, Belliveau JW, Wald LL. Degenerate mode birdcage volume coil for sensitivity-encoded imaging. Magn Reson Med 2003; 50(5): 1107–1111.

12 Moody HJ. The systematic design of the Butler matrix. IEEE Transaction on Antenna and Propagation 1964: 786–788.

13 Nistler J. et al, Using a mode concept to reduce hardware efforts for multi channel transmit array, 2006, ISMRM, Seattle, Washington, USA, p. 2024

14 Grissom W, Yip C-Y, Noll DC. A new method for the design of RF pulses in Transmit SENSE, Proceedings of the 2nd International Workshop on Parallel Imaging, Zurich, Switzerland 2004. p. 95.

15 Saekho S, Boada FE, Noll DC, Stenger VA. Small tip angle three-dimensional tailored radiofrequency slab-select pulse for reduced B1 inhomogeneity at 3 T. Magn Reson Med 2005; 53(2): 479–484.

16 Ulloa J, P. I, Hajnal JV. Exploring 3D RF shimming for slice selective imaging. 2005; ISMRM. Miami Beach, Florida, USA. p 21.

17 Saekho S, Yip C-Y, Noll DC, Boada FE, Stenger VA. A Fast-kz 3D Tailored RF Pulse for Reduced B1 Inhomogeneity. 2005; ISMRM. Miami Beach, Florida, USA. p 22.

Acknowledgments

We would like to thank Melanie Schmitt for her valuable assistance in the preparation of this article.

Proven Outcomes to Redefine Healthcare.

Introducing Siemens Medical Solutions Diagnostics. Combining the strengths of **Diagnostic Products Corporation** and **Bayer Diagnostics**, along with a comprehensive portfolio of industry-leading imaging and IT products, Siemens Medical Solutions becomes the world's first full-service diagnostic company. Now we can provide more customized and innovative solutions for your diagnostic needs. Together, we're taking you closer than ever to personalized healthcare. In a way that only Siemens can.

www.siemens.com/diagnostics

SIEMENS
medical

DX-Z1017-1-7600

Image Gallery
MAGNETOM Symphony, A Tim System

Dr. Cheng from VGH-Healthtech International in Taiwan made these artistic images of flowers on a MAGNETOM Symphony, A Tim System, using the VIBE sequence. The flowers had Gd for one day to give enhancement for the fine detail of fiber. High-resolution images (512 x 512) with about 0.3–0.5 mm resolution have been acquired using the knee coil. Postprocessing was done using VRT (Volume Rendering Technique) or MIP (Maximum Intensity Projection).

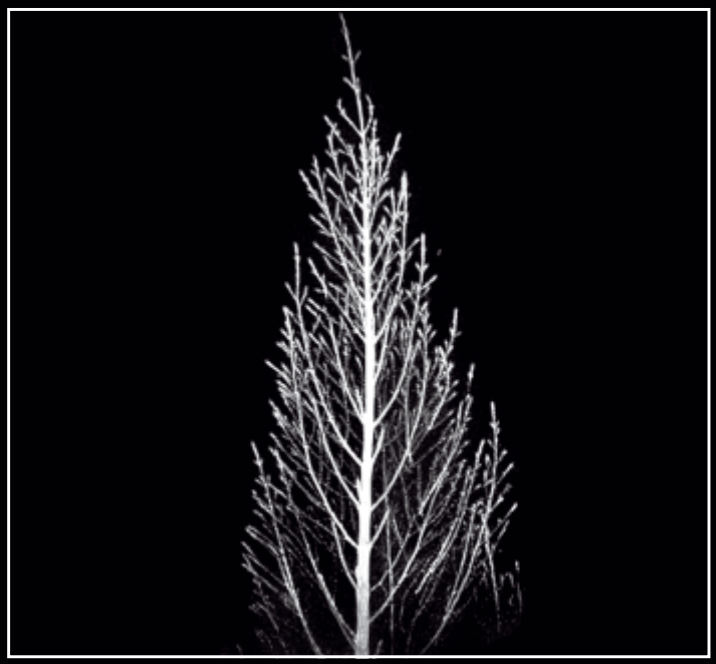

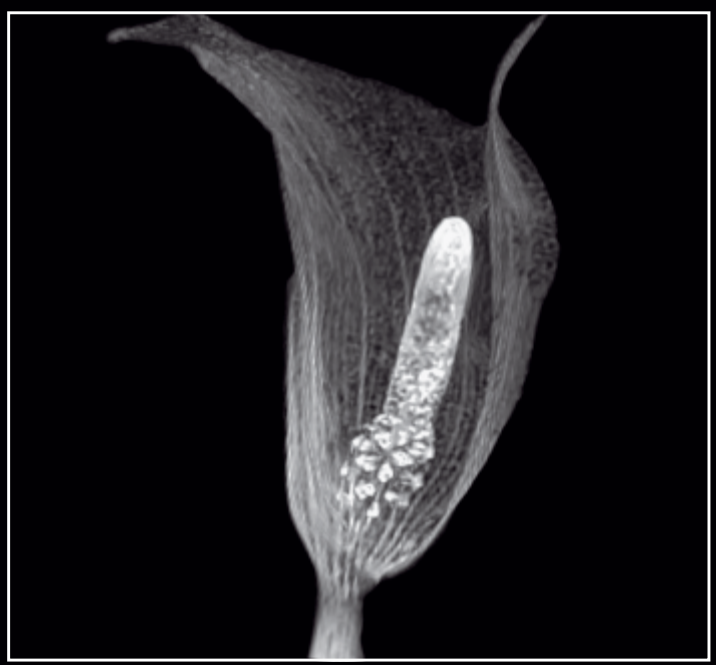

MAGNETOM Symphony With New Applications Power-class with *syngo* MR A30

With more than 2,000 installations worldwide – constantly maintained at the leading edge of MRI technology – MAGNETOM Symphony now has been powered with the latest applications thanks to new software *syngo* MR A30. For further up-to-date information please visit our internet pages at www.siemens.com/mr and select MAGNETOM Family.

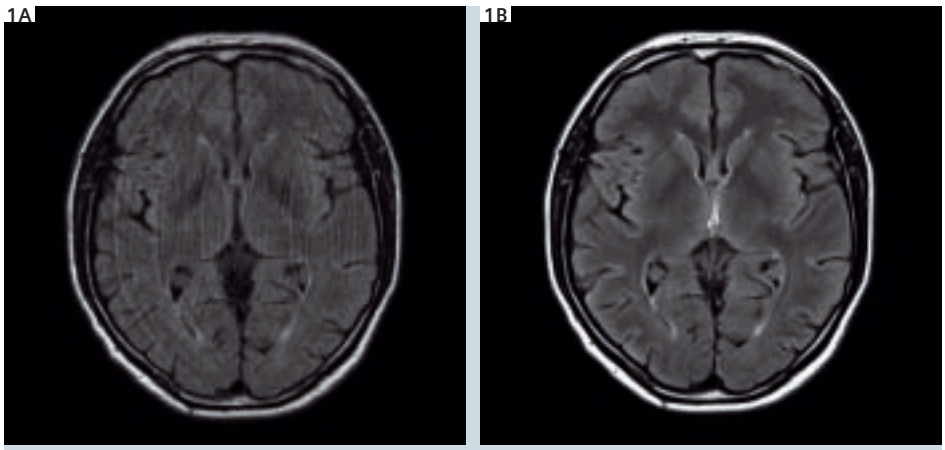

1 **Head imaging, TIR (Turbo Inversion Recovery) DarkFluid. 1A: Without motion correction. TR 8000 ms, TI 2500 ms, TA 2:24 min, SL 5 mm, FoV 230 mm. 1B: With *syngo* BLADE. TR 9500 ms, TI 2500 ms, TA 2:03 min, SL 5 mm, FoV 250 mm.**

Courtesy of MR Bremen Nord, Germany.

syngo BLADE

Capable of robust imaging in all applications areas and in all 3 orientations even in cases of severe movement, *syngo* BLADE motion correction enables facilities to increase patient throughput and decrease costs.

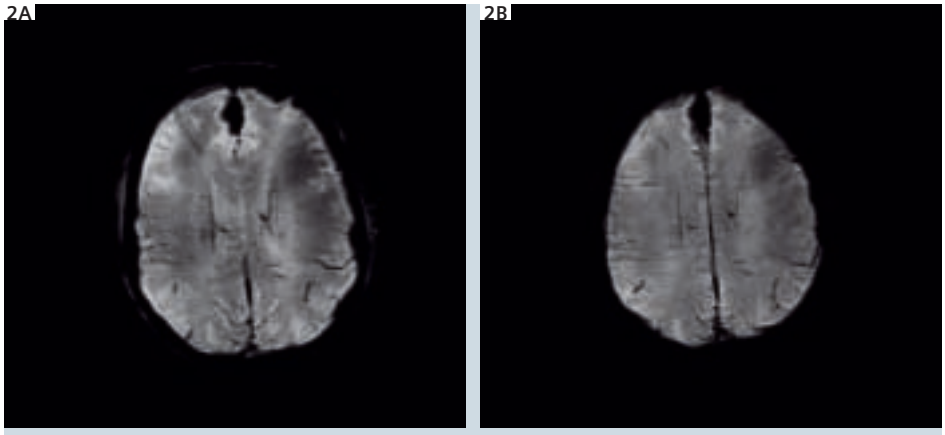

2 **Falx cerebri calcification. 3D SWI, minIP (minimal Intensity Projection) image. 2A: TA 2:45 min. 2B: TA 2:45 min.**

Courtesy of Dr. Hancken, Stade, Germany

syngo SWI

This technique exploits the susceptibility differences between tissues. *syngo* SWI (Susceptibility-Weighted Imaging) opened the door for improved contrast and improved detection of hemorrhage and microhemorrhage. It is also an excellent method to pick up abnormalities in iron and calcium in different anatomical locations in the brain.

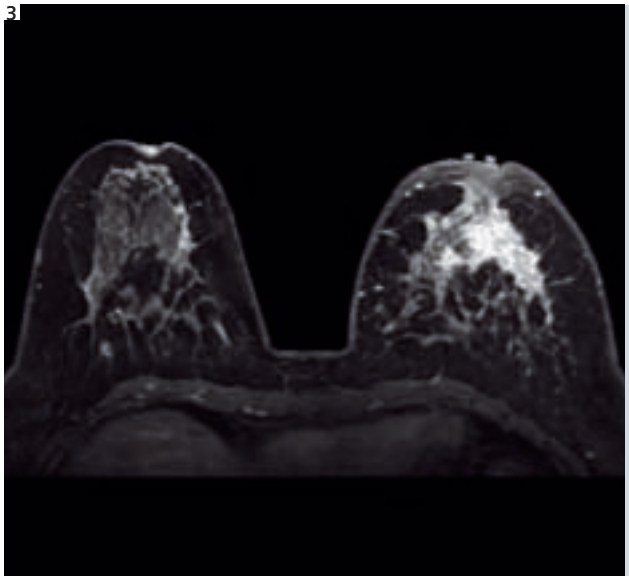

3 **3D breast imaging with 0.8 mm isotropic resolution. *syngo* VIEWS, Water Excitation, post chemo therapy, inflammatory carcinoma. TR 10.2 ms, TE 4.6 ms, eff. SL 0.8 mm, matrix 512, FoV 320 mm.**

Courtesy of Cedars-Sinai MRI, USA.

syngo VIEWS

syngo VIEWS is a 3D FLASH sequence with Water Excitation that enables 3D bilateral breast imaging with high spatial and temporal resolution, providing excellent diagnostic capabilities in breast disease. All this is working in combination with the Siemens-unique Parallel Imaging algorithm *syngo* GRAPPA to reduce scan time.

4

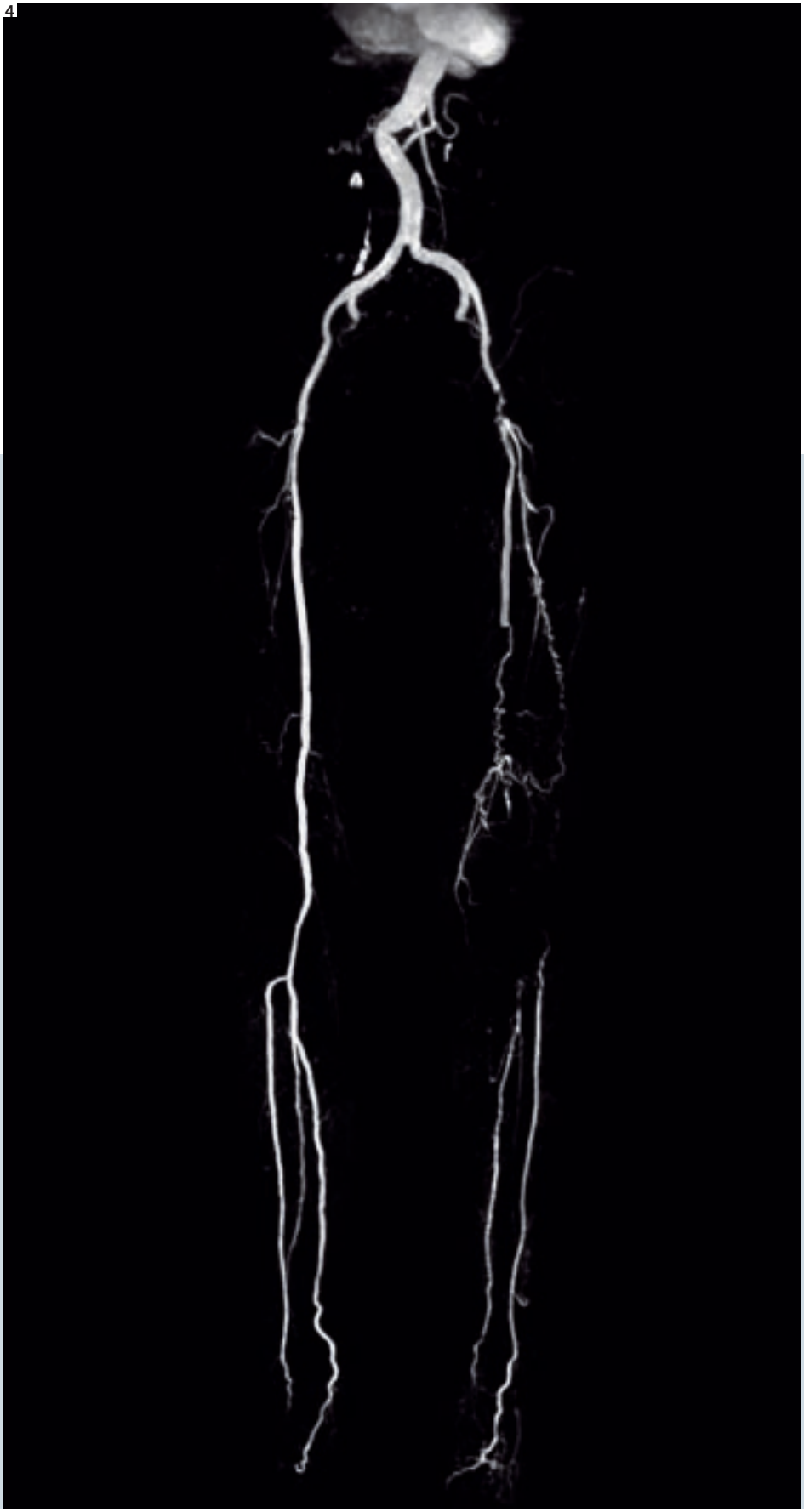

Composing *syngo*

This application provides dedicated evaluation software for creating full-format images from overlapping MR volume data sets of the different anatomical structures like the spine, vascular structures acquired at multiple stages.

4 **Composed image from the level of the abdominal aorta to feet vessels. Contrast enhanced peripheral MR Angiography (pMRA) with Fat saturation, MIP (maximum intensity projection). PAT factor 2, FoV 470 mm. Coil combination of Body Array, Spine Array, and Peripheral Angiography Array (PAA).**

Courtesy of AKH Linz ZRI, Linz, Austria.

A) Abdominal level, TA 15 s, eff. SL 1.6 mm, partitions 64, matrix 384.

B) Upper leg level, TA 11.7 s, eff. SL 1.45 mm, partitions 60, matrix 512.

C) Lower leg level, TA 17.3 s, eff. SL 1.3 mm, partitions 88, matrix 44.

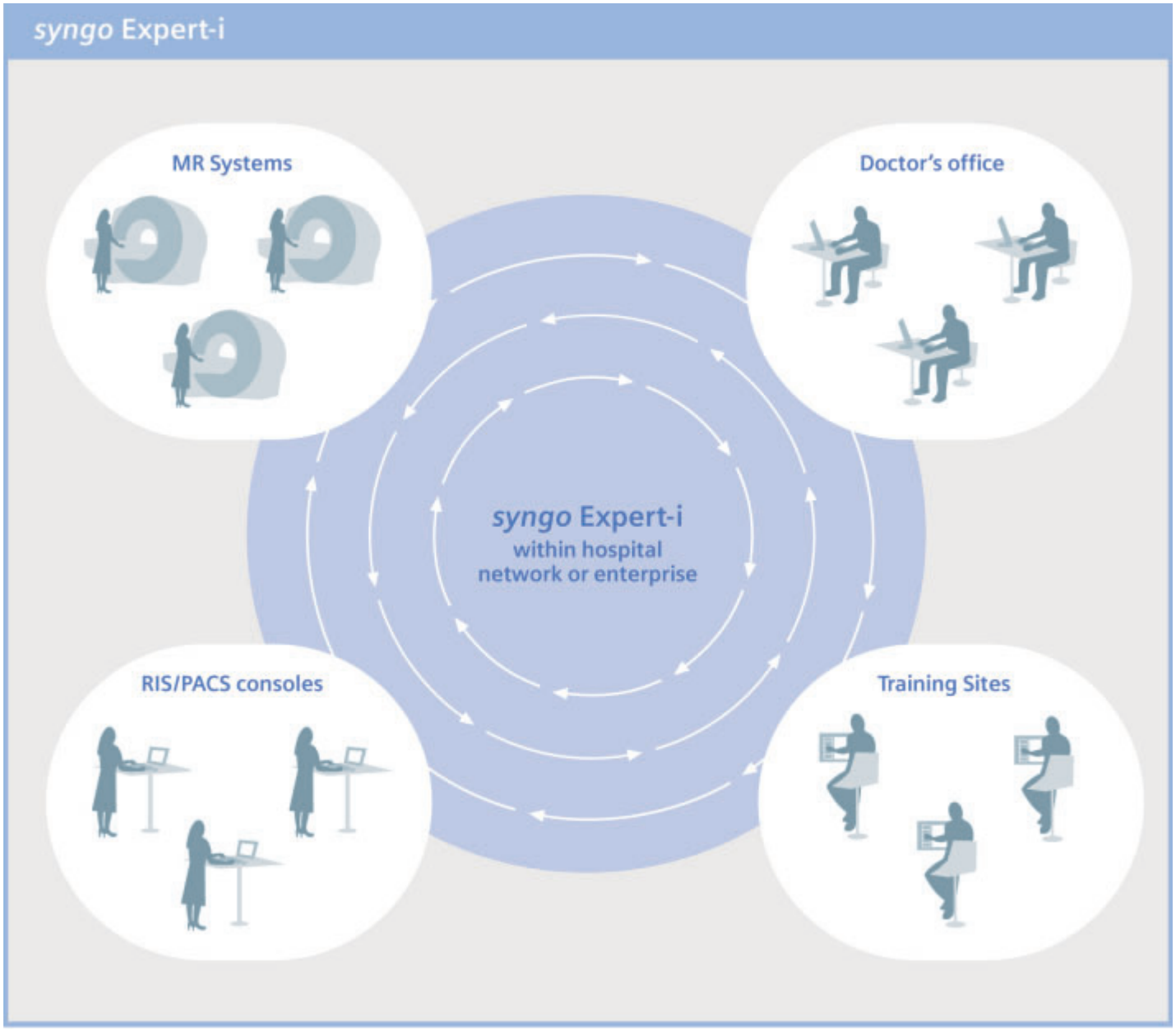

syngo Expert-i

syngo Expert-i offers an intelligent solution to remotely access your Siemens MR scanner and/or *syngo* MultiModality WorkPlace (Leonardo) from anywhere in the enterprise IT network. You can easily view the entire patient set-up, imaging data, and all sequences performed in real-time.

Inline Image Filter

Image Filters help to suppress unnecessary noise and improve the overall image appearance. With the Inline capability we help you to reduce your post-processing steps and shorten the total examination time. By including the filter in the protocol it will automatically process the images.

DVD / USB writing

With the DVD burning functionality, you save money and time. *syngo* MR A30 enables you to store up to 25,000 images on a single DVD compared to only 4,000 at 256 x 256 matrix on a CD. READ and WRITE DVD-R Media with 4.7 GB are supported.

Your verdict: “Great job – keep doing what you’re doing!”

Nearly 200 readers from 30 countries participated in the survey in the MAGNETOM Flash 3/2006. Thank you!

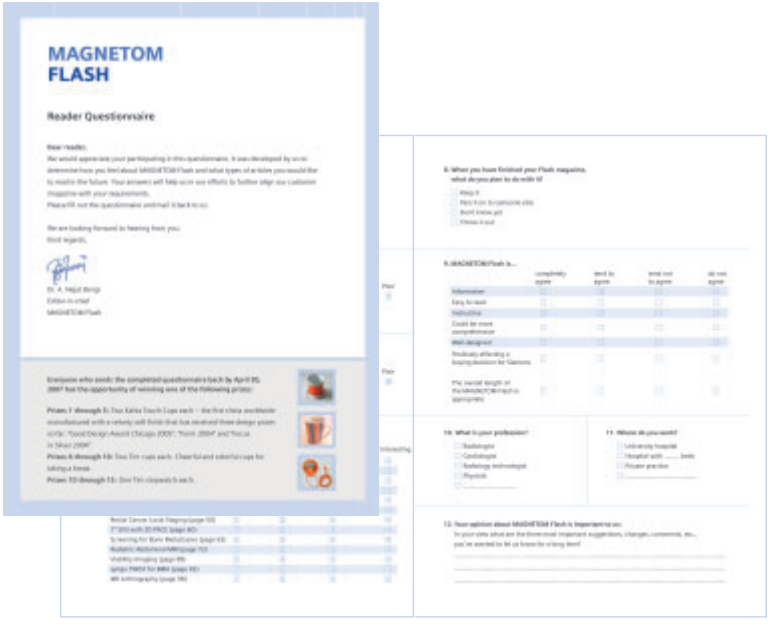

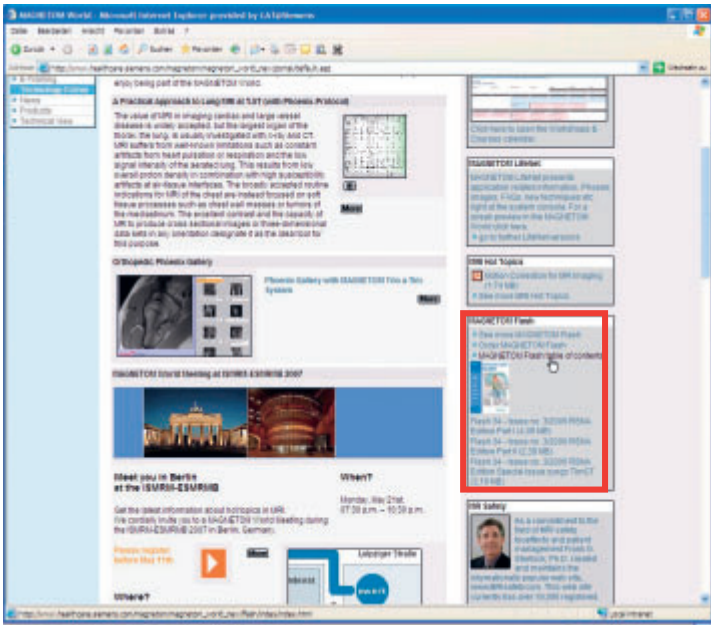

Application hints

Your evaluation of the selection of topics was positive: “Good” (61%) or “Exceptional” (38%). The favorite topic suggested for future issues was scanning tips and techniques. Your wish is our command: In this issue of MAGNETOM Flash we launch a “How I do it” section, starting with application hints for MR knee examinations and two articles on MR imaging of the carpometacarpal joint of the thumb and of the forefoot.
When asked to rate your interest in the articles that appeared in the MAGNETOM Flash issue 3/2006, you gave the highest scores to the new *syngo* applications. SPACE in head imaging led the ranks (57% “Very Interesting” and 30% “Interesting”), followed by motion correction with *syngo* BLADE (53% “Very Interesting”, 39% “Interesting”), and *syngo* TWIST (53% “Very Interesting”, 33% “Interesting”).

Table of content and Online version

Since the majority of you (70%) keep your MAGNETOM Flash issues for further reference, we now provide a table of contents for all of the issues since 2002. Please go to www.siemens.com/magnetom-world and select “MAGNETOM Flash table of contents” from the box on the right hand-side. For those of you who asked for online versions of the magazine, the MAGNETOM World webpage also contains pdf files for the current articles and – by selecting “see more MAGNETOM Flash” – you will find the electronic versions of most articles since 2002.

The MAGNETOM Flash editorial team would like to thank everyone who participated in the survey for your enthusiastic and constructive comments. They will be extremely helpful for future issues. One response was particularly heart-warming. A radiologist from Arizona, USA, gave us the following feedback, in German: “Please do not change anything. I am looking forward to each new issue. Flash is full of valuable information.” Oh, and the headline is from a technologist from Australia.

Innovations '07 Siemens Education Symposium for Medical Technologists and IT Customers

August 12 – 15, 2007
Pennsylvania Convention Center and Philadelphia Marriott Hotel
Philadelphia, Pennsylvania, USA

Register now for Innovations '07 and take advantage of this education opportunity to sharpen your skills, share experiences with your colleagues, and learn new techniques to enhance patient care and optimize system efficiency.
This program offers a total of 16.5 Category A ASRT continuing education credits.
Sessions will allow you to experience the latest innovations in MR for 3T, Breast MR, Cardiac MR, functional MRI (fMRI), and the newest hybrid technology, MR-PET. You will learn how to improve your workflow, optimize image quality, and troubleshoot artifacts with the "Tips and Tricks", Siemens Uptime, iPAT (integrated Parallel Acquisition Techniques) and Tim (Total imaging matrix) sessions. An update on MR Safety will also be highlighted.

For more information and to register, visit www.usa.siemens.com/med-innovations/eNewsletter.

Early registration fee and hotel reservation deadline date: July 20, 2007.

Philadelphia, Pennsylvania, USA.

All Siemens Medical Solutions customers are invited to participate.

On account of certain regional limitations of sales rights and service availability, we cannot guarantee that all products included in this brochure are available through the Siemens sales organization worldwide. Availability and packaging may vary by country and is subject to change without prior notice. Some/All of the features and products described herein may not be available in the United States.

The information in this document contains general technical descriptions of specifications and options as well as standard and optional features which do not always have to be present in individual cases.

Siemens reserves the right to modify the design, packaging, specifications and options described herein without prior notice.
Please contact your local Siemens sales representative for the most current information.

Note: Any technical data contained in this document may vary within defined tolerances. Original images always lose a certain amount of detail when reproduced.

Order No. A91MR-1000-32C-7600
Printed in Germany
CC MR 01000 WS 050720.

Contact Addresses

In the USA:
Siemens Medical Solutions USA, Inc.
51 Valley Stream Parkway
Malvern, PA 19355
Tel.: +1 888-826-9702
Tel.: 610-448-4500
Fax: 610-448-2254

In Japan:
Siemens-Asahi
Medical Technologies Ltd.
Takanawa Park Tower 14 F
20-14, Higashi-Gotanda 3-chome
Shinagawa-ku
Tokyo 141-8644
(+81) 354238489

In Asia:
Siemens Medical Solutions
Asia Pacific Headquarters
The Siemens Center
60 MacPherson Road
Singapore 348615
(+65) 9622-2026

In Germany:
Siemens AG, Medical Solutions
Magnetic Resonance
Henkestr. 127, D-91052 Erlangen
Germany
Telephone: +49 9131 84-0

Headquarters
Siemens AG, Medical Solutions
Henkestr. 127, D-91052 Erlangen
Germany
Telephone: +49 9131 84-0
www.siemens.com/medical

www.siemens.com/medical